COMPUTERISED EVALUATION OF FURNACE FIELDS

C.C.Rabey

September 1974

Submitted in fulfilment of the requirements for the degree M.Sc.(Eng).

University of Cape Town

ACKNOWLEDGEMENTS

1. To Mr. M.G. Rodd for his guidance and encouragement.

2. To the National Institute for Metallurgy for their financial and technical support.

3. To the staff of the Electrical Engineering Department, U.C.T., for their assistance and patience.

4. To Mr. G. Sommer for his endless supply of information and enthusiasm about the project.

S Y N O P S I S

The concept of using a submerged arc furnace for the reduction of ore to semi-refined metal was introduced early in the nineteenth century, and although much research has been done on the operation of the furnace, its design and construction still remain more of an art than a science. The aim of this thesis is to investigate, by means of various models, some of the basic parameters and fields of the arc furnace in an attempt to increase the understanding of its operation.

LIST OF CONTENTS.

CHAPTER 1

THE ARC FURNACE

Arc furnaces fall into two categories - the open arc furnace and the submerged arc furnace. The former is extensively used in the steel industry for melting down scrap and is, in general, much smaller than its counterpart which is used in the mining industry as a first step in the refining of certain metals. The two types of furnace, although they work on the same basic principle, have entirely different modes of operation and associated design and control problems. The effective circuit for a single phase is shown in Figure 1.1. The charge is loaded into a crucible and an arc struck between it and the electrode. The load impedance, and hence the power input, can be varied by changing the height of the electrode tip. Very high current densities are used, so the impedance of the busbars has a very significant effect and hence the designers must go to great lengths to keep it as low as possible. This is achieved by using many conductors with small cross-sectional areas (to reduce the skin effect) for a single busbar. The outgoing conductors are interlaced with the return path lines (as far as is practicable) in an attempt to reduce the self inductance of the system. For higher power density furnaces a polyphase system is used with more electrodes. The most common shape furnace in use today is a circular one with three electrodes arranged at

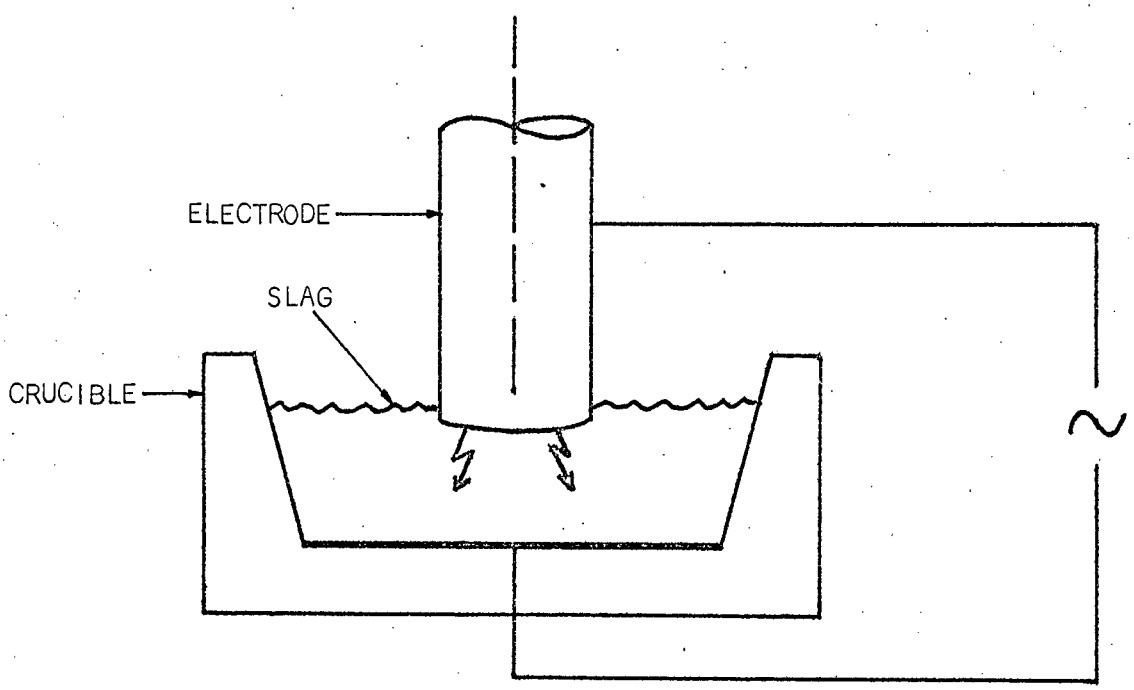

FIGURE 1.1(a) A DIAGRAMMATIC REPRESENTATION OF AN ARC FURNACE

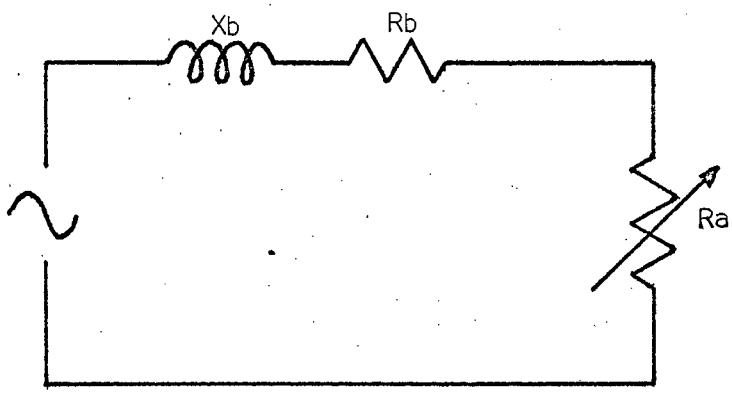

Ra=Arc Resistance
Rb=Busbar Resistance
Xb=Busbar Reactance

FIGURE 1.1(b) EQUIVALENT CIRCUIT OF AN ARC FURNACE

the corners of an equilateral triangle (Figure 1.2). The melt forms the star point of the system.

1.1 THE OPEN ARC FURNACE.

As mentioned previously, these are largely used for melting down scrap iron i.e. they are only used for heating purposes. The crucible is loaded with the scrap and the electrodes lowered onto it and an arc is struck. The operator can then set the size of arc he requires and it is kept constant by a fast-response control system which keeps the impedance presented to the supply at a steady value by varying the vertical position of the electrode tip. This is possible because the electrodes used are fairly small, sintered carbon rods which are light enough to permit quick movement, and necessary because as the metal melts the level of the surface sinks so the electrode must follow. As the process proceeds the type of arc required for optimum performance changes so the operator must periodically make manual adjustments to the controller. At the end of the meltdown the electrodes are removed and the metal discharged. In many furnaces the entire superstructure supporting the electrodes and their mountings can be swung away and the crucible tilted to empty the metal.

The characteristics of this furnace, then, are that it is generally fairly small, reasonably well controlled and most of the input power is dissipated as heat in the arc. Very little heat is generated due to conduction currents in

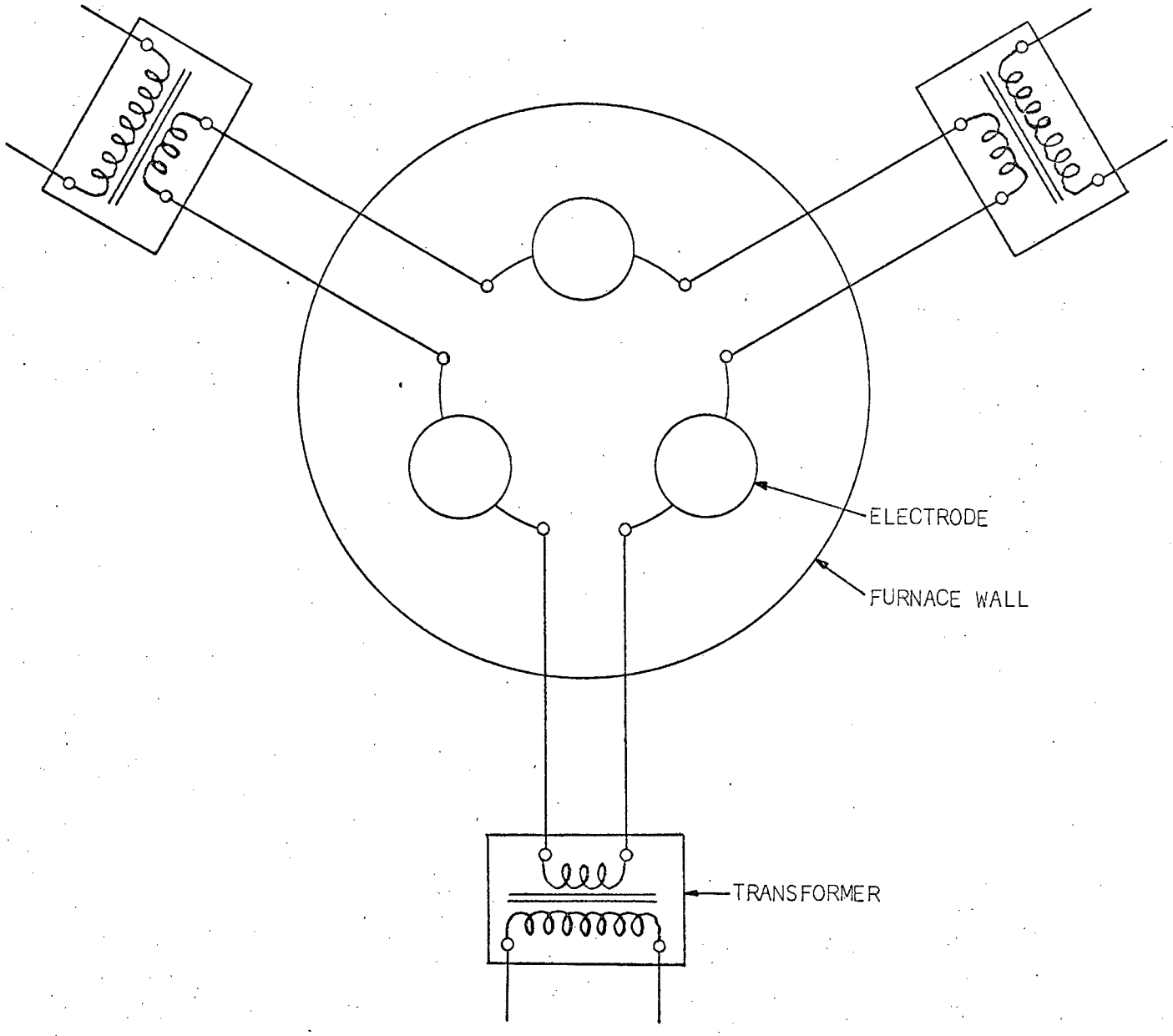

FIGURE 1.2 TYPICAL PLAN OF AN ARC FURNACE

the burden. The operator can see where the electrode tips are and the type of arc that has formed and so has fairly good control over the situation. The process is not continuous, but the time interval elapsing while the furnace is emptied and recharged is made as short as possible so that the bowl does not lose too much of its heat.

1.2 THE SUBMERGED ARC FURNACE.

In contrast to the open arc furnace, the submerged arc furnace is usually a massive beast which should operate continuously for several years until the fire-brick lining wears thin. The burden in this case consists of a mixture of ore, coke and flux which is heated up by the arcing and current flow and in the process is reduced to a semi-refined metal alloy. This settles out as a layer on the floor of the bath and is tapped off at various intervals. The remainder of the material forms a slag which is withdrawn from a higher tap-hole and recycled. Raw materials are fed in continuously by feedshoots through the roof of the furnace.

The electrodes used in these furnaces are much larger than the open arc electrodes and are actually submerged a few feet into the burden. The top layers of the charge are still granular material and very little of the total current flows through it. This small current and rising gases serve to preheat the mixture. The majority of the reaction and power dissipation occurs in a small area around the electrode tip (References 1, 2, 3). The actual

mechanism of the transport of current in the furnace is not entirely clear and depends to a fair amount on the product being refined. Loe (Reference 3) claims it takes place from particle to particle by means of small electric arcs, while Otani, Saito, Usui and Chino (Reference 4) observed by means of a peep-pipe fairly large arcs from the electrode tip to the slag. In the furnace modelled in this thesis (Reference 5) the current flow appears to be entirely by conduction. The physical composition of the furnace contents is also very complex, but can, for analytical purposes, be broken up into several distinct regions. Figure 1.3 shows the cross section of a typical submerged-arc furnace as suggested by Loe.

Since the feed is continuous there is no rapid change in furnace resistance so there is no need for the fast electrode-position control. However, during the process the metal layer will rise in between tapping and the electrodes will slowly burn away so there must be some means of moving the electrode. This is accomplished by hydraulic jacks, but movement is very slow due to the massive size of the carbon rods. The electrodes cannot be premanufactured and so are made continuously as the operation proceeds (Soderburg electrodes). At the top of the electrode (above the holding clamps and power contacts) the electrode has a thin metallic sheath. As it moves down new sections are welded on and filled with graphite and pitch. The closer to the reaction zone this gets the hotter the electrode becomes

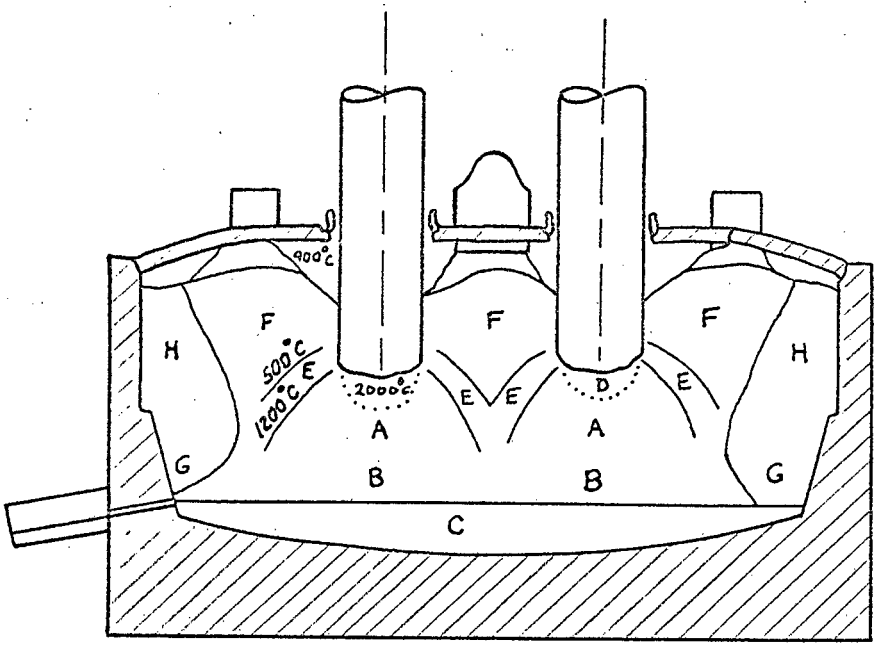

FIGURE 1.3 TYPICAL CROSS-SECTION OF AN ARC FURNACE (LOE)

A: Coke bed

B: Slag bath penetrating lower part of coke bed

C: Metal bath

D: Highest temperature zone

E: Prereduction and smelting zone

F: Preheating zone

G: Solidified slag

H: Spongy material

(due to heat conduction and current flow) until the basic materials melt and start to bake. By the time the section reaches the slag area the metal sheath has been melted away and all that remains is a solid carbon block.

To determine the position of the electrode tip is very difficult and also vital for efficient operation. If too high, the lower areas of the slag will cool and start to freeze, if too low the electrode will overheat and burn. Obviously the operator cannot see where the tip is, and although the electrode-hearth voltage gives some indication of the height, these signals are subject to error due to the large magnetic fields in the area (Reference 13). At present, this measurement is done more by guesswork and operating experience than anything else.

As can be seen, the process is fairly complicated and must run continuously. Any sudden shutdown which may occur could cause a lot of trouble because, unless the bath can be cleared quickly, the contents may freeze and then the only means of clearing it is with explosives. Once cleared there still remains the problem of starting it up again. This involves slowly heating it up over several weeks, baking new electrodes and rekindling the reaction. Economically this is a disaster because the whole operation will take about a month.

The size of the furnace prevents experimental set-ups - once built the system is there to stay. Very little

can be done to change the design without the costs running to almost the price of a new furnace, so it must be very carefully prepared. The most common design in use today is the circular furnace with three electrodes (Figure 1.2). However, with the pressing demand for larger operations more electrodes have to be added. Six electrodes in a circular furnace have been tried, but the largest furnace yet (100MW) is a rectangular furnace with six electrodes in a line. This is effectively three single phase furnaces lumped into one bath and many of the mutual effects between phases (which are apparent in the circular furnace) are eliminated. This is the type of furnace that has been modelled in this project because of the rising interest in its design.

1.3 DEVELOPEMENT OF THE SUBMERGED-ARC FURNACE.

The first submerged-arc furnaces came into commercial operation late in the nineteenth century and their design has remained to a large extent a matter of arbitrary decision. Very little of the planning is made out to ensure most suitable metallurgical conditions, the basis being to consider it from an electrical point of view. Most of the concepts used today have been derived from masses of data collected from small furnaces built on a trial and error basis. Different sizes and shapes of furnace seemed to be more efficient for the production of different types of metals. This led to the development by F.V. Andreae of

the electrode periphery concept

$$k = \frac{E\pi D}{I}$$

where k = electrode periphery resistance

D = electrode diameter (in inches)

E = electrode-hearth voltage

I = current per electrode

He found that for a particular smelting operation the product of furnace resistance and electrode circumference was more or less constant. Together with Kelly he determined a large number of k factors from operating plants and the latter (Reference 2) presented a typical range of k factors for different submerged-arc operations. This was the first attempt at assigning a cell constant to a furnace. Andreae later expanded on the k concept (Reference 1) and, assuming the energy to flow radially from the electrode in an area proportional to the power input, showed that the radius of the active zone should be equal to the diameter of the electrode. Kelly used this to calculate the optimal dimensions for furnaces. These principles have affected the design of submerged arc furnaces to the present.

One of the most important parameters to calculate when designing a furnace is the resistance of the burden in terms of the dimensions of the system and the specific resistivity of the charge. Morkramer was the first to

attempt a theoretical determination and suggested

$$R = \rho\pi D$$

where R = charge resistance

ρ = charge resistivity

D = diameter of electrode

This equation assumes the current to flow from the electrode to the hearth through a volume shaped like a truncated cone.

Kjolseth (Reference 6) theoretically examined the Tysland Hole furnace and proposed the formula

$$R = \frac{\rho}{2\pi S}\left(1 - \frac{D}{\left(1 - \frac{D}{4H}\right)\left(2H-S\right)}\right)$$

where S = electrode immersion

H = depth of charge

This he found gave better agreement with measurements taken from the furnace. Hallvard Nilsen (Reference 7) using a salt solution model with a single phase supply, found an empirical cell constant

$$K = \frac{0.1517}{D}\frac{\left(\frac{H-S}{D}\right)^{0.24}}{\left(\frac{S}{D}\right)^{0.45}}$$

where $K = R/\rho$ and the other symbols are as before. He also calculated the resistance offered assuming the current to flow from electrode to hearth along various regular geometric lines. The most accurate solution was within sixteen percent of the empirical answer, but the theoretical model failed to account for any interelectrode current flow.

Downing and Urban (Reference 8) also proposed a formula for calculating the cell constant by using a relationship between the capacitance and resistance of the system, and they obtained a fairly reasonable correlation between the theoretical and measured results.

Recently a lot of work has been done by the National Institute for Metallurgy (South Africa) concerning the actual current distribution in the bath (Reference 9). A salt solution model was used and the two components of current (viz. electrode-electrode and electrode-hearth-electrode paths) were measured. For all electrode depths they found that at least seventy percent of the current went via the hearth.

All these models used so far have been scaled replicas using a cold saline solution as the charge. The validity of these results when applied to a large real system is questionable because in the models only small currents could be used (not even in proportion for its size to the real currents) and so any effects due to the magnetic fields would be lost. Also the actual size of the components

in the real world systems might play an important part e.g. skin effect in the electrodes would be negligible on a model but will be significant for an electrode four feet in diameter. In this thesis an attempt is made to show the actual current distribution in a model furnace and then, using a mathematical simulation, transform these fields to what might be expected in a large furnace.

CHAPTER 2

A PHYSICAL MODEL

It was decided to build a scale model of an operating furnace and to extract information from this which could then be compared to and correlated with any data available from the actual furnace. A minicomputer was to be employed to help obtain and record the data.

In all submerged-arc furnaces the contents of the hearth can be divided into three specific zones - the matte or molten metal on the floor of the bath, the slag - where the majority of the reduction process takes place, and the top layer of raw materials which acts as an heat jacket. This has been the theory behind the design of furnaces and has in fact been shown by some quite fantastic experiments (Reference 3) in which a furnace has been 'frozen' and then 'dissected'.

The top insulating layer of raw materials consists of lumps of ore and flux and coke mixed in the correct proportions and, for all intents and purposes, has both electrical and thermal insulating properties. The small amount of current it does draw only serves to preheat the material prior to it being dissolved into the next layer - the slag. For a small model such as the one used in this project, this layer can be left out. The heat generated

in the model is far too small to warrant a heat jacket covering the surface.

This leaves only the slag and the matte to be simulated in the model. Various sets of experiments have shown that the metallic phase has a much higher conductivity than the slag even at the operating temperature (Reference 9) so all the power can be assumed to be dissipated in the upper layer. This was achieved by using a saline solution (as slag) in a plastic bath with a stainless steel bottom. This does assume that the two layers have a horizontal interface in the furnace, but, for normal operation of a furnace, this is a very fair approximation.

The contents of the model are stationary. In a real furnace there must be some movement of the layers since raw materials are being added and refined metal is being extracted all the time. Tests carried out on the furnace which was modelled (Reference 9) have shown that the residence time of the material is fairly long (36 hours) so the movement is very slow. Hence the 'stagnant pool' effect of the model should not affect the correlation between any real and simulated results.

The furnace chosen as the guidelines for the dimensions of the model was a platinum resistance furnace situated at Rustenburg in the Transvaal. This furnace has six electrodes in a line, each adjacent pair being supplied by a different phase with its own transformer. Its electrical

consumption is 19,5MVA and it operates at a power factor typically in the region of 0,95. The reasons for choosing this furnace as the basis of the model are:

(a) It is almost completely resistive i.e. it has a minimal amount of arcing. Since arcing can never be simulated in a saline solution model, the proposed model will be more valid.

(b) It operates efficiently - if it can be ascertained why this one works so well, others may be designed on the same lines.

(c) It is a very quiet furnace which makes the task of obtaining data for correlation much easier. Most other large submerged arc furnaces, particularly the ferro-alloy ones, produce huge volumes of gases during the reaction which form large bubbles under pressure. Eventually these pockets burst shooting hot material in all directions. This makes the furnace almost impossible to approach, let alone take any measurements.

(d) A lot of information was already available about the internal structure of the furnace from investigations carried out by a team from the National Institute for Metallurgy.

(e) Because of the in-line positioning of the electrodes the mutual effect of the three phases is very small. The system can, on the small scale anyway, be reduced to three separate single phase furnaces lumped into one.

This greatly simplifies any theory.

(f) For economic reasons larger furnaces than are operating at present are to be built. There were theories that the in-line furnaces may be more efficient at the higher power consumption levels than the more common circular furnaces with electrodes arranged in a triangular formation. Hence data on this specific design needed to be amassed.

The disadvantages of the small saline-solution model proposed is that one cannot obtain the high current densities encountered in a full-scale industrial furnace, hence one does not have the associated large magnetic fields. This does of course mean that it is far easier to take more meaningful measurements fromthe model, but the effect any magnetic flux may have on the electric field, and hence the current path, is lost. In a real furnace, especially those designed to produce ferro-alloys, the contents will have a fairly high magnetic permeability which also increases the magnetic effects. Again, the salt solution falls down here. Other aqueous solutions using ferro-magnetic ions such as iron or nickel would not really help here either because the solutions would be too weak to have any noticeable effect. Actual arcing from the electrode to the slag and from one particle to another in the burden, although very small in the system being simulated, can never be obtained using a salt solution as the conductive medium. Iron smelting furnaces also exhibit this small arcing effect (Reference 3) but in

ferro-alloy furnaces it has been seen (Reference 4) to be in predominance, so a model as used here would give fairly dubious results. Inhomogeneity due to temperature gradients and operation of the furnace (i.e. reaction zones, incomplete mixing of the raw materials, inconsistency in the charge constituents and particles instead of liquid) are also very difficult if not impossible, to obtain in a model of this kind. Ideas of using a paste or a series of layers of immiscible liquids were considered but rejected for practical reasons. The considerable reactance always present in an arc-furnace circuit (because it is of the same order of magnitude as the resistance offered by the charge) is completely lost in the model. The little inductance present in the feeding busbars is completely swamped by the resistance of the electrolyte in the tank, no matter how high a conductivity used. Using a higher frequency supply to the model furnace to enhance the reactance had little effect - the resistance still predominated.

Despite these drawbacks it was decided to construct the model and see what information could be obtained from it. This model could then, hopefully, be modelled mathematically and simulated on a computer. The simulation could then be modified to overcome the inadequacies of the physical model.

The tank representing the furnace was built to approximately one-thirtieth full scale. This makes it large enough to be able to get in and make accurate position read-

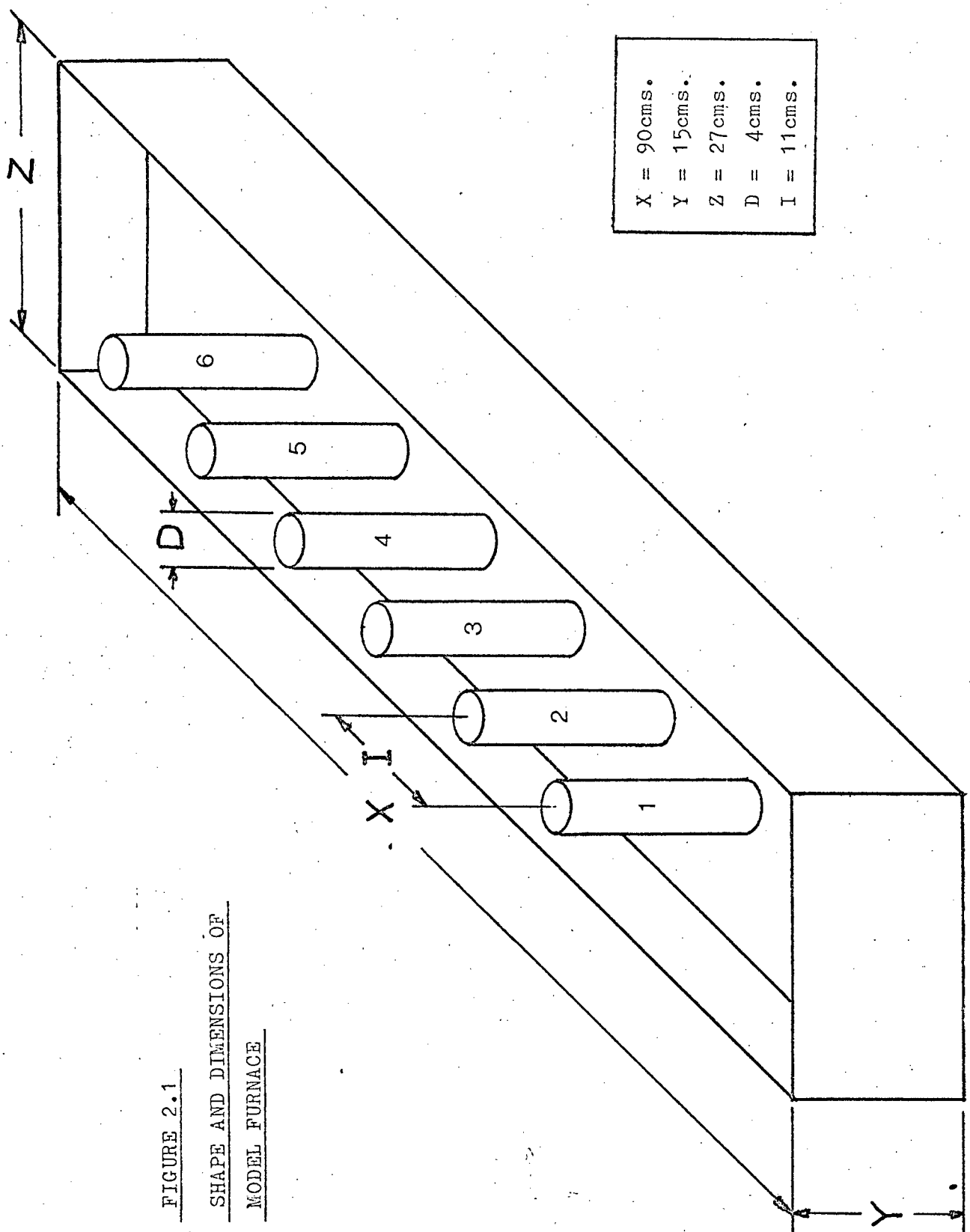

FIGURE 2.1

SHAPE AND DIMENSIONS OF MODEL FURNACE

ings of the electrodes, depth of solution and voltage probe, and yet not so large that voltage pickup in the measuring leads cause erroneous analog readings. The dimensions and layout are shown in Figure 2.1. The bath was made of P.V.C. with a stainless steel plate covering the bottom. The whole tank was not made of metal because it was felt that since in the actual furnace the walls are made of firebrick they should be non-conducting. The metal base is brought to a terminal to provide a reference point for all electrical measurements. The six electrodes were made of carbon in order to avoid the corrosive effects of the salt. The shape of the electrode was a plane cylinder with a flat end. The slight taper and rounded bottom observed on the real electrodes was considered too small to be worth worrying about. Each electrode was positioned vertically by a stepping motor mounted on a frame enclosing the tank. The horizontal position of the electrode can be altered by moving the motor mounting. The adjacent pairs of electrodes were fed from the three phase supply, through three independent variacs to afford variation of a single phase if required, then through isolation transformers. These transformers were rated as 12.5A at 12V. The electrical circuit diagram is given in Figure 2.2.

The use of stepping motors for controlling the depth of immersion of the electrodes was instigated by the idea of using a digital computer to control the variables of the model and to extract the data. These motors have

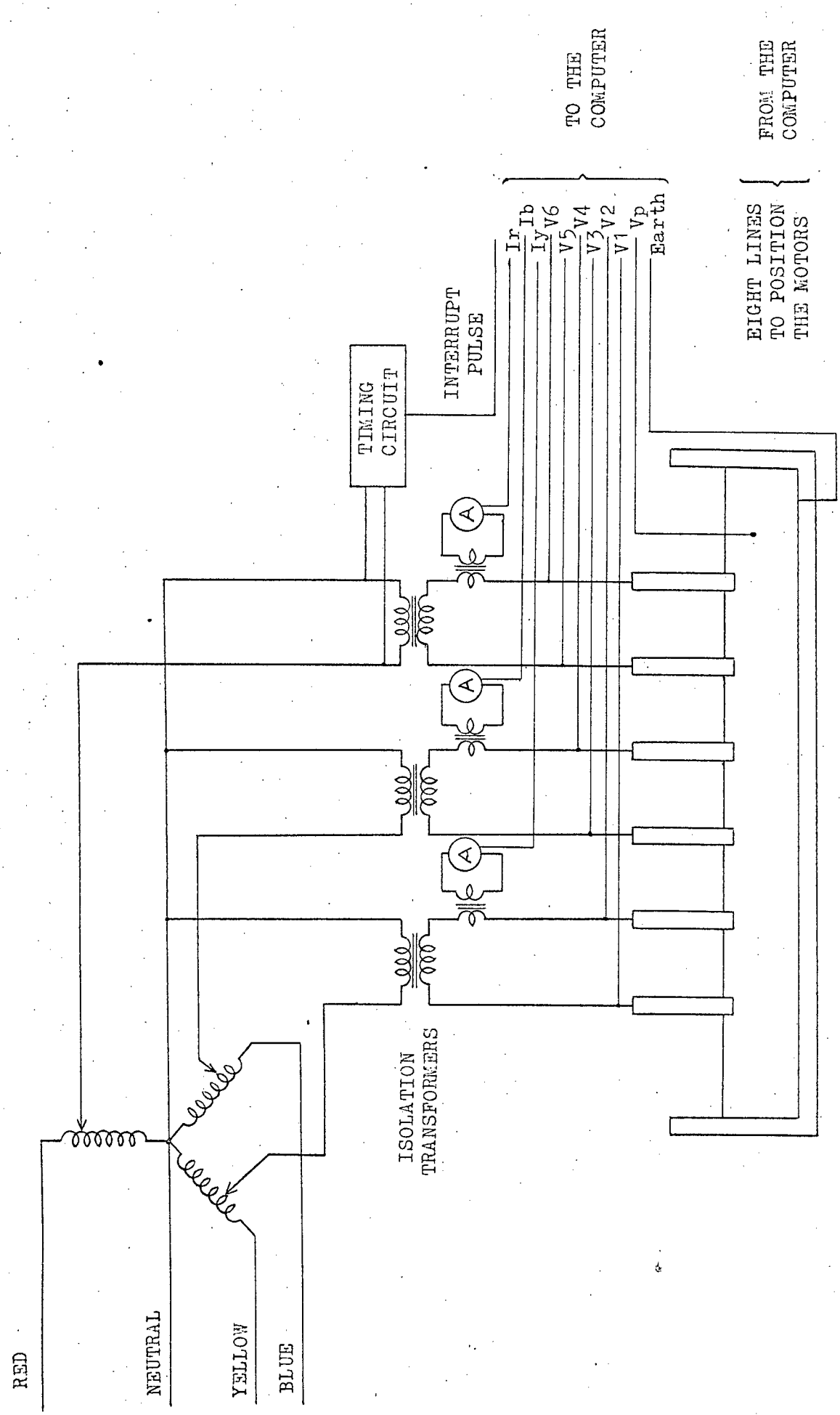

FIGURE 2.2 ELECTRICAL CONNECTIONS TO THE MODEL

been developed as digital devices which can be directly controlled, via a driving circuit, by a string of pulses emanating from the computer. One of the chief advantages is that no feedback, regarding position, is necessary. A more detailed description of the theory and operation of a stepper motor, together with the circuit used to decode the controlling signal pulses is given in Appendix A. It is sufficient to say here that by applying a pulse and a direction signal to the driving circuit, the motor will move one step in the desired direction. The motors chosen for the project are capable of delivering a torque of fifty ounce-inches which is more than enough for the purpose. The maximum speed at which they can run is one hundred steps per second i.e. they can be driven by a pulse train of 100Hz. One full revolution consists of two hundred individual steps. The movement of the motor is transmitted to the electrodes via a suspension wire wrapped around a pulley on the motor shaft. These pulleys were machined so as to have a circumference of five centimetres i.e. by moving the motor one step the electrode will move a quarter of a millimetre. This gives a positioning resolution which is in excess of the general accuracy of the whole system.

The various electrical parameters (the six electrode-hearth voltages and the three line currents) are fed through a multiplexer to the analogue-to-digital converter and into the computer. Since alternating signals are being measured the computer also requires a synchronising signal to indicate

when measurements should be taken so that all readings are made at the same instant of the cycle. This is achieved by a zero-dectector monitoring one of the phases, which sends the appropriate pulses to the interrupt facility on the computer. The instant at which the pulse is generated can be varied over the full period of one cycle. The positioning of the electrodes is remembered by the computer - the system is initialised at the start and all consequent movements are recorded in memory.

The model was now at a stage where one could measure the voltages of the electrodes relative to the base and the current flowing for any possible configuration of electrodes. A lot of information can be gained from this such as curves of resistance versus electrode depth but this setup hardly warrants the expense of a minicomputer and the associated positioning mechanisms and, in any case, is not the prime aim of this project. What the model was wanted for was to investigate and plot out the potential and electric fields found in the slag (salt solution) and hence determine the current distribution. This could be done in two ways - by analogue means or by digital means.

(i) Analogue determination of field.

This method is well illustrated by the use of Teledeltos paper in the mapping of two-dimensional fields. The model is set up and a probe moved around in the volume until a point at a specified potential is found.

The probe is then moved in a path so as to follow that potential line and its path is plotted. By repeating this performance with different potential values a potential field plot can be built up. The problem arises when one wishes to draw the electric field which, for the quasi-static case, is the plot of the gradient of the potential field. Also, when one has a three-dimensional model the probe can travel anywhere along a surface instead of a line, which can give one quite weird answers. Instruments have been developed and are available for automatically plotting fields in this manner, but they are expensive and the amount of information one can extract from the results is much less than can be obtained using digital methods. The analogue method also favours the use of direct current models which for the project definitely rules it out as a method of solution as it is required, eventually, to look at three phase effects.

(ii) Digital determination of fields.

The digital approach to measuring a field is to take as many samples as are required, to give a specified accuracy, of the potential at certain, preselected points in space and/or time and then use interpolation techniques to display the required information. The accuracy of these results depends on the total number of samples taken (as should be expected from Information theory). The advantage of the digital method is that once one has

scanned the model and stored the data, one effectively has the model represented by a three (or four if time is taken into account) dimensional matrix. This can then be operated upon mathematically by a digital computer to give other related fields such as the electric field and the energy distribution. The field can also be shown at a certain point in time (if it is time variant) and not as an R.M.S. field as in the analog case.

Clearly the digital method leaves one with the data in a more convenient form for processing and so this was chosen.

The next problem was what to measure, and how to go about it. Obviously there must be some form of detector in the bath which can be moved to any specified coordinates. What to measure was no problem because basically there was no choice. The magnetic field was far too small to detect. The current density at any point could possibly be found using three short-circuited search coils arranged orthogonally and measure the induced current in each one and hence get the three components of the said vector. However to get any decent sort of reading the coils would have to have a fairly large cross-sectional area which would affect the accuracy of any measurement taken on such a small-scale model. The only alternative left was to measure the electric potential at the tip of a probe, relevant to some reference point which,

for convenience sake, was taken as the metal plate on the floor of the bath.

How to scan the bath resolved itself. Initially it was intended to have a large number of probes equally spaced out in a horizontal plane. The probes would all be connected up to a multiplexer and so the computer would be able to access any one and measure the potential at that point. By moving the measuring plane up or down a three-dimensional matrix of samples could be obtained. The advantage of such a system is that a complete horizontal plane can be sampled in a matter of a few cycles. Against it is its inherent inaccuracy. To interpolate a reasonably accurate field plot one must take the points fairly close together, and to position the probes accurately they must be made of some fairly solid material to give them rigidity. With the massive number of probes required and the amount of foreign matter in the bath the fields must get distorted. Further, the cost of a multiplexer will be prohibitively high to get the resolution required. Another factor ruling out this mode of analysis is that one cannot readily take readings of the field below the electrodes - which is the most important area in the tank. Similar problems are encountered if one uses a line of probes which can be moved in two directions to get the full coverage of the bath. These methods are fine if one already has an equation giving the field in the bath and only one or two points at strategic positions are needed to evaluate the constants in the formula in order to calculate the field

everywhere. But when one wants to map the field using only the measured data a fine sampling mesh is imperative. This leaves only the possibility of one probe which can be moved in all three directions (X, Y and Z) and so access any point in the model.

Ideally the probe should be positioned by the computer, but to achieve this one has to have a very sophisticated drive mechanism. The system adopted in this project only enables the computer to move the transducer in a two-dimensional scan - to change the third coordinate the operator has to make manual adjustments. The scanning device used consists of a horizontal track clamped above the tank, running along the whole length of it (referred to as the X-direction). Along this set of rails runs a trolley which holds the probe. The probe is made of stainless steel wire insulated by a layer of resin. Stainless steel was chosen to eliminate the possibility of an electrode potential being set up between the tip of the probe and the reference plate and the insulation made fairly thick to minimise any disturbing effects on the field by the presence of the probe. The wire was bent into an L-shape so that measurements can be taken directly below the electrodes. Two stepping motors fixed at the one end of the track can move the probe to any point in a vertical plane parallel to the line of the electrodes by means of a complex system of wires and pulleys. Hence the computer can control two of the degrees of freedom of the sensor - the X and the Y (vertical). To obtain the three dimensional matrix of data

samples a scan is done in one plane and the points stored, then the whole track is moved manually (in a horizontal direction at right-angles to the line of the electrodes - the Z direction) by the desired increment to the next plane, the scan repeated and so on until completed.

The speed at which the probe moves is about two and a half centimetres per second which is not too fast to disturb the electrolyte. The accuracy with which it can be positioned should again be a quarter of a millimetre since the same size pulleys are used on the motors. However, with the various wires etc. used to transmit the motion to the trolley the accuracy is probably reduced to about half a millimetre.

All the analogue signals to the computer (the six electrode voltages, the three line currents and the probe voltage are fed into buffer amplifiers before going into the multiplexer. These only have unity gain, but their purpose is primarily to isolate the signals from each other - and provide a bit of protection for the multiplexer. The analogue-digital converter is capable of measuring between plus and minus ten volts with ten bit accuracy. This gives a resolution of twenty millivolts.

Finally, one of the most important pieces of equipment used in the model - the computer. The machine used was a VARIAN 620I minicomputer having twelve kilowords fast storage and two magnetic tape drives for backup mass-storage. Because of the intricate and somewhat cumbersome peripherals

the machine cannot be easily moved around. Since the computer cannot be taken to the model the next best thing would be to bring the model to the computer. However, the model with its associated instrumentation and power supplies was not an easy thing to move either, and since the computer was not dedicated to this project the equipment could not be set up and left in the computer room for the simple reason that there was not enough space. Furthermore, the corrosive solutions used and the steam produced when operating would completely nullify the effect of keeping the computer in a dust-free, air-conditioned room. To overcome this problem, and also to enable the computer to be used for other projects in the laboratories, a high-speed data-link was built. What this piece of equipment effectively does is to bring the computer, with its associated peripherals, into the laboratory. The speed at which the input and output devices are accessed is slightly reduced due to the delay introduced in the transmission line but this does not significantly affect the results obtained since only low frequencies (maximum of 400Hz) were used on the model. For a more detailed account of the design and operation of this link refer to Thorning (Reference 18).

Communication between the operator and the computer was by means of a teletype with a large cathode-ray visual display. Hence the operator could type in instructions and the computer could reply with numbers or graphs. Permanent copies of any output displayed on the screen could be

obtained using a hard copy-unit - a device which electronically scans the screen and reproduces the display on paper by photographic means.

CHAPTER 3

VARIAN PROGRAMMING

The use of a minicomputer to extract information from a small model resistance furnace may seem to be rather extravagent, but when one considers how many readings are to be taken and processed for just one field plot, the proposition becomes more real. Further, the potential field which is measured does not show the information required in the best way, but should first be transformed into related fields using mathematical operations. Another advantage of using a digital measuring system is that the fields which one hopes to obtain, although they are time-varying, can be frozen at any one point in the time cycle depending on the instant at which the operator has instructed the computer to sample. To measure the fields in a three phase system this is absolutely imperative because the resultant fields consist of rotating vectors which also vary sinusoidally in magnitude. If one merely measured the R.M.S. value of these vectors the results would be meaningless because the direction of the field cannot be shown at any instant. However by freezing the picture at various points in the cycle the complete action of the process can be seen. The speed with which the results can be displayed also favours the use of a computer for this study. If drawn out by hand it would take several hours to produce a field plot. With the digital processor the information is displayed in a matter of seconds and any peculiarities

noticed can be followed up immediately with closer examination before any of the conditions change. Besides having the results processed and drawn out more quickly one also gains in the time taken to acquire the data. The accuracy with which the analog signals are measured and the positioning of the sensing device are also greatly improved by automation basically because the human element is eliminated.

The programmes developed can be split up into three categories. These are data acquisition, data processing and data presentation.

3.1 DATA ACQUISITION

This part of the program can be described as the real-time part. It does the actual controlling of the model. As mentioned in the previous chapter there are eighteen parameters over which the computer has control - the positions of the six electrodes, the X-Y coordinates of the sensing probe, the three line currents, the six electrode voltages and the probe potential. The motors can be moved in either direction by means of pulses originating in the EXC card (Appendix B) and applied to the motor drive circuits (Appendix A). The ten analog signals are fed to the A-D converter, and thence into the computer, via a multiplexer under direct control of the central processor. The operator controls the whole operation by means of a few simple commands which are entered via a teletype.

Data from the model can be acquired in two ways,

depending on what is ultimately required for display purposes. For some plots the whole field of points is required, for others only a few are needed.

(i) Field Data Acquisition

For field analysis by computer a matrix of numbers representing the field must be stored in memory. By means of the EXC interface card the computer can position the probe anywhere in one vertical plane through the model. Varying this plane position manually and storing all the information gives the required set of figures. In this part of the program, therefore, it is the computer's task to move the probe in a scan in such a way that all the points specified by the operator are sampled in the quickest possible way. This is best achieved using a scan as shown in Figure 3.1. The flow chart showing the mode of operation of the routine used to attain this objective is shown in Figure 3.3.

The first block of data requested of the operator by the computer defines the dimensions and fineness of the sampling mesh used in the scan (all the dimensions are in millimetres). The frame of reference used is as explained in Chapter 2 - Y=0 lies on the surface of the electrolyte and increases as one approaches the bottom, X=0 is arbitrarily assigned to be one side of electrode number three. As an

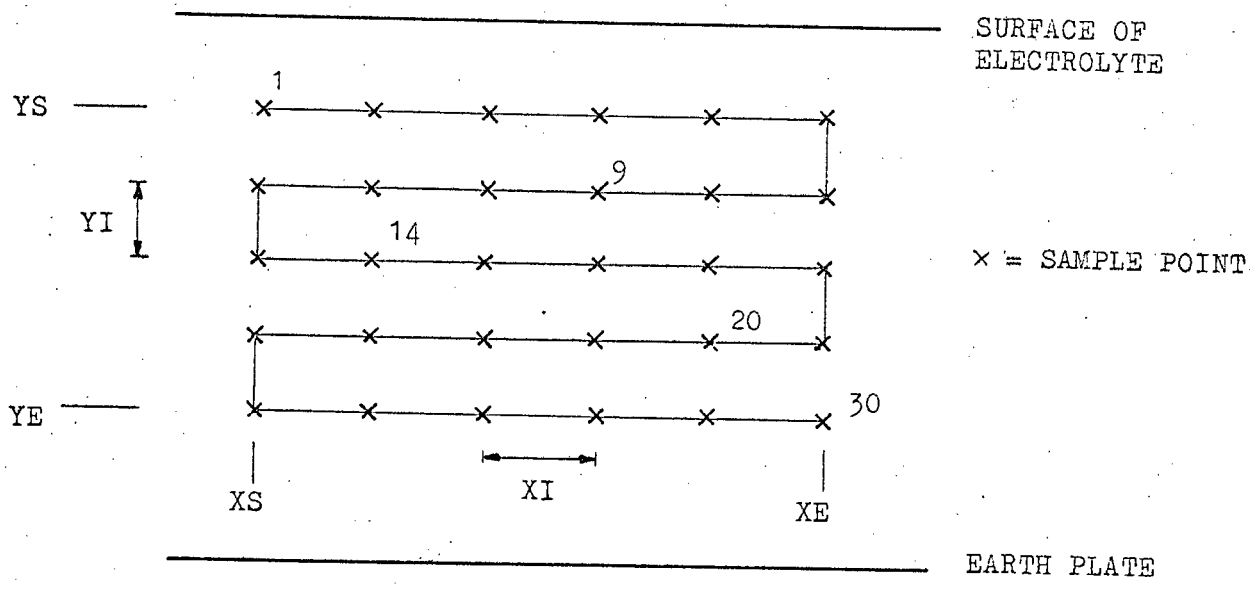

FIGURE 3.1 SCAN PATH

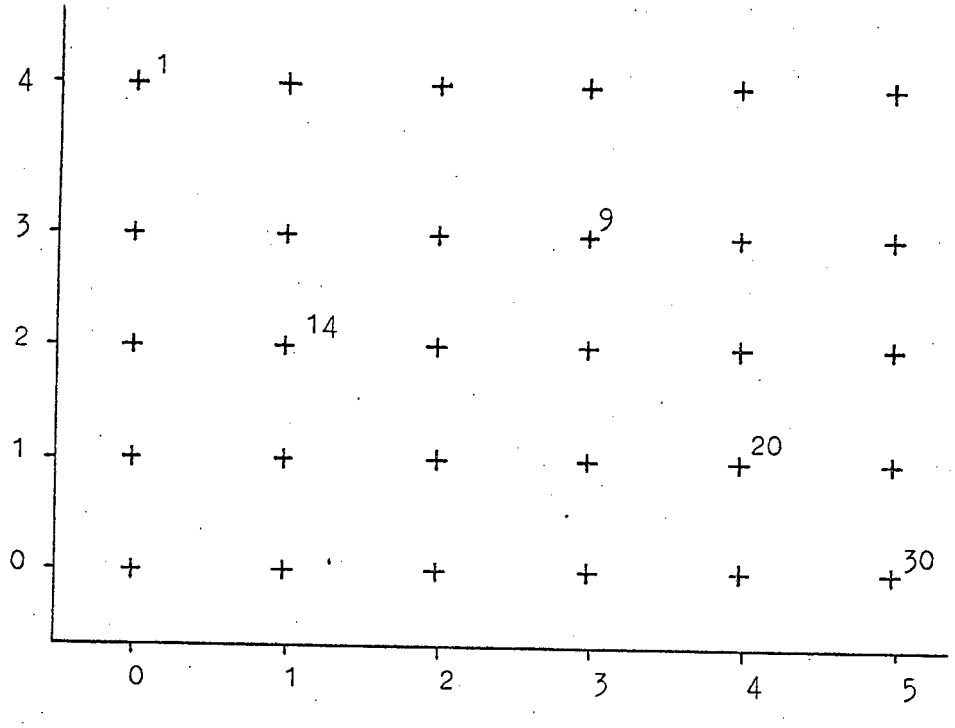

FIGURE 3.2 DATA STORAGE PATTERN

example, the input

0,100,5,

0,45,5,

would indicate to the computer to scan horizontally from position 0mm to position 100mm and take a sample every 5mm along the way, and to do this at level 0mm, 5mm, 10mm and so on to a depth of 45mm.

The next block of data assigns the depth of immersion of the electrodes. The format used is

X,D,

where X refers to the electrode number (A to F) and D indicates the depth in millimetres to which it should be submerged. If nothing is specified the system remains unchanged.

The next step is to initialise the system i.e. to move the probe to the start of the scan and the electrodes to their assigned positions. This is done in two stages. First the INIT routine takes the input information and calculates the direction and number of steps each motor must make to achieve this set up. These results are passed to the MOVE routine which controls the movements of all eight motors and so, as it's name implies, moves the elements to the initial positions. This is done by

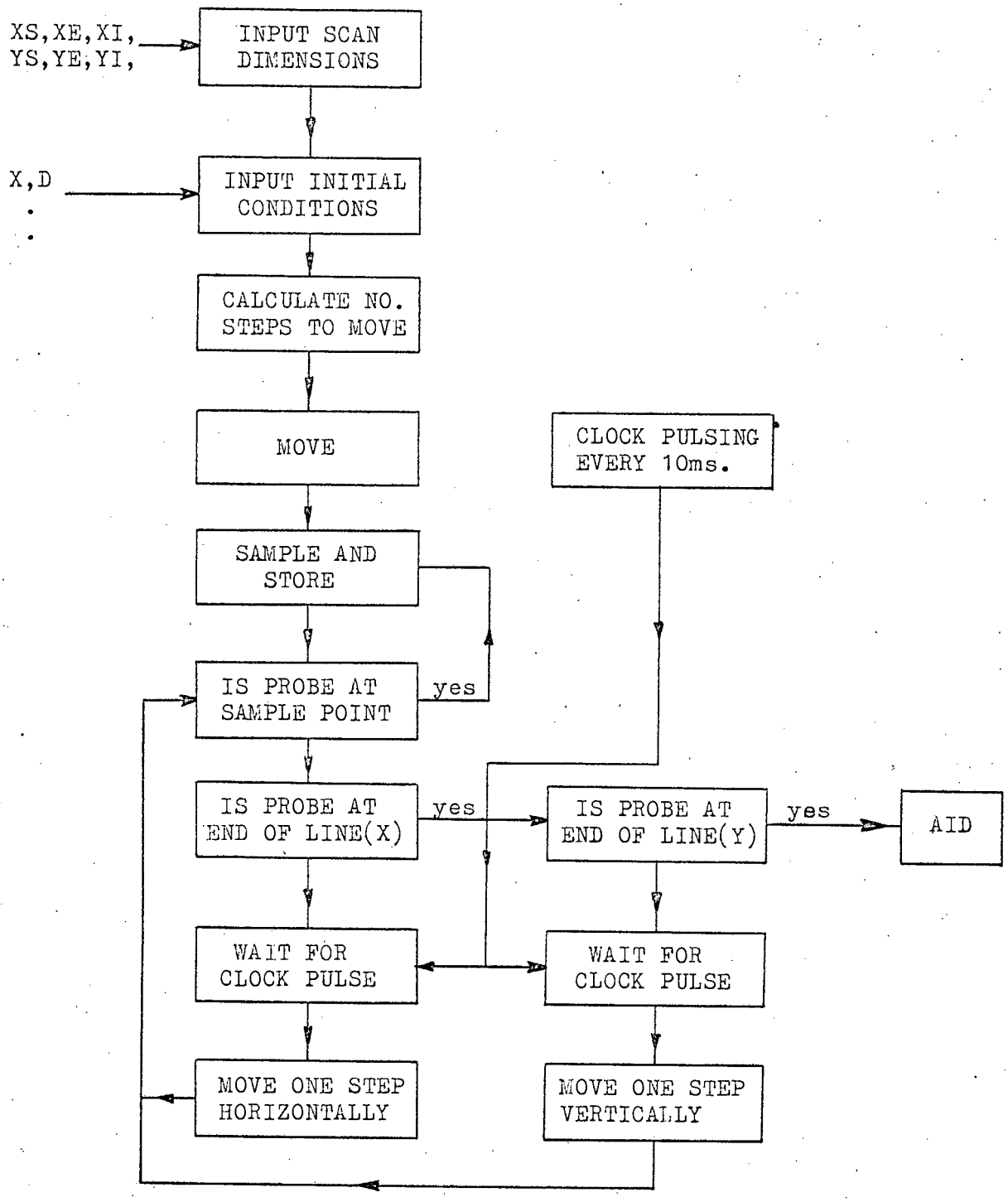

FIGURE 3.3 FLOW CHART OF SCAN ROUTINE

outputting the correct number of pulses to each motor drive circuit. The routine has been flow-charted in Figure 3.4. The stepper motors have a maximum speed of one hundred steps per second (to give the required torque). The required spacing between the consecutive pulses is obtained by means of the computer's real-time clock which is set to interrupt the flow every ten milliseconds. At each pulse the computer jumps into a loop which looks at the position of each motor individually, moves it one step in the correct direction if required i.e. if it is not at the final position specified when the routine MOVE was entered, records the change then moves on to the next motor. When all the motors have been interrogated the computer either jumps back to what it was doing before the interruption or just sits in a non-operational loop and waits for the next pulse. The non-operational loop is necessary, though time-wasteful, because often the computer cannot do anything until all the information has been collected. When all the motors have been moved to the specified positions the clock is switched off and the program continues with the next block.

Once the system has been set up the operational scan can commence. The first sample point is the starting point i.e. the initial position of the

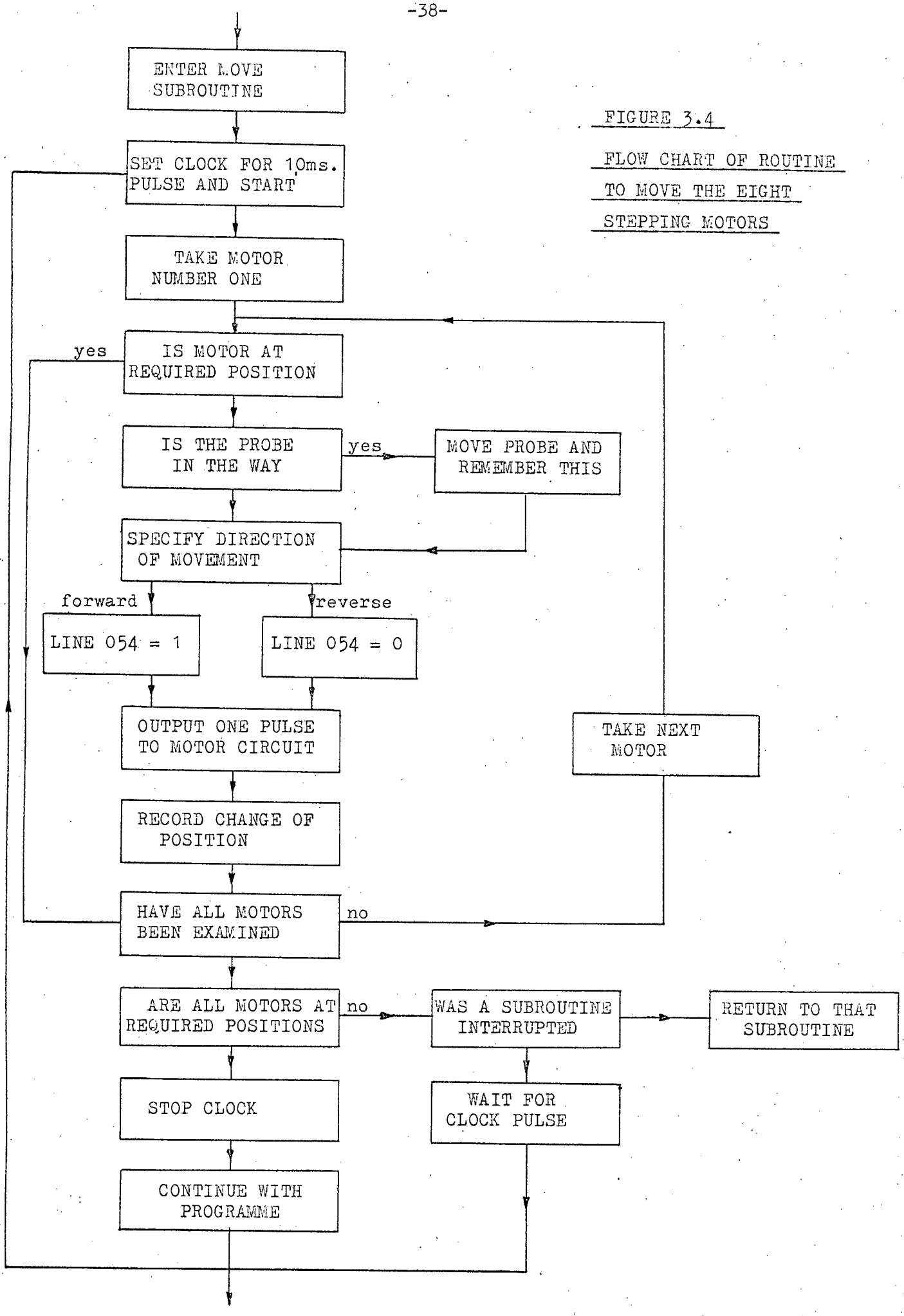

FIGURE 3.4

FLOW CHART OF ROUTINE TO MOVE THE EIGHT STEPPING MOTORS

probe. The instant in the cycle of the furnace supply at which the potential is sampled is determined by an interrupt pulse to the computer via the interrupt module (see Appendix B for description of operation). The interrupt pulse is generated by an external source (Appendix C) which is connected to the furnace supply for synchronisation. It detects the zero crossings and then outputs a pulse. This pulse can be delayed (manually) for a period of up to twenty milliseconds i.e. one full cycle at 50Hz. This interrupt pulse directs the program into a sampling routine which chooses the channel of the multiplexer to be used, samples the potential at that point, converts it to a digital representation and stores it in memory. The next point in the scan is then calculated, the number of steps to move each motor evaluated and passed to the MOVE routine which positions the probe at the next sample point. When all the samples have been taken and stored, the computer jumps back to the control routine and awaits further instructions.

A small point which should be mentioned here is the method of storing the data. It is not stored in the order it is taken but rather with a one to one correspondence with position i.e. the first line is stored starting with (XS,YS) going up to (XS,YE)

(see Figure 3.2) then the next line (XS+1,YS) to (XS+1,YE) and so on. This facilitates handling of it at a later stage.

Another essential part of the program, indicated in Figure 3.4 but as yet unexplained, is the AVOID routine. If one of the electrodes has been immersed to such a depth that it will be in the way of the probe as the probe makes its scan how is the computer to prevent a collision? This is the duty of the AVOID routine. Before any motor is moved this subprogram looks at the position of the probe in relation to the electrodes. If it will collide with the electrode by moving one step it is first moved down the required number of steps to pass below before continuing. The fact that the probe has gone 'off course' is remembered, and as soon as it is clear of the electrode it is brought back on its original track. While below the electrode the input channel to the A-D converter is changed. The scan path should require the probe to sample in the electrode, therefore the multiplexer is switched so that the potential of the electrode is measured. This assumes that the electrode is a perfect conductor i.e. at constant potential - a fair approximation in the model.

(ii) Parameter Variation Data Acquisition

The other data acquisition program available allows the operator to plot any two of the eighteen parameters available (seven potentials, three currents and eight positions) against each other while varying one or more of the independent variables. The flow chart of the program is given in Figure 3.5.

The inputs requested by the computer are:

(a) The X and Y axes - the variables to be plotted are entered, together with an approximate idea of the range of values these will take. This is to accommodate scaling. The variable names are

A - position of electrode 1

B - position of electrode 2

C - position of electrode 3

D - position of electrode 4

E - position of electrode 5

F - position of electrode 6

G - horizontal position of probe

H - vertical position of probe

I_1 - line current between electrodes 1 and 2

I_2 - line current between electrodes 3 and 4

I_3 - line current between electrodes 5 and 6

V_1 - potential of electrode 1

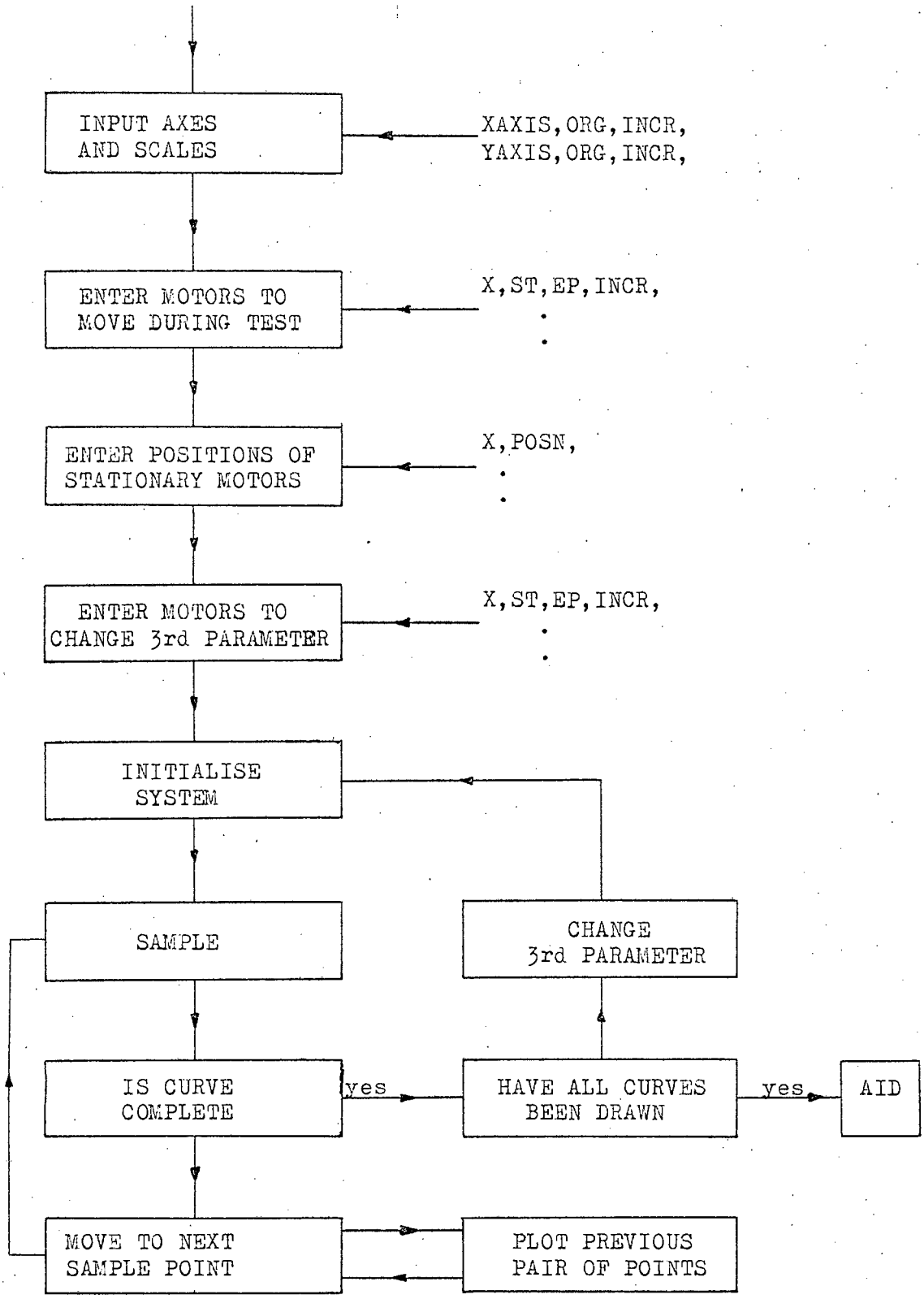

FIGURE 3.5 FLOW CHART OF OPERATION OF PARAMETER PLOT

V_2 - potential of electrode 2

V_3 - potential of electrode 3

V_4 - potential of electrode 4

V_5 - potential of electrode 5

V_6 - potential of electrode 6

V_7 - potential of probe

(b) The dynamic motors - these are the motors to be moved during the test. They are specified together with their starting positions, finishing positions and the interval between samples. All the distances are given in millimetres.

(c) The stationary motors - these are the motors to move to give a specified boundary condition e.g. the immersion of a particular electrode. They are identified together with their required position (in millimetres). Default condition leaves the system as it was.

(d) The third parameter - if a family of curves is desired the changes to be made between each curve must be specified. The motors to achieve this change must be given with start, end and increment values. Default condition gives only one curve.

With this information the computer takes over and initialises the model (using the INIT and MOVE

routines) and draws and scales the axes on the display screen. The test is carried out in much the same way as was the scan in (ii), except in this case two samples are taken at each specified point - one for each axis. Since the motors can only be moved once every ten milliseconds and it takes four steps to move one millimetre, the minimum time, between samples is forty milliseconds. This is a long time for the computer to sit in a loop and do nothing, so in this time the sample just taken is plotted on the screen and joined up to the rest of the curve. Hence one gets the curves drawn out as the data is collected. This could not be accomplished with the field scan, because the graphic output obtained from that data requires the whole field of values for calculation purposes.

When the line is complete i.e. the dynamic motors reach the endpoints, the PARAM routine re-initializes the system according to the instructions given in (d) and the next curve in the family plotted out.

3.2 DATA PRESENTATION

One of the biggest problems one is faced with in a project of this nature is how to display the information once one has it. The data represents a field varying in four dimensions - three directions and time, and the only

means of showing it is on a two-dimensional screen. The method adopted has been to show one plane at a time, and by superposition of the planes (usually mentally) one hopes to gain an idea of what is happening. Three types of plot have been developed for this purpose viz :

(i) Equipotential plot:-

this draws contours of equipotentials in a plane of a scalar field.

(ii) Vector plot:-

this draws the magnitude and direction (two dimensions only) in a plane of a vector field at discrete intervals.

(iii) Three-dimensional plot:-

this attempts to show the variation in two directions of magnitude of a scalar field over a certain plane.

(i) Equipotential Plot

The flow chart for this section is shown in Figure 3.6. The plane to be displayed as a series of contours (i.e. a semi-analogue representation) has been digitised and now resides in the core as a series of numbers. The operator can specify, via the teletype, the value of the equipotentials to be plotted and then it is the computer's job to work out the path these lines take and draw them

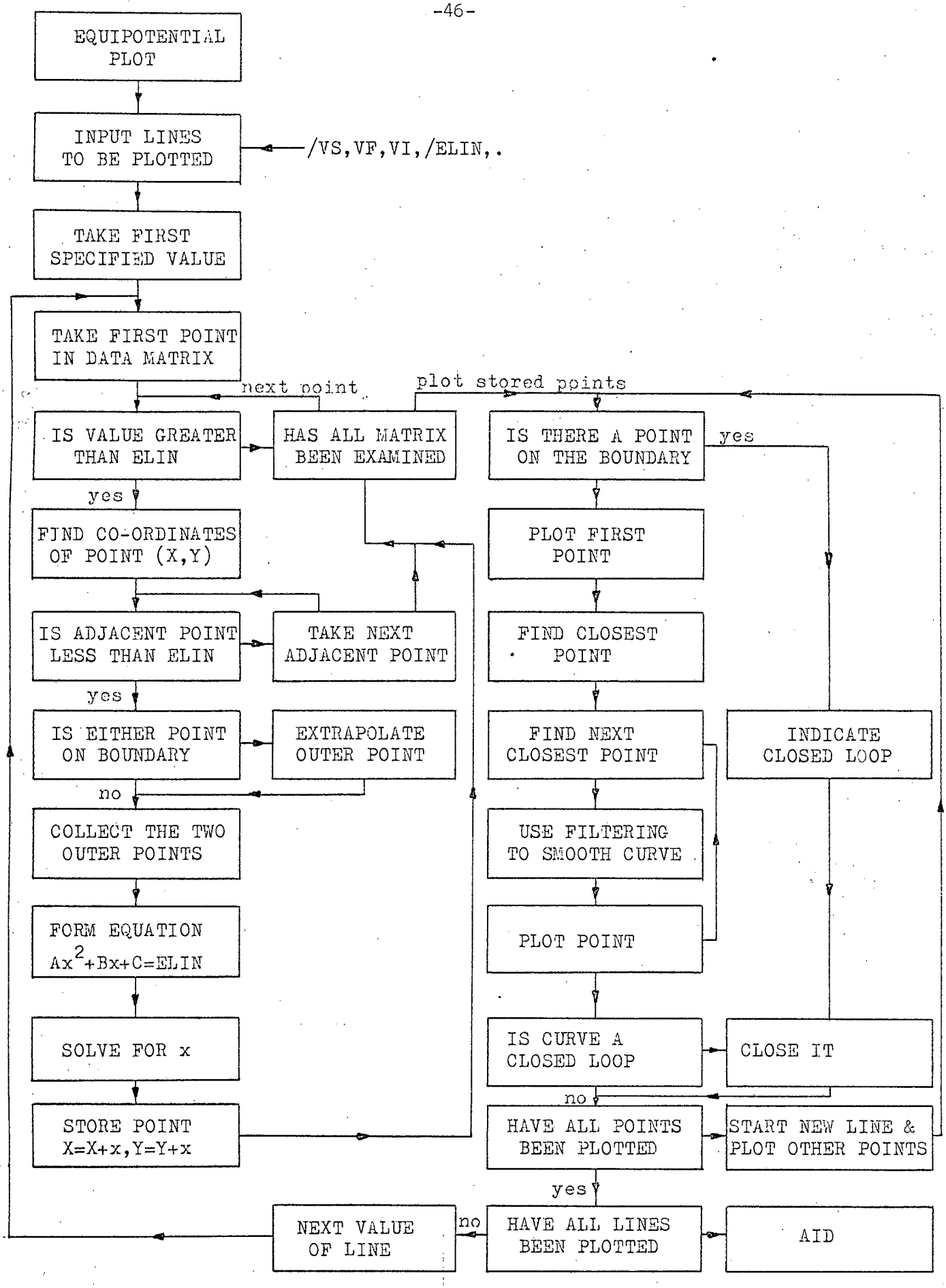

FIGURE 3.6 FLOW CHART OF ROUTINE TO MAKE EQUIPOTENTIAL PLOT

out on the screen. Obviously these contours will pass through points which were not on the 'cross hairs' of the scan and so were not sampled, thus some attempt at converting the digital representation back to an analog field must be made so that these locations can be found. This is done by using Bessel's interpolation technique which fits a parabola to four consecutive points in the array. From this the position of the desired potential can be calculated.

To save space in the core, each contour is calculated individually. Taking the first line, value say ELIN, the data array is scanned for a sample greater than this value. The surrounding eight points (See Figure 3.7) are examined for a value less than ELIN. If one is found, the contour must pass between these points, if not the computer continues its search through the array. Assuming two suitable points are found (A and B in Figure 3.7) the two outer points on a line drawn between these two (C and D) are taken and the best-fit parabola through these four points is calculated. From this the position of point E (the point where the curve equals ELIN) can be found and the X-Y coordinates of that location stored. This continues until all possible locations of ELIN on this finer grid are found. If any of the two inner points (A and B) happens to lie on the boundary

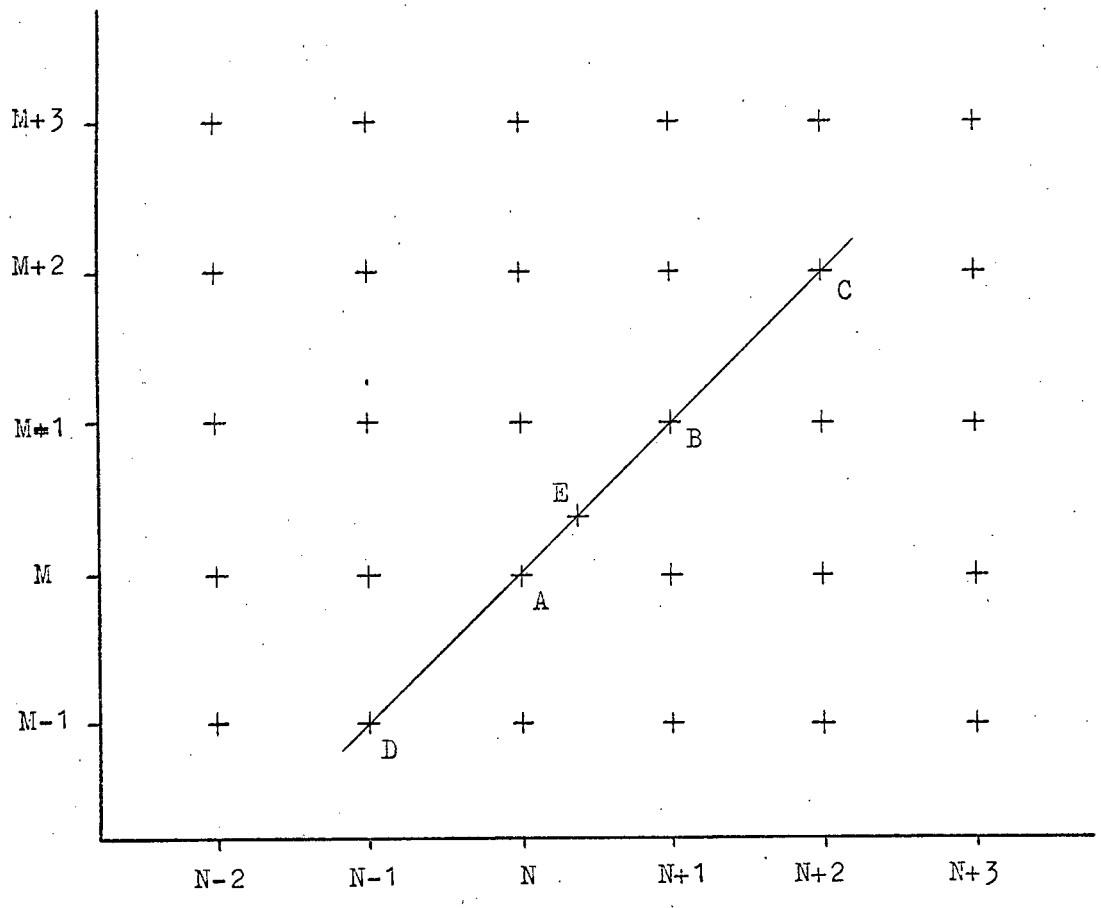

FIGURE 3.7 INTERPOLATION TECHNIQUE

THE POSITION OF THE REQUIRED VALUE IS FOUND BY FITTING A PARABOLA TO THE FOUR POINTS SHOWN AND INTERPOLATING.

POINT A > REQUIRED VALUE (ELIN)
POINT B < ELIN

of the matrix in such a way that one of the two outer points is undefined only the three available points are used, and the equation used is modified to account for this.

Once the points have been found they must be plotted and linked up in the correct sequence. The starting point should lie on a boundary - if not it must be a closed loop and so the last point will equal the first. Having found an origin, the program looks for the nearest point, within a certain radius, in the list made previously, and joins it to the first. This continues until the contour is completed and all the points plotted. This may necessitate more than one line. The rest of the contour values are then plotted.

This method of deriving the contours will give an accurate diagram of the field held as data, but as can be seen in Figure 3.8 is a very noisy plot. This can be attributed to the fact that when one changes from an analogue to a digital system the original field must be distorted in some way. Obvious causes of this distortion are rounding-off error (the data logger can only register in discrete levels) and inaccurate probe positioning. One can, therefore, be justified in filtering the output to get a cleaner picture. This can be done by con-

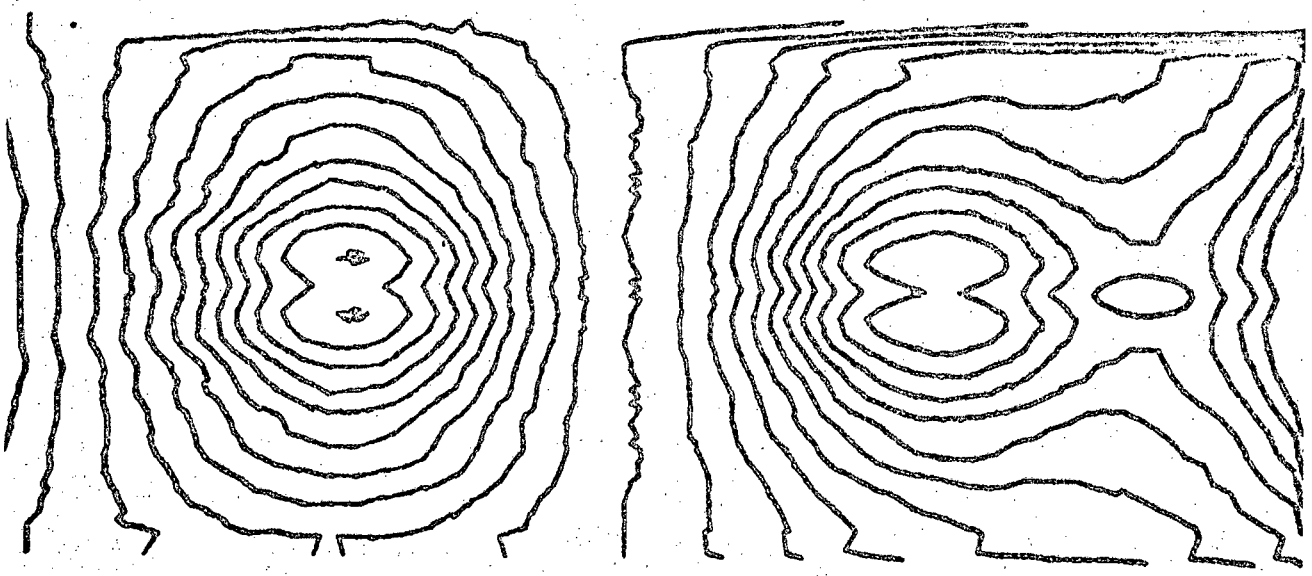

FIGURE 3.8(a) EQUIPOTENTIAL PLOT WITH NO SMOOTHING OF CONTOURS

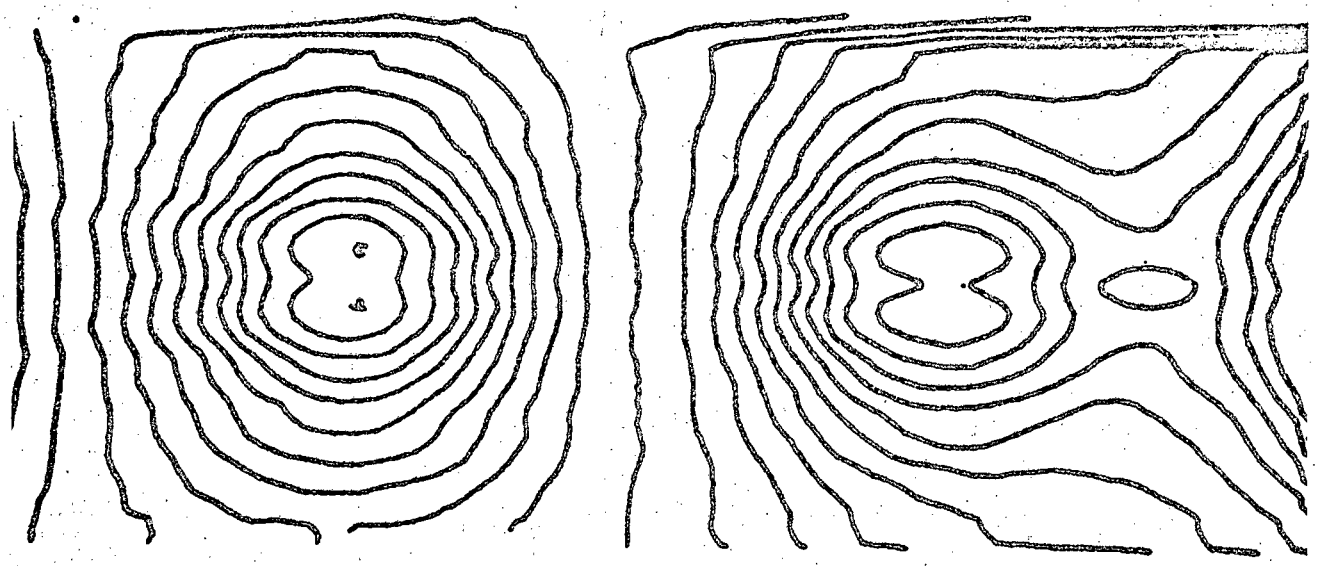

FIGURE 3.8(b) EQUIPOTENTIAL PLOT AFTER CONTOURS HAVE BEEN SMOOTHED

volving the noisy signal with the same function used to transform the analogue field to the digital field. This has been incorporated in the program and the effect can be seen in Figure 3.8(b). Note that the filter has no effect on the principle curves, only the noise.

(ii) Vector Plot

This display mode shows the gradient, or as good an approximation as is possible with a digital computer, of a scalar function on a plane through the field. The output medium unfortunately only permits one to show two of the components - those that lie in the plane being viewed.

The two components making up the vector are calculated for each point on the mesh imposed on the model. A picture of the field is then displayed by a series of lines indicating the magnitude and direction of the field at the point of origin. This, the origin, is marked with a cross. Figure 3.9 is an illustration of what this routine produces.

(iii) Dimensional Plot

If one has a series of curves representing the variation of a function along a set of parallel lines, and these curves are imposed on each other, but with the origin of each slightly displaced from the previous one, an image giving a perspective view of the function is obtained. This is what

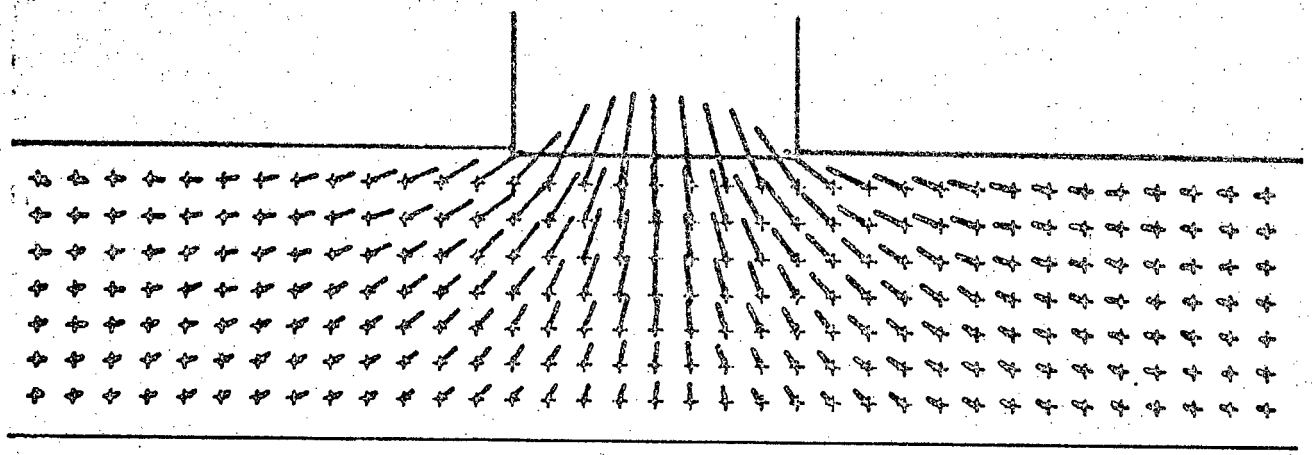

FIGURE 3.9 EXAMPLE OF A VECTOR FIELD PLOT

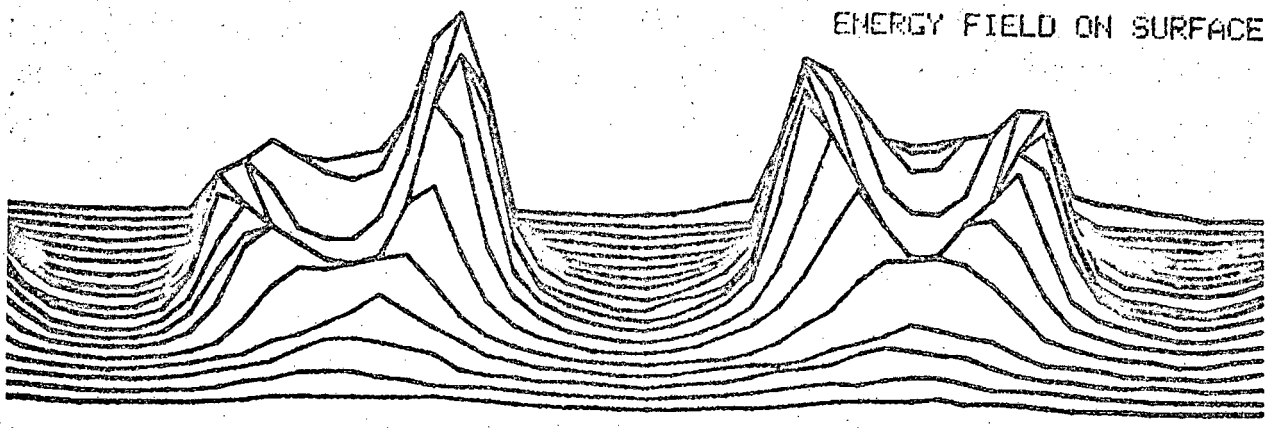

FIGURE 3.10 EXAMPLE OF A THREE-DIMENSIONAL FIELD PLOT

has been achieved with this display - an example is given in Figure 3.10. The magnitude of the function as it varies over a plane has been plotted.

3.3 DATA MANIPULATION

Using the routines in section 3.1 one can obtain an array of numbers representing the value of potential at any point in the model. This information, as such, is of no real importance, but from it one can obtain fields of a more useful nature by performing various mathematical operations on the whole matrix. These fields would be the electric field, from which one can easily derive the current distribution in the bath, and hence the power density distribution. From the energy field it should be possible to get some inclination as to what the temperature profile of the system should look like and from that a plot of the heat flow.

Section 3.2 describes how fields, held in a block of core memory, can be presented on paper. The purpose of this section is to explain the necessary interfacing between the two previous ones i.e. the transformation of data obtained in 3.1 to a matrix of values which can be used by 3.2.

The sampled field is stored as a series of vertical planes parallel to the X and Y axes (see figure 2.1). Because of space limitations in the computer memory, these have to be kept on magnetic-tape. Clearly, by selective readout, one can obtain from these readings a set of values

representing the field over any one of the three sets of planes parallel to the coordinate axes. A subroutine has been incorporated which does just this. Once one has the required plane stored in the correct block of core it can either be plotted out straight away (as an equipotential or perspective plot) or mathematically manipulated to give an associated field.

Since the model can only use small currents and the frequency of these is low (50 cycles) the magnetic fields produced will be negligible. Hence the system can be defined as a quasi-static case and the electric field vector ($\underline{E}$) can be obtained from the simple relation

$$\underline{E} = -\text{grad } V.$$

where V is the potential field already stored.
From Taylor's theorum, the difference equation to obtain the gradient can be obtained

$$f(x+h) = f(x) + hf'(x) + h^2 f''(x) \ldots\ldots$$

If terms in h^2 and above can be neglected, the result

$$f'(x) = \frac{f(x+h) - f(x)}{h}$$

is obtained. Using this the gradient

$$\underline{E} = \hat{\underline{x}}E_x + \hat{\underline{y}}E_y + \hat{\underline{z}}E_z$$

can be calculated, where

$$E_x = \frac{V_{x+1,y,z} - V_{x,y,z}}{h} \qquad E_y = \frac{V_{x,y+1,z} - V_{x,y,z}}{h}$$

$$E_z = \frac{V_{x,y,z+1} - V_{x,y,z}}{h}$$

For the vector plot 3.1(ii) only the two components in the plane are required.

From the electric field it is easy to plot the current distribution because, since the medium used is an homogeneous solution, the current is simply related to E by the equation

$$\underline{J} = \sigma \underline{E}$$

where $\underline{J}$ = current density

σ = conductivity of the electrolyte

To obtain the power density distribution the same routine is used. Power dissipation at a point can be calculated from

$$P = I^2R$$

Since I is linearly related to E this leaves the relation

$$P \propto E^2$$

Now the third component of the field vector cannot be ignored, so the plane above the one used previously must also be read off the magnetic tape so that Ey can be

calculated (assuming a horizontal plane is being used). From the three components it is a simple matter to obtain $P = E_x^2 + E_y^2 + E_z^2$ at each point and store it as a scalar field. This can then be displayed in any of the scalar forms.

Where the power is dissipated, the heat is generated. Hence the power distribution should be proportional to the temperature profile. So, if this field is differentiated again using the foregoing method and the resultant vector multiplied by the heat capacity of the system and then plotted out a map showing the heat flow in the particular plane being examined should be obtained. This will, of course, only hold if the medium is homogeneous, isotropic and at a steady state condition. In the actual furnace a lot of the energy is used in the reducing action and so does not appear as heat. However, if one can consider that the ratio of energy used for heating and reducing is constant, there should still be some correlation between the temperature profiles of the furnace and the model. An indication of the main reaction zones should also be seen.

The various instructions needed to shift the data in core to obtain the various outputs described are entered using a mini control routine. An example of the input instructions is given in Figure 3.12. The plane is specified by its direction and level no. (Figure 3.11) and the type of plot can be chosen from

C - contour plot

D - dimensional plot

E - energy plot

F - field plot

If an energy (E^2) plot is desired the processor calculates the field and then again requests the type of presentation.

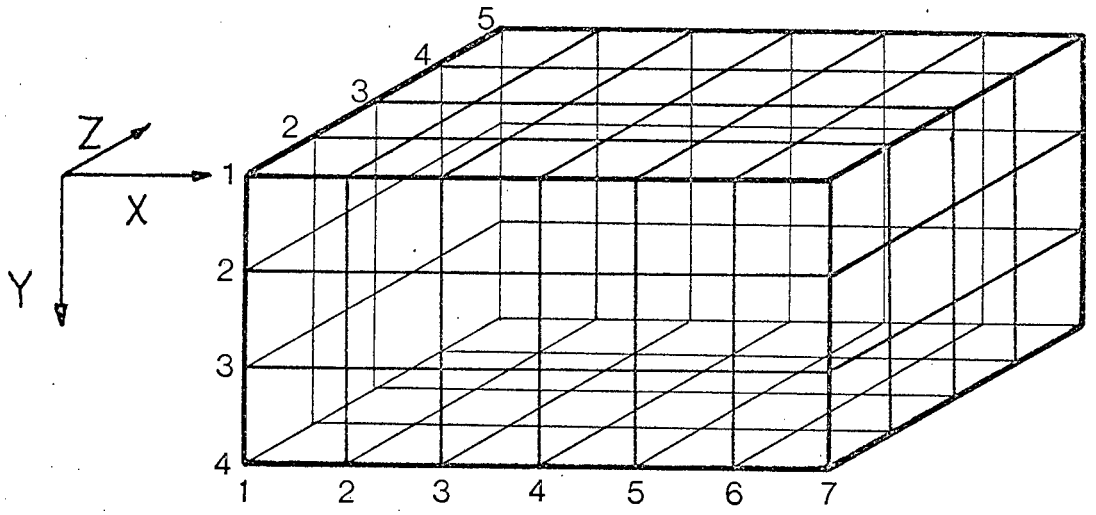

FIGURE 3.11 DIAGRAM TO INDICATE DEFINITION OF PLANES IN MODEL

```
UGIVE PLANE  XZ
PLANE NO,OF 0010:-3,
TYPE OF PLOT:-C
PLOT EQUIPOTENTIALS OF VALUE  /0,500,20,/.
```

FIGURE 3.12 EXAMPLE OF CONTROL STATEMENTS FOR DATA MANIPULATION

3.4 THE OPERATING SYSTEM

In order to make the program as versatile as possible there must be some way in which the operator can access any of the various routines i.e. he must be able to tell the computer which routines to run, when and in what order. To accomplish this the VARIAN general debug routine, AID, has been modified and used. The instructions used have been tabulated in table 3.1. Several seemingly unnecessary instructions have been added, but this is because a terminal was used to obtain the data. The graphs are plotted on a cathode-ray screen of a teletype. There are two such screens available, one at the terminal end and one at the computer end. To get a permanent copy of the display a hard-copy unit was used. This unit was connected to the teletype at the computer end. One cannot keep running backwards and forwards to make copies etc. so the graphs are drawn on both screens and the functions which are normally local modes of the teletype (e.g. make a copy, erase the screen) are executed using software initiated at the terminal end.

A further necessity needed, especially when operating a long way from the computer console, is the ability to interrupt the program at any stage. Say for instance something goes wrong, or incorrect instructions have been entered, there must be some way in which the operator can get back to the control program and make corrections. This has been incorporated and is initiated by pushing the two buttons, on the keyboard, Control and A.

A special routine has also been inserted for writing the data on magnetic tape, recording also the plane number and the scan dimensions.

3.5 PROGRAM LANGUAGE

All the programming done on the VARIAN computer was written in DAS - the standard VARIAN assembler language. A brief discussion of the instructions used in this language is given in Appendix D. The full listing of the programs has been included in the accompanying program file.

Symbol	
A	Display/change A register
B	Display/change B register
Cx	Display/change location x
Dx,y,	Dump on paper tape locations x to y inclusive
E	Erase both screens
F	Make a vector plot using data just sampled
Gx	Jump to location x
H	Make a permanent copy of the display
Ix,y,z	Insert z in locations x to y inclusive
J	Write a file mark on the magnetic tape
K	Reset all peripherals
L	Read in from paper tape
M	Jump to scan routine
N	Jump to parameter plot routine
O	Display/change overflow register
P	List all programs on the tape
Q	Jump to semi-local mode
R name	Read program name from magnetic tape
Sx,y,z	Search locations x to y for the word z
Tx,y	Trap to location y from location x
Ux	Select magnetic-tape unit x
V	Jump to data manipulation routine
W name	Write program name on magnetic tape
X	Display/change x register
Y	Jump to initialise routine
Z	Display from location x onwards

TABLE 3.1 MODIFIED AID INSTRUCTION SET

CHAPTER 4

A MATHEMATICAL MODEL

The physical model described in Chapter Two was an exact replica of a real furnace and a lot of useful information was gained from it. However it does suffer from several serious drawbacks because of its size and these may lead to distorted pictures as to what form the fields take in an operational furnace. The electrodes, for example, are only four centimetres in diameter in the model and the current distribution in them will be fairly uniform, but in the actual furnace these conductors are four feet in diameter and so, because of the skin effect, the current will tend to flow more in the outer regions of the electrode. The current density possible in the model is much lower than required - for a true scale model it should draw approximately three hundred amps. The highest achieved in the experiments was only twenty amps. This reduces the intensity of the magnetic fields and practically eliminates any effect they may have had. In an attempt to overcome these faults a mathematical formulation of the system was prepared in terms of the furnace's electrical properties and the current distribution obtained from this compared to the experimental results.

4.1 ELECTRO-MAGNETIC THEORY

The basis of the theoretical model lies in Maxwell's

electromagnetic equations which, in their most general form, can be stated as follows

$$\text{Curl } \underline{E} = -\frac{\partial \underline{B}}{\partial t} \qquad (1)$$

$$\text{Div } \underline{B} = 0 \qquad (2)$$

$$\text{Div } \underline{D} = \rho \qquad (3)$$

$$\text{Curl } \underline{H} = \underline{J} + \frac{\partial \underline{D}}{\partial t} \qquad (4)$$

The equation of continuity is also used viz :

$$\text{Div } \underline{J} = \frac{\partial \rho}{\partial t} \qquad (5)$$

where $\underline{E}$ = electric field (V/m)

$\underline{B}$ = magnetic induction (weber/m^2)

$\underline{J}$ = current density (amp/m^2)

ρ = free charge density (coulomb/m^3)

$\underline{D}$ = displacement vector (coulomb/m^2)

$\underline{H}$ = magnetic field (amp-turn/m)

$\underline{D}$ is defined by $\underline{D} = \varepsilon \underline{E} + \underline{P}$ where $\underline{P}$ is the polarization per unit volume. $\underline{H}$ is defined by $\underline{H} = (1/\mu)\,\underline{B} + \underline{M}$ where $\underline{M}$ is the magnetisation per unit volume. For a linear isotropic medium $\underline{P}$ and $\underline{M}$ are zero so

$$\underline{B} = \mu \underline{H} \qquad (6)$$

$$\underline{D} = \varepsilon \underline{E} \qquad (7)$$

$\underline{J}$ and ρ are the physically measurable quantities and $\underline{E}$ and $\underline{B}$ are the physical fields i.e. they can be interpreted as force per unit charge and thus have a physical meaning.

Also introduced to facilitate the solution of these equations are the fields V, the scalar potential, and $\underline{A}$, the vector potential. These arise from equation (2):-

$$\text{div } \underline{B} = 0$$

which implies that $\underline{B} = \text{curl } \underline{A}$ (8)

where $\underline{A}$ can be uniquely defined by specifying div $\underline{A}$.

From (1) $\text{curl } \underline{E} = \frac{-\partial \underline{B}}{\partial t} = -\frac{\partial(\text{curl } \underline{A})}{\partial t}$

which implies $\text{curl}\left(\underline{E} + \frac{\partial \underline{A}}{\partial t}\right) = 0$ (9)

which implies $\underline{E} + \frac{\partial \underline{A}}{\partial t} = -\text{ grad } V$

where V is uniquely defined to within an arbitrary constant. The scalar potential, V, is the generalisation of the electrostatic potential which is obvious if one sets $\frac{\partial \underline{A}}{\partial t} = 0$ in equation (9)

Both V and $\underline{A}$ can be proved unique by the uniqueness theorum which is described in most of the literature on electromagnetic fields.

From these equations a completely general set of boundary conditions can be obtained for the interface between any two media (Reference 20). These can be written

$$\underline{n} \times (\underline{E}_2 - \underline{E}_1) = 0 \qquad (10)$$

$$\underline{n} \cdot (\underline{B}_2 - \underline{B}_1) = 0 \qquad (11)$$

$$\underline{n} \cdot (\underline{D}_2 - \underline{D}_1) = \rho_s \qquad (12)$$

$$\underline{n} \times (\underline{H}_2 - \underline{H}_1) = \underline{J}_s \qquad (13)$$

where $\underline{n}$ is the unit vector normal to the junction plane, ρ_s is the surface charge density and $\underline{J}_s$ is the surface current density. The subscripts 1 and 2 refer to the different media.

A further useful boundary condition can be obtained from the continuity equation (5) (Reference 19)

$$\underline{n} \cdot (\underline{J}_1 - \underline{J}_2) = \frac{\partial \rho}{\partial t} \qquad (14)$$

Classes of Problem:

Electromagnetic problems can usually be classified in one of two ways depending on the frequency of time variation (assuming harmonic fields). These are the static case and the radiation case. The difference arises in the approximations made to reduce the equations to a soluble form, and the accuracy of these solutions will depend on the frequency of operation.

For the radiation problem the high frequencies involved necessitate consideration of retarded potentials. For the static case curl $\underline{E} = 0$ since $\frac{\partial \underline{B}}{\partial t} = 0$ and so $\underline{E}$ can be defined in terms of a scalar potential. In the problem of the furnace, although the time varying term cannot be ignored completely (since the currents are very large, $\underline{B}$ will have a significant value) because of the low frequency used (fifty cycles) the idea of a retarded potential can be disregarded completely. This will only be meaningful if the ratio $^{c}/_{f}$ (where c = velocity of light and f =

frequency of operation) is of the order of the dimensions of the apparatus. In this case c/f is approximately six thousand kilometers whereas the furnace has a maximum dimension of thirty meters. The problem, then, seems to be a quasi-static case - in which the term $\frac{\partial \underline{B}}{\partial t}$ is not entirely ignored.

Assumptions For Furnace Model

Maxwell's equations, as set out above, are completely general and can be used to solve any problem. However, to obtain a unique solution for any particular situation the boundary conditions must be specified. For a mathematical treatise of the fields in an arc furnace certain assumptions pertaining to its structure and the materials of which it is composed must be made in order to reduce it to something simple enough to be solved. Many of these were assumed when making the physical model (Chapter Two).

The Furnace Walls : these are assumed to be vertical and to be made of non-conductive material. In practice, at the high temperatures involved, the walls may be slightly conductive and the transition from molten slag to solid wall will not be sharply defined. A solid layer of slag will form on the wall and give a slight taper to the bath. However, the current density in this area is small and the percentage error introduced by this approximation will be less than the general accuracy of the solution.

The Slag : this is assumed to be a layer of homogeneous, isotropic material in which all current flow is by conduction. The justification for this approximation was discussed in Chapter Two. The surface is a horizontal plane in contact with the air. Similarly the bottom of this layer forms a horizontal boundary with the matte. In a real furnace, the upper boundary will be more or less horizontal, but since the majority of the reaction takes place below the electrodes the actual surface shape is not too critical. The level slag-matte interface is also postulated by other workers in this field (Loe, Figure 1.3).

The Electrodes : these are considered to be circular rods with a plane base projecting into the slag. Any taper of the sides or rounding-off of the base is ignored.

Conductivity of Materials : the matte and the electrodes are assumed to be perfect conductors compared to the slag (the ratio of the conductivities is less than 0.004). This greatly simplifies the boundary conditions. The slag is taken to be a conductor with uniform specific conductivity, σ, throughout its volume. This has been measured as approximately 0,25mhos/cm. The raw material lying in a layer on top of the slag is of a porous nature and as such has been assumed to have the electrical and magnetic properties of free space. Hence it has been ignored in the model.

Motion of Contents : the material in the model furnace has been defined to be static. In the real furnace there will

be a stirring effect caused by the rotating magnetic fields and a flow towards the tap-holes, but this is very slow compared to the frequency of operation and will not affect the solution.

4.2 THE STATIC PROBLEM

It is required to determine the current distribution in the bath of the furnace. This can be obtained from the vector formulation of Ohm's law

$$\underline{J} = \sigma \underline{E}$$

since the slag has been assumed to have a uniform conductivity. Hence a means of calculating the electric field, $\underline{E}$, within the furnace boundaries must be found.

For the static case all time derivatives are equal to zero and so the term $\frac{\partial B}{\partial t}$ in Maxwell's first equation will fall away. If simulating the physical model described in Chapter Two this will be a very reasonable assumption since both the magnetic fields and the frequency are low. Hence equation (1) reduces to

$$\text{Curl } \underline{E} = 0 \quad \text{which implies} \quad \underline{E} = -\text{grad } V \qquad (15)$$

Since the contents of the furnace have been assumed to be conductive no charge is expected to build up and so the free charge density, ρ, will equal zero. Thus from equation (3)

$$\text{div } \underline{D} = 0 = \varepsilon \text{ div } \underline{E} \quad \text{(since the slag is homogeneous)}$$

$$\text{i.e. div } \underline{E} = 0$$

which on substitution in equation (15) gives

$$\underline{\nabla^2 V = 0} \qquad \text{(La Place's equation)}$$

Having established an equation which describes the system, one must now find boundary conditions so that a unique solution for the specific problem can be obtained.

(a) The Floor of the Furnace

The floor of the furnace is covered with a layer of molten metal - the matte - which has been assumed to be a perfect conductor. Hence it cannot sustain an electric field and so must be at an equipotential. Since the potential field is only defined to within an arbitrary constant it is convenient to specify the potential of the matte as zero.

(b) The Electrodes

These too have been assumed perfect conductors and so will also be areas of equipotential. The value is specified as the potential difference or voltage of the electrode with respect to the matte.

(c) The Air-Slag Boundary

This is more difficult to define and must be specified in terms of the gradient of the field. Firstly, from the boundary condition given in equation (10) the tangential component of the electric field must be continuous across the boundary. Hence

$$\underline{E}_{t1} = \underline{E}_{t2}$$

For the normal component, equation (14) is used. Since time deriviatives are zero this reduces to $\underline{n}.(\underline{J}_1-\underline{J}_2)=0$ i.e. the normal component of the current density is continuous. The air does not conduct any current hence $\underline{J}_n$ must equal zero. Since the slag has been assumed to be entirely ohmic, $\underline{J} = \sigma\underline{E}$ and σ is non-zero, the only solution is $\underline{E}_n = 0$. Hence for the slag-air boundary :

$$\underline{E}_{n1} = \underline{E}_{n2} = 0$$

$$\underline{E}_{t1} = \underline{E}_{t2} \qquad \text{where } \underline{E} = -\text{grad } V$$

(d) The Wall-Slag Interface

The same boundary conditions apply at this junction as in (c) since the walls are assumed to be non-conductors, and the conductivity is the only condition peculiar to the interface.

This completes the mathematical description of the furnace for the static case. An equation has been derived which describes the fields in an area for which boundary conditions can be defined. The means of solution is described in Chapter 5.

4.3 THE QUASI-STATIC CASE IN TERMS OF POTENTIALS

A very useful relationship was obtained for the static case using the potential fields. This suggests that a similar treatment of Maxwell's equations, but this time not ignoring the time dependent terms, might yield a better

approximation to the fields in the furnace. In terms of potentials, Maxwell's equations become

$$\underline{E} = -\text{grad } V - \frac{\partial \underline{A}}{\partial t}$$

$$\underline{B} = \text{curl } \underline{A}$$

$$\text{div } \underline{D} = \rho$$

$$\text{curl } \underline{H} = \underline{J} + \frac{\partial \underline{D}}{\partial t}$$

For the problem in question the medium is an homogeneous, isotropic conductor, and all time variations are harmonic i.e. $\underline{E}(r,t) = \underline{E}(r)e^{j\omega t}$

Hence the above equations can be further simplified to

$$\underline{E} = -\text{grad } V - j\omega \underline{A} \qquad (16)$$

$$\underline{B} = \text{curl } \underline{A} \qquad (17)$$

$$\text{div } \underline{E} = 0 \qquad (18)$$

$$\text{curl } \underline{H} = \sigma \underline{E} + j\omega\varepsilon \underline{E} \qquad (19)$$

Since the slag has a fairly high conductivity (approximately 0.25 mhos/cm) and the frequency of operation is low (fifty cycles per second)

$$\sigma >> \omega\varepsilon \qquad (\omega\varepsilon \text{ is approximately } 3 \times 10^{-9} \text{ mhos/cm})$$

so the last term in equation (19) can be ignored.

The divergence of $\underline{A}$ must also be specified to define it uniquely. The Lorentz gauge is the most convenient to use and is given by $\text{div } \underline{A} = -\mu\varepsilon' \frac{\partial V}{\partial t}$ where $\varepsilon' = \varepsilon + \frac{\sigma}{j\omega} \simeq \frac{\sigma}{j\omega}$ is the effective permittivity of the medium in the problem.

From equation (16)

$$-\text{grad } V = \underline{E}+j\omega\underline{A} \quad \rightarrow \quad \text{div } (-\text{grad } V) = \text{div } (\underline{E}+j\omega\underline{A})$$

$$\rightarrow \nabla^2 V = -j\omega \text{div} \underline{A} \qquad (\text{since div } \underline{E}=0)$$

$$\underline{\nabla^2 V = j\omega\mu\sigma V} \qquad (20) \quad (\text{from Lorentz gauge}).$$

Also, from equation (19)

$$\text{curl } \underline{B} = \mu\sigma\underline{E} \quad \rightarrow \quad \text{curl } (\text{curl } \underline{A}) = \mu\sigma\underline{E}$$

$$\rightarrow \nabla(\text{div}\underline{A}) - \nabla^2\underline{A} = -\mu\sigma(\text{grad } V + j\omega\underline{A})$$

$$\underline{\nabla^2\underline{A} = j\omega\mu\sigma\underline{A}} \qquad (21) \quad (\text{from Lorentz gauge}).$$

Thus the fields in the furnace can be described by equations involving the potentials. However, to solve these equations, boundary conditions must be specified, and in this case neither of the potentials can be identified with any physically measurable quantities of the furnace. Hence a further formulation, this time in terms of physical fields, must be made.

4.4 MATHEMATICAL FORMULATION IN TERMS OF FIELDS

Since the aim of the model is to determine the current distribution in the slag of the furnace, the required field is the electric field since this is linearly related to current density by Ohm's law. This quantity can also be physically measured on the furnace so defining boundary conditions should present no problem. Hence a formulation in terms of $\underline{E}$ is sought.

Again, starting with Maxwell's equation (4)

$$\text{curl } \underline{H} = \underline{J} + \frac{\partial \underline{D}}{\partial t}$$

Since there is no charge accumulation in the slag, displacement currents can be taken as zero

Hence $\text{curl } \underline{H} = \underline{J}$

$\rightarrow$ $\text{curl } \underline{B} = \mu\sigma\underline{E}$ (homogeneous medium).

From Maxwell (1)

$$\text{curl } \underline{E} = \frac{-\partial \underline{B}}{\partial t} = -j\omega\underline{B} \qquad \text{(assuming harmonic fields)}$$

Thus $\text{curl (curl } \underline{E}) = -j\omega \text{curl } \underline{B}$

$$\underline{\text{curl (curl } \underline{E}) = -j\omega\mu\sigma\underline{E}} \qquad (22)$$

The boundary conditions have still to be defined in order to uniquely specify the problem. Several of these can be obtained from the static case (4,2) where the condition specified a gradient continuity. The boundary conditions used are :-

(a) On the walls

$\underline{E}_t$ is continuous across the boundary

$\underline{E}_n = 0$ since current is continuous across a boundary and is equal to zero in the wall

(b) In the electrodes

The assumption that the electrodes are perfect conductors can now be waived as the boundary condition can be specified in terms of current. Axial current flow is assumed and the non-uniform current distri-

bution due to the skin effect can be taken into account. Hence

$$E_{axial} = E_{in} \qquad \text{(proportional to current flow)}$$

$$E_{radial} = 0$$

(c) The Air-Slag Interface

The same conditions apply as in the static case i.e.

$\underline{E}_t$ is continuous across the boundary

$\underline{E}_n = 0$ since current must be continuous

(d) The Slag-Matte Interface

The matte is assumed a perfect conductor i.e. $\underline{E}$ cannot exist in it. Since $\underline{E}_t$ is continuous across the boundary, $\underline{E}_t = 0$. For the normal component, $\underline{E}_n$, the continuity equation, $\text{div}\underline{J}=0$, is used. Since $\underline{E}_t=0$ this leaves only the normal component

$$\text{i.e.} \quad \frac{\partial \underline{J}_n}{\partial n} = 0 = \sigma \frac{\partial \underline{E}_n}{\partial n} \qquad \text{(since homogeneous)}$$

Hence the boundary conditions for this interface are

$$\underline{E}_t = 0$$

$$\frac{\partial \underline{E}_n}{\partial n} = 0$$

Skin Effect in the Electrodes

To complete the boundary conditions for the model defined in terms of $\underline{E}$, the current distribution in the

electrodes must be calculated. If the electrodes are taken as long cylindrical rods, in which all current flow is axial the current density $\underline{J}$ is given by (Reference 2 1)

$$\underline{J}(r) = \frac{jmI}{2\pi R} \frac{\text{ber}(mr) + j\,\text{bei}(mr)}{\text{ber}'(mR) + j\,\text{bei}'(mR)} \qquad (23)$$

where

R = radius of conductor

r = distance from axis of conductor

$m^2 = \omega\mu\sigma$ (properties of electrode)

I = total current flowing through electrode

ber (x) and bei (x) are the Kelvin functions and the prime denotes differentiation.

CHAPTER 5

SOLUTION OF THE EQUATIONS

Determination of the fields in the furnace is now merely a matter of solving the equations derived in the previous chapter. Ideally one would like to obtain an analytical solution. Using this the effect of varying the different parameters e.g. electrode size, electrode spacing, current input, crucible dimensions etc., could be studied and the results obtained used for improving, or maybe merely proving, present design. However the complexity of the system and the geometric awkwardness of the boundaries of the model make this impossible, so one has to resort to using numerical approximations to the answer. These solutions may still be used to study the effect of varying parameters, but instead of merely changing a variable in an equation to obtain the curve, the whole field must be recalculated for each change and the graph plotted using these results. The accuracy of the solution will depend on the computer facilities available and the validity of the assumptions made in deriving the equations.

There are several means of solving partial differential equations numerically, the most common being that of the method of finite differences. In this case the differential calculus, $\frac{\partial V}{\partial x}$, is replaced by difference calculus, $\frac{\delta V}{\delta x}$, where δx is a small but finite change in x. A grid is drawn over the

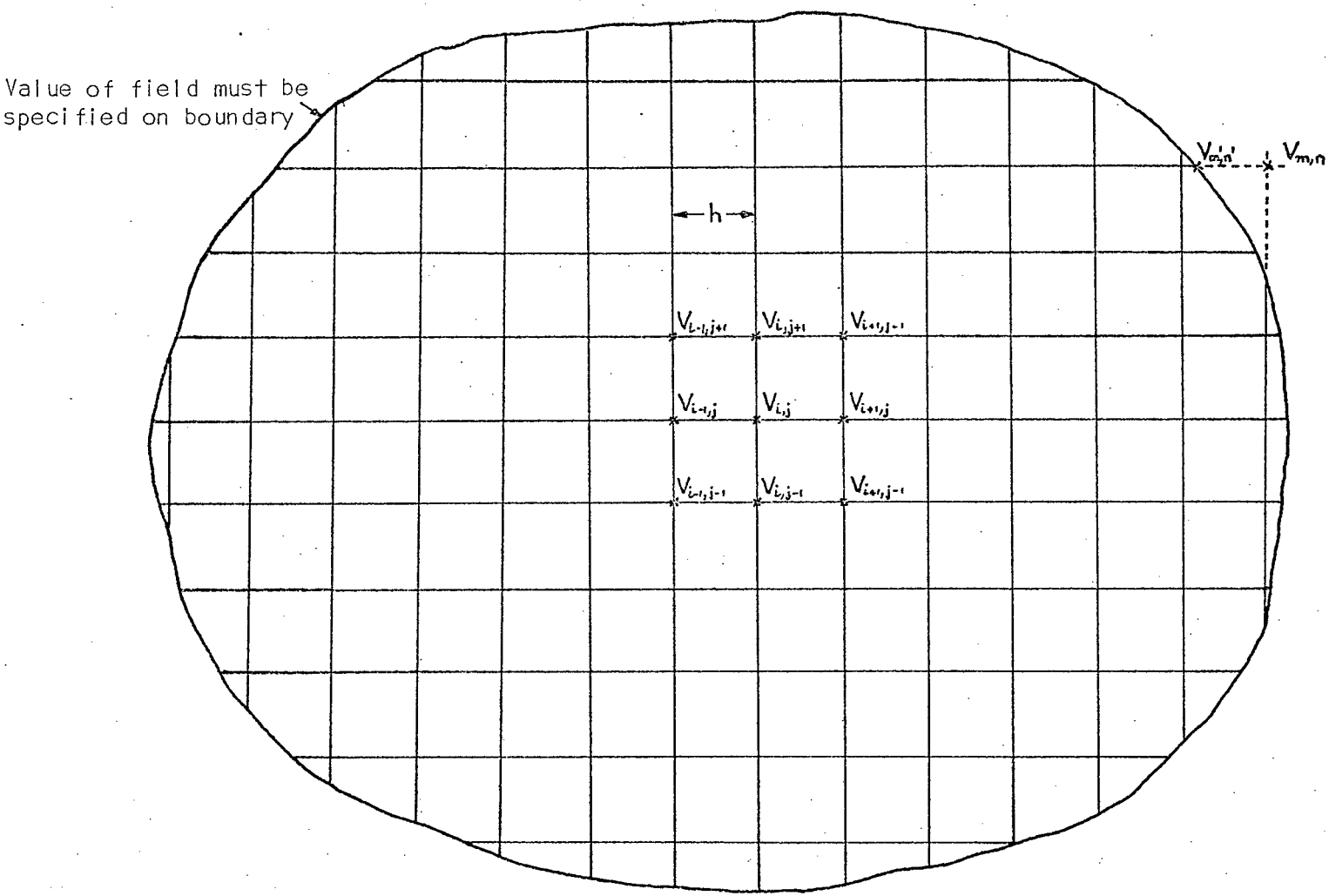

FIGURE 5.1 A BOUNDED AREA WITH IMPOSED MESH NECESSARY FOR SOLUTION OF EQUATIONS BY NUMERICAL MEANS

bounded area in which the field is required (Figure 5.1) and the difference equation at each nodal point is formed. This gives a set of N linear equations in N unknowns. Simultaneous solution of this set now gives a numerical approximation to the answer. However, to obtain any reasonable accuracy a fairly fine grid must be used which implies a large number of nodal points and a correspondingly massive matrix to be solved. Because of limited core-storage on the computer it is more convenient to solve these linear equations iteratively, such as by the Gauss-Seidel iterative method in the form of a relaxation.

5.1 THE METHOD OF SUCCESSIVE OVER-RELAXATION

In a relaxation process the answer is obtained by a series of iterations, each cycle using the result of the previous one to obtain a better approximation. In the first cycle, an estimate of the value of the function at each point on the grid (Figure 5.1) is made ($\underline{x}^{(o)}$). Then, using the difference equation relevant to the problem (in general $\underline{A}\underline{x} = \underline{B}$) the error at each point, or residual vector $\underline{r}$, is calculated and reduced to zero by making appropriate changes to the value of one or more of the components of $\underline{x}$. These changes are called relaxations. Obviously each change in $\underline{x}$ affects some or all of the remaining residuals which must then be recalculated. The process is repeated until the required accuracy is obtained. In general, for the n^{th} iteration

$$\underline{r}^{(n)} = \underline{B} - \underline{A}\underline{x}^{(n)}$$

and then $\underline{x}^{(n+1)} = \underline{x}^{(n)} + \underline{r}^{(n)}$

As an example of this technique take the solution of La Place's equation in two dimensions. The difference equation is derived using Taylor's expansion

$$f(x+h) = f(x) + hf'(x) + h^2f''(x)/2! \ldots.$$

$$f(x-h) = f(x) - hf'(x) + h^2f''(x)/2! \ldots.$$

Adding and rearranging

$$f''(x) = (f(x+h) + f(x-h) - 2f(x))/h^2$$

with an error of order h^4

Applying this to the problem in question at the point (i,j) (Figure 5.1)

$$\nabla^2 V = \frac{\partial^2 V}{\partial x^2} + \frac{\partial^2 V}{\partial y^2}$$

$$= \frac{V_{i+1,j} + V_{i-1,j} + V_{i,j+1} + V_{i,j-1} - 4V_{i,j}}{h^2} = 0$$

Substituting the values for V the residual can be calculated as

$$R_{i,j} = V_{i+1,j} + V_{i-1,j} + V_{i,j+1} + V_{i,j-1} - 4V_{i,j}$$

If $V_{i,j}$ is now increased by $R_{i,j}/4$ the residual at point (i,j) will be reduced to zero and the residuals at the surrounding

points will be increased. At the boundaries this simple relationship may not hold since one or more of the points referenced may lie beyond the border line (e.g. point (m,n) in Figure 5.1). In this case the value of the point where the grid cuts the boundary line is taken (point (m',n')) and the difference equation readjusted to account for this change in position. Using many iterations the required field can be calculated to quite a high degree of accuracy.

The rate of convergence of this simple relaxation scheme can be considerably improved by means of the successive over-relaxation method. Instead of reducing the residual at each point to zero every cycle it is over-relaxed according to the equation

$$\underline{x}^{(n+1)} = \underline{x}^{(n)} + \alpha \underline{r}^{(n)}$$

where α is termed the relaxation factor. It can be proved (Reference 25) that the S.O.R. method of solving equations is convergent for $0<\alpha<2$, but normally α will lie in the range 1 to 2. If it is less than 1 the process is called under-relaxation. The optimum value of α for maximum rate of convergence is difficult to calculate and depends on the size and shape of the boundary. A rough figure can be obtained from one of the few proposed formulae (Reference 24) and then refined using a trial and error method. The actual value is quite critical - a change in α of 0.05 can halve the number of relaxations required to obtain a specified accuracy.

5.2 SOLUTION OF THE STATIC EQUATION.

The first mathematical model proposed was for the static case and can be expressed as La Place's equation. The furnace as described to the computer is shown in Figure 5.2. To save computer time and space only a single phase 'furnace' has been modelled and this only in two dimensions - a vertical plane through the axes of the two electrodes. In this plane there should be no z-component of current (where the z direction is perpendicular to the plane of the page) due to the symmetry of the system. Only one plane should be necessary to attempt a correlation with the field obtained in the physical model. From the real system it was found that, for the static case at any rate, the three phase furnace could be viewed as three single phase furnaces lumped together. The field for the polyphase system could be derived by simply summing the fields for the individual phases. This suggests a similar approach for the mathematical model - three sets of values are obtained, taking into account the different instantaneous voltages and electrode positions for the three phases, and are then summed algebraicly to give the desired result.

The programme developed has been written so as to be as general as possible. The various dimensions of the furnace as shown in the diagram can be changed using the first data card. The second data card specifies the mesh spacing (h) and the required accuracy of the solution, and the final data card dictates the depths of immersion and voltages

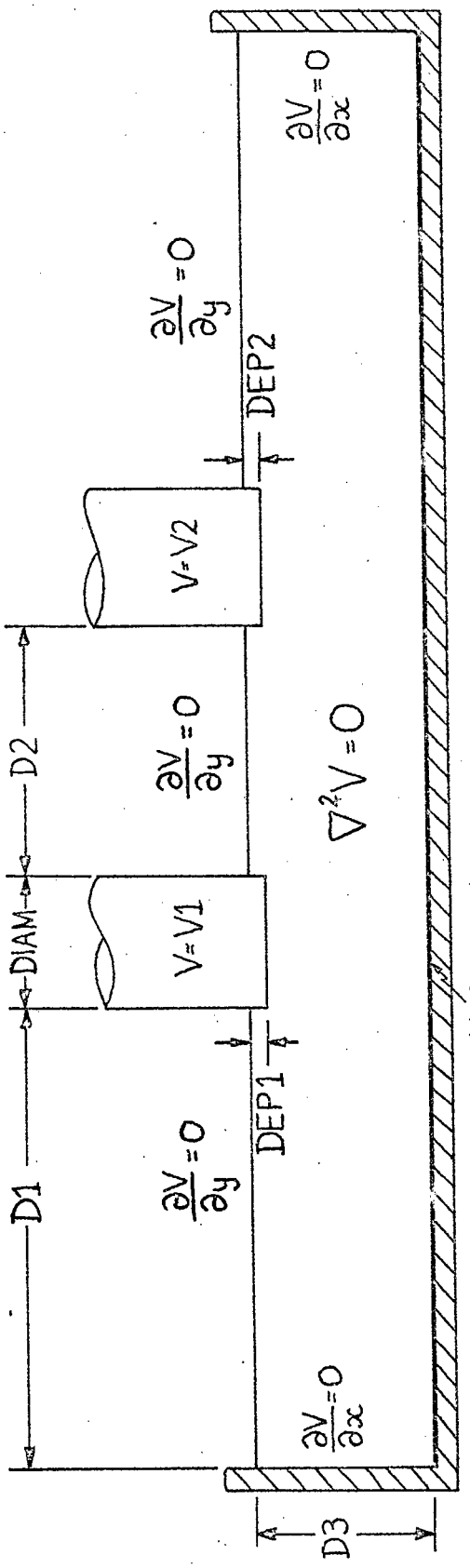

FIGURE 5.2 THE FURNACE AS DESCRIBED BY THE COMPUTER MODEL DEFINED IN TERMS OF THE SCALAR POTENTIAL V

of the two electrodes. Since the electrodes may not be submerged to the same depth there is no general symmetry to the boundaries so the whole field must be calculated. The program and flow-chart has been included in the program file.

The first task of the computer is to set up the boundaries and their associated boundary conditions and estimate the field. This estimate can either be the result from the previous field calculation (stored on tape) or is made zero everywhere. Once the system has been defined the job of solving the particular problem is tackled. The difference equation used in the relaxation process is the one derived in the previous section, and the over-relaxation factor was set at 1,72. Theoretically the order in which the residuals are relaxed should affect the speed of convergence - the highest residual being reduced first. However the computer takes more time finding the largest value than it does to relax the whole field once, so a systematic relaxation is used. When the required accuracy has been obtained a further relaxation is carried out, this time using a more accurate difference equation in that nine points are involved in its formulation. Again it is derived from Taylor's series, this time taking the expansion further to higher powers. Referring again to Figure 5.1, and defining

$$V_1 = V_{i+1,j} + V_{i-1,j} + V_{i,j+1} + V_{i,j-1}$$

$$V_2 = V_{i+1,j+1} + V_{i+1,j-1} + V_{i-1,j+1} + V_{i-1,j-1}$$

the nine point difference equation can be written (Reference 25)

$$\nabla^2 V_{i,j} = \frac{4V_1 + V_2 - 20V_{i,j}}{6h^2} = 0$$

The error in this case is of the order h^6

Once the potential field has been established it is a small matter for the computer to calculate an approximation to the electric field. This is then printed out and plotted.

5.3 SOLUTION OF THE FIELD EQUATION.

The second model, defined in terms of electric field, can be stated as curl (curl $\underline{E}$) = $-j\omega\mu\sigma\underline{E}$. This can be expanded giving

$$\nabla^2\underline{E} - \nabla(\text{div } \underline{E}) = j\omega\mu\sigma\underline{E}$$

In the slag there is nó free charge density so div $\underline{D}$ and hence div $\underline{E}$ will equal zero. The equation reduces to

$$\nabla^2\underline{E} = j\omega\mu\sigma\underline{E} \quad (24) \text{ consistent with div } \underline{E} = 0$$

The boundary and the relevant boundary conditions presented to the computer have been shown in Figure 5.3. Again only a two dimensional field with two electrodes was simulated. The value of EIN at any point in the electrode will depend on the size of the conductor, the specified input current, the conductivity of the electrode and the frequency of the supply, and is calculated from equation (23). Just how much the size of the components affect the current distribution can be seen in Figure 5.4 where two cases have been calculated. The first is for a 4cm electrode (i.e. the model electrodes) and the current can be seen to be uniform through-

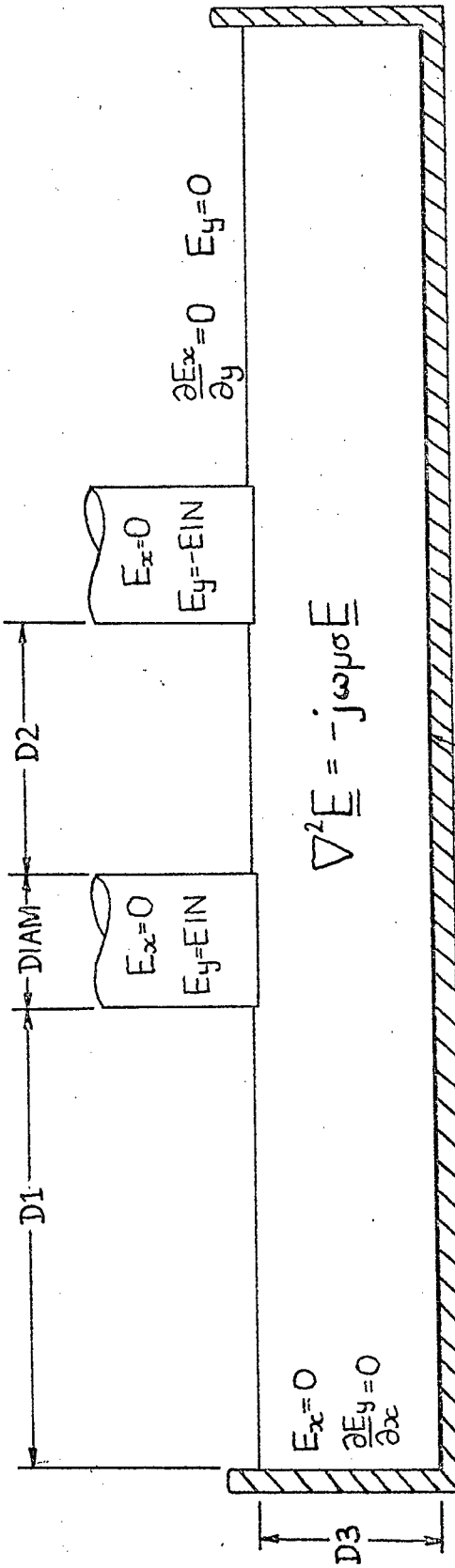

FIGURE 5.3 DIAGRAM SHOWING THE BOUNDARY CONDITIONS OF THE MODEL FURNACE SIMULATED ON THE COMPUTER IN TERMS OF ELECTRIC FIELD

out. For the second plot, a 1.2m diameter electrode was used (this is the size of the real electrode). The field can be seen to be far from uniform, and a phase displacement is introduced.

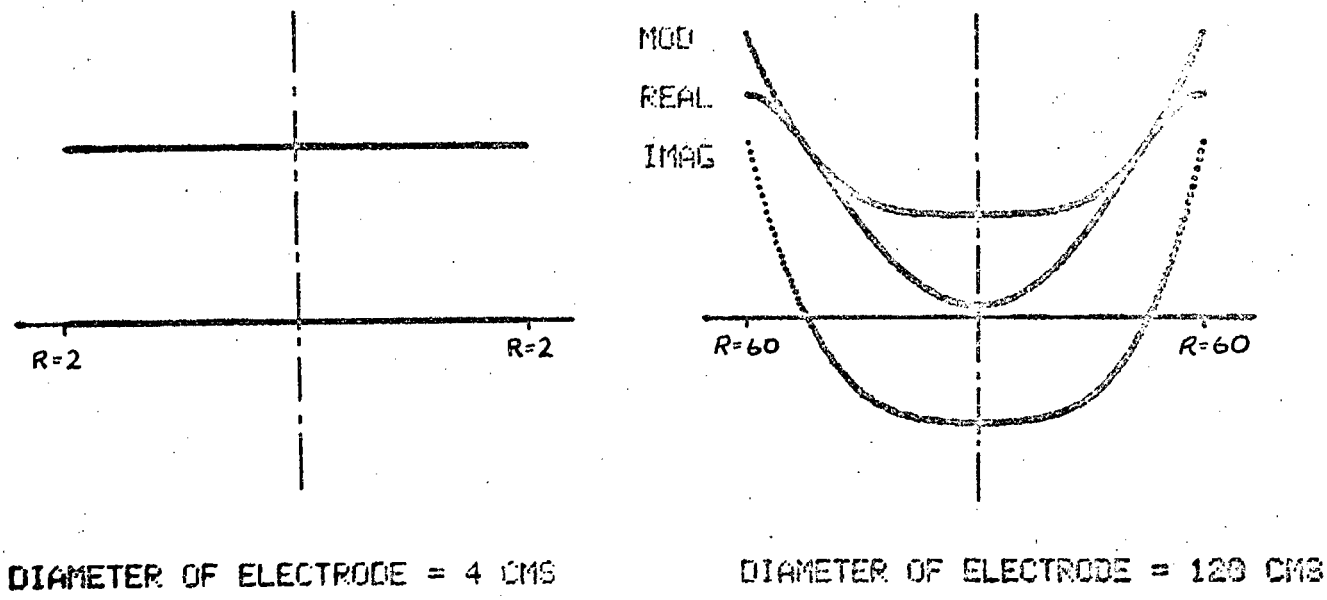

FIGURE 5.4 EFFECT OF CONDUCTOR SIZE ON CURRENT DISTRIBUTION

Solution of the field equation (24) was not as easy as it would first appear, because the condition that div $\underline{E}$ = 0 over-specifies the problem. There are effectively three equations (because $\underline{E}$ is a vector, equation (24) can be considered as two independent equations) and only two unknowns (the two components of $\underline{E}$). A lot of time was spent trying to solve equation (24) by brute force, with little success. Then an analogy was made to the magnetic case where a vector potential was formed. Since div $\underline{E}$ = 0 (in the area where the solution is required viz : the slag) a vector potential $\underline{T}$ may be defined where $\underline{E}$ = curl $\underline{T}$. For the two dimensional

case $E_z = 0$ and $\frac{\partial}{\partial z} = 0$ and so this reduces to

$$\underline{E} = \hat{\underline{x}} \frac{\partial T_z}{\partial y} - \hat{\underline{y}} \frac{\partial T_z}{\partial x} \qquad (25)$$

Substituting this into equations (24)

$$\nabla^2 \underline{E} = \hat{\underline{x}} \frac{\partial}{\partial y}\left(\frac{\partial^2 T_z}{\partial x^2} + \frac{\partial^2 T_z}{\partial y^2}\right) - \hat{\underline{y}} \frac{\partial}{\partial x}\left(\frac{\partial^2 T_z}{\partial x^2} + \frac{\partial^2 T_z}{\partial y^2}\right)$$

$$= j\omega\mu\sigma\left(\hat{\underline{x}} \frac{\partial T_z}{\partial y} - \hat{\underline{y}} \frac{\partial T_z}{\partial x}\right)$$

Since $\underline{E}$ is a regular function in the area in question, $\underline{I}$ will also be regular, and, because of the boundary conditions peculiar to this specific problem, the above equation can be simplified to

$$\underline{\nabla^2 T_z = j\omega\mu\sigma T_z} \qquad (26)$$

Having found an equation for the model in terms of $\underline{I}$ the next step is to define boundary conditions.

On the floor of the bath

$$\frac{\partial E_y}{\partial y} = 0 = -\frac{\partial^2 T_z}{\partial x \partial y} \qquad E_x = 0 = \frac{\partial T_z}{\partial y}$$

On the sides

$$E_x = 0 = \frac{\partial T_z}{\partial y} \qquad \frac{\partial E_y}{\partial x} = 0 = -\frac{\partial^2 T_z}{\partial x^2}$$

On the surface

$$\frac{\partial E_x}{\partial y} = 0 = \frac{\partial^2 T_z}{\partial y^2} \qquad E_y = 0 = \frac{-\partial T_z}{\partial x}$$

On the electrode surface

$$E_x = 0 = \frac{\partial T_z}{\partial y} \qquad E_y = EIN = \frac{-\partial T_z}{\partial x}$$

If the electrode is submerged in the slag, obviously some current will flow through the sides. Since across a boundary it is the normal component of $\underline{D}$ and the tangential component of $\underline{E}$ that is continuous the condition that div $\underline{E} = 0$ will not hold here since the two materials have different permittivities. Hence the $\underline{T}$ model can only be used if the electrodes are on the surface of the slag, when the boundary condition will specify the value of $\underline{E}$ at the base of the electrode but in the slag. This solution will still be valuable since it is the region below the electrodes which is of prime importance in a furnace.

The programme developed to solve the field using the vector potential $\underline{T}$ follows similar lines to that described in section 5.2. Again the data cards specify the furnace dimensions, accuracy of solution and power input (in terms of current flow). Other quantities are also necessary viz. the conductivities of the slag and electrodes and the frequency of supply. The potential field must now be calculated using complex numbers since phase delays can occur in conducting media. This doubles the amount of computer-core necessary

and quadruples computation time. Since both electrodes lie at the same level, the $\underline{I}$ field will be symmetric about the middle line (parallel to the Y axis) of the bath, so only half the field need be calculated. In setting up the boundary, the different boundary conditions must be taken into account. The current flow in the electrodes is calculated using a routine employing the series approximation to the Bessel functions. Again the equation is solved by relaxation, using the two difference equations for improved accuracy. After calculating and printing the electric field, another routine calculates and prints out the error in this field using the three equations defining it in terms of $\underline{E}$. The program and flow chart has been included in the accompanying file.

CHAPTER 6

RESULTS AND CONCLUSIONS

The results obtained from the physical model were most interesting though somewhat frustrating. The first set of readings taken were very pleasing in that what was expected was obtained, indicating that the programming and the theory behind the field derivation is correct and valid. However, variation of the power parameters (current and frequency) in an attempt to change the current distribution and ascertain the trend likely to take place on scale-up proved rather fruitless. The current drawn was altered by changing the conductivity of the solution and the frequency of the supply increased using a laboratory alternator. Any change that did occur was very small and beyond the resolution of the measuring system. The current could only be increased by a factor of twenty (1 to 20 amps) and the frequency changed from 50Hz to 400Hz. Skin effect is related to the square root of frequency (equation (23)) so to achieve the same conditions as in the real furnace the supply should be increased by a factor of 900 (since the model is $\frac{1}{30}$ scale) and the current drawn should be 300 amps. This was quite impossible, and even it could have been achieved would have given dubious results - the voltage pick-up in the measuring leads would be as large as the signals being measured and the contents of the bath would quickly boil away. However, the mathematical model affords another means of scale-up, so the

information from the tank is not entirely wasted.

For the majority of the experiments the conductivity of the electrolyte was about 0,2 mhos/cm (200g NaCl/1000g water). This is approximately the same value as that of the slag in the Rustenburg furnace. The depth of solution was normally 5cms. (corresponding to the 5 ft. slag layer). A fair amount of heat was developed in the electrolyte and this had a marked effect on the readings, so the model had to be left on for about half an hour before any consistent readings could be taken. The system had no measurable reactance (even at the high frequencies used) and an electrode-hearth resistance (electrode at surface of liquid) of half an ohm. The normal frequency of operation was 50Hz.

The results obtained using the parameter plot routines did not show anything new or spectacular, merely what other researchers had done on models of circular furnaces. The Hallvard Nilsen formula (Reference 7) for resistance vs. depth of electrode showed the best correlation even though he derived this using a three-electrode round furnace. This is not surprising since, as shown later, the interelectrode spacing is such that the main fields associated with the individual electrodes barely interact. The sharp voltage drop at the tip of the electrode (as observed by Kjolseth) is shown in Figure 6.1. The potential along a line at different levels in the solution in a plane through the axis of the electrode has been shown. The electrode tip was at the surface of the 'slag' (0mm). The voltage has dropped to one

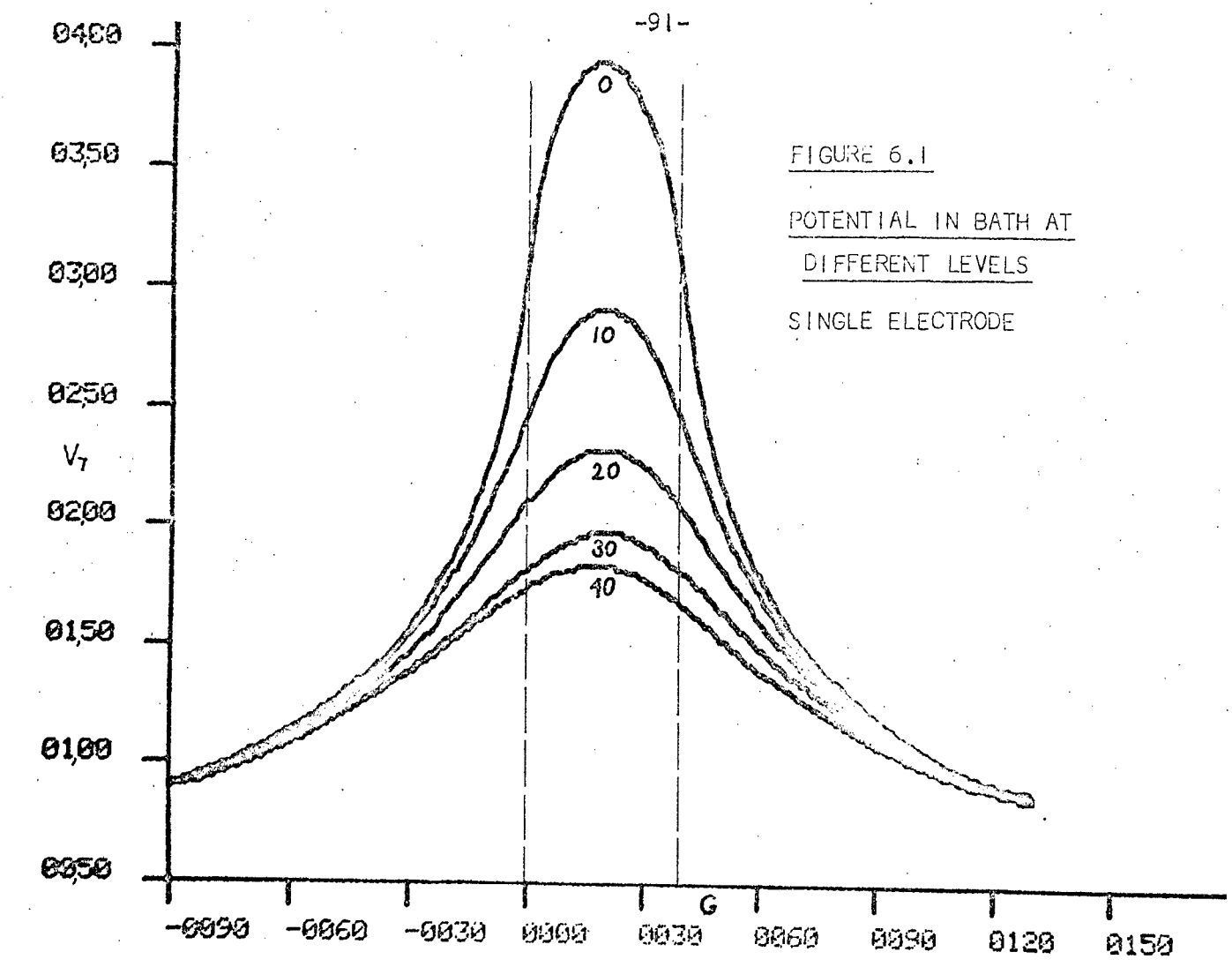

FIGURE 6.1

POTENTIAL IN BATH AT DIFFERENT LEVELS

SINGLE ELECTRODE

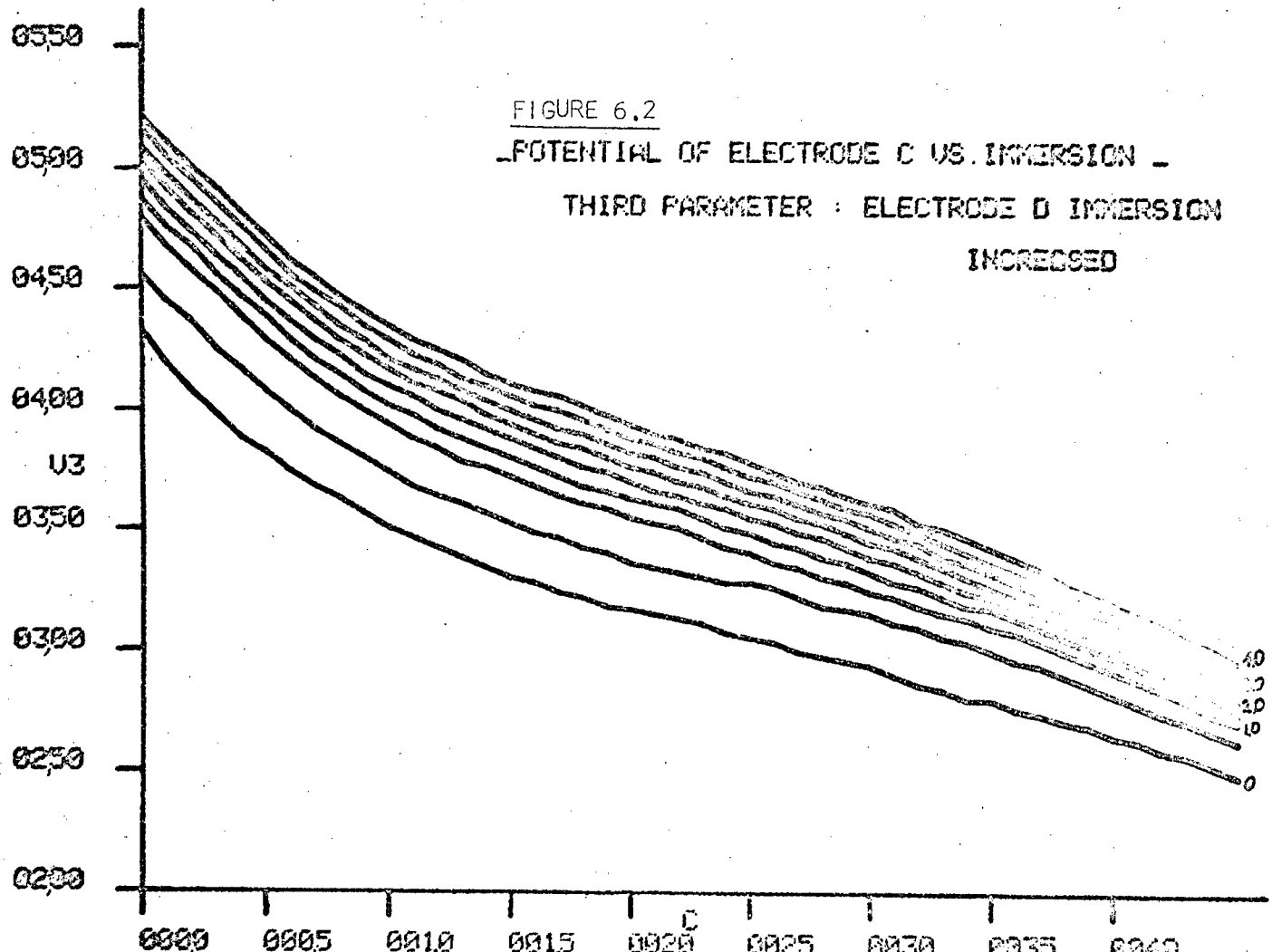

FIGURE 6.2

POTENTIAL OF ELECTRODE C VS. IMMERSION

THIRD PARAMETER : ELECTRODE D IMMERSION INCREASED

third of its maximum value within 4cm (i.e. one electrode diameter). The curves for the different levels all have a similar shape, only the magnitude varies. Note also that the graphs do not tend to zero indicating that there is still an electrode potential set up between the probe and the earth-plate despite the precautions taken. However, since the useful results involve the gradient of this scalar field, the offset will disappear. Figure 6.2 shows the variation of the electrode-hearth voltage as the depth of one electrode was changed. The applied potential difference between the two electrodes was constant (8V). This is a useful set of curves for determining the boundary conditions for the static mathematical model. Plots involving more phases and different power inputs showed similar characteristics.

Moving on to the more useful data display, the field plots, the simplest case involving only one electrode is considered first. Figure 6.3 shows the fields in the XY plane and Figure 6.4 for the XZ plane. The equipotential plot in 6.3(a) does not really convey much information which can be related to the furnace since voltage measurement in the slag is almost impossible and very inaccurate due to pick-up. The other field plots attempt to show the current distribution. The lines indicate the magnitude and direction of the current at the point marked with a cross. The distance between each sample point (cross) was 5mm. This was found to be the optimum size mesh since the Z positioning of the measuring trolley could not be placed with more than

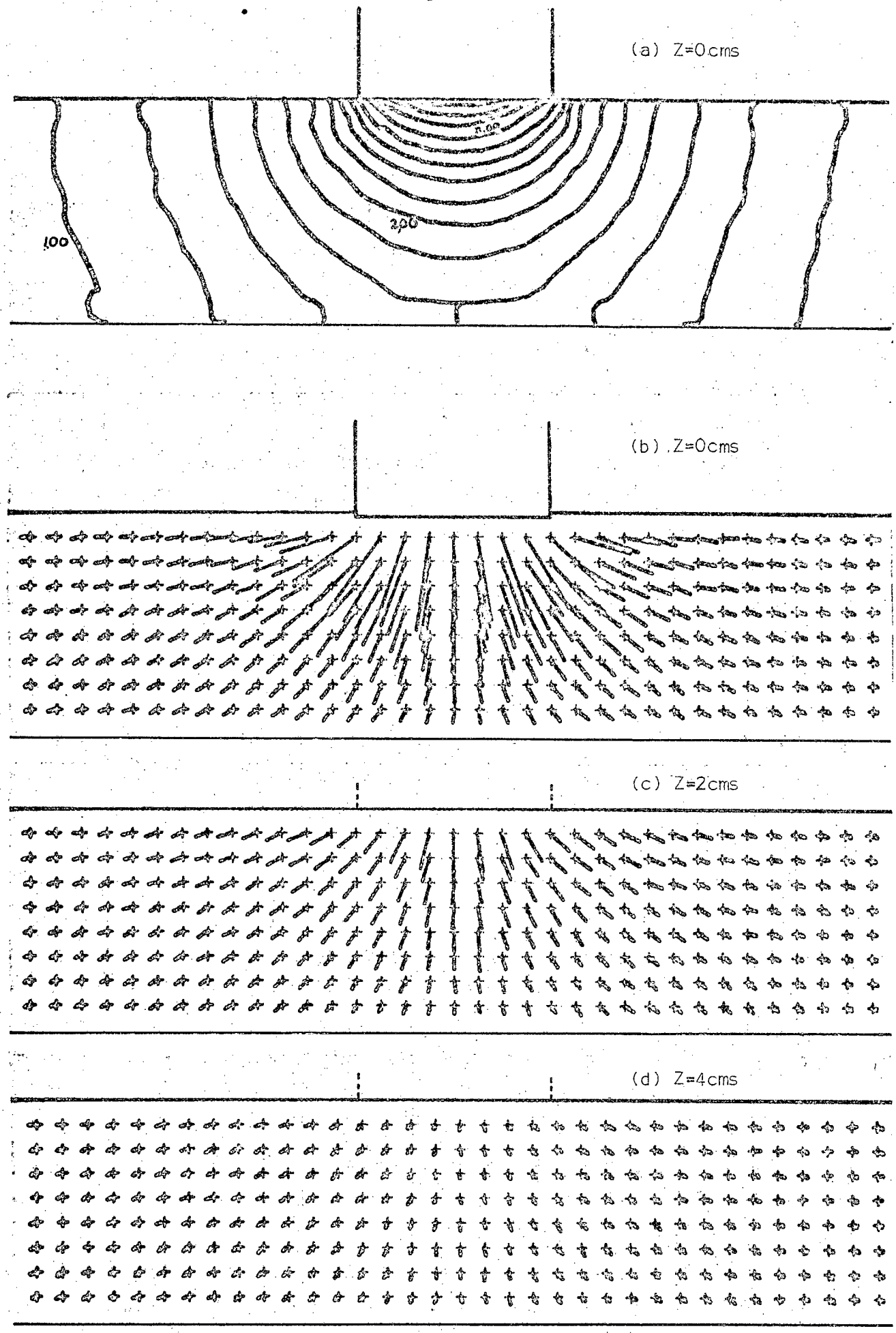

FIGURE6.3 FIELDS IN THE X-Y PLANE FOR THE SINGLE ELECTRODE CASE

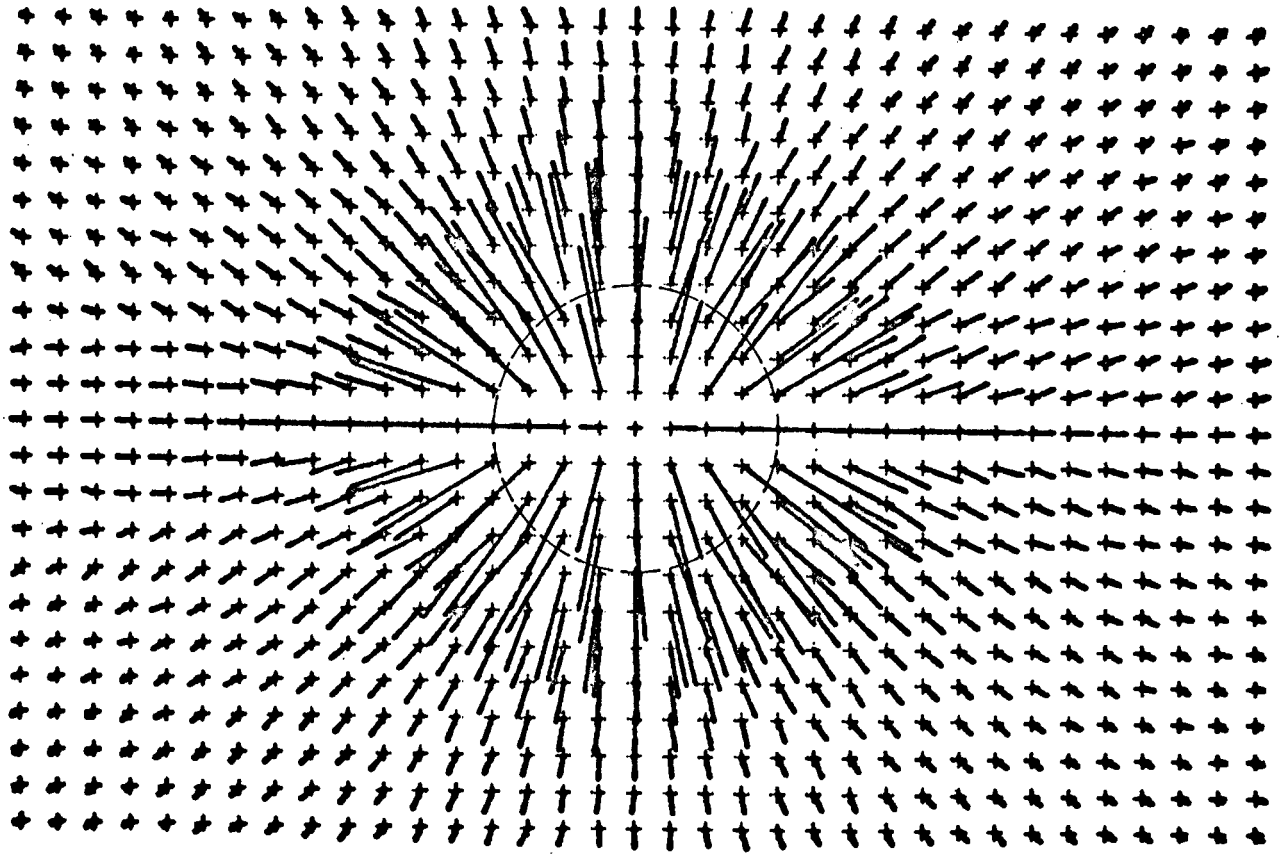

(a) Y=0cms

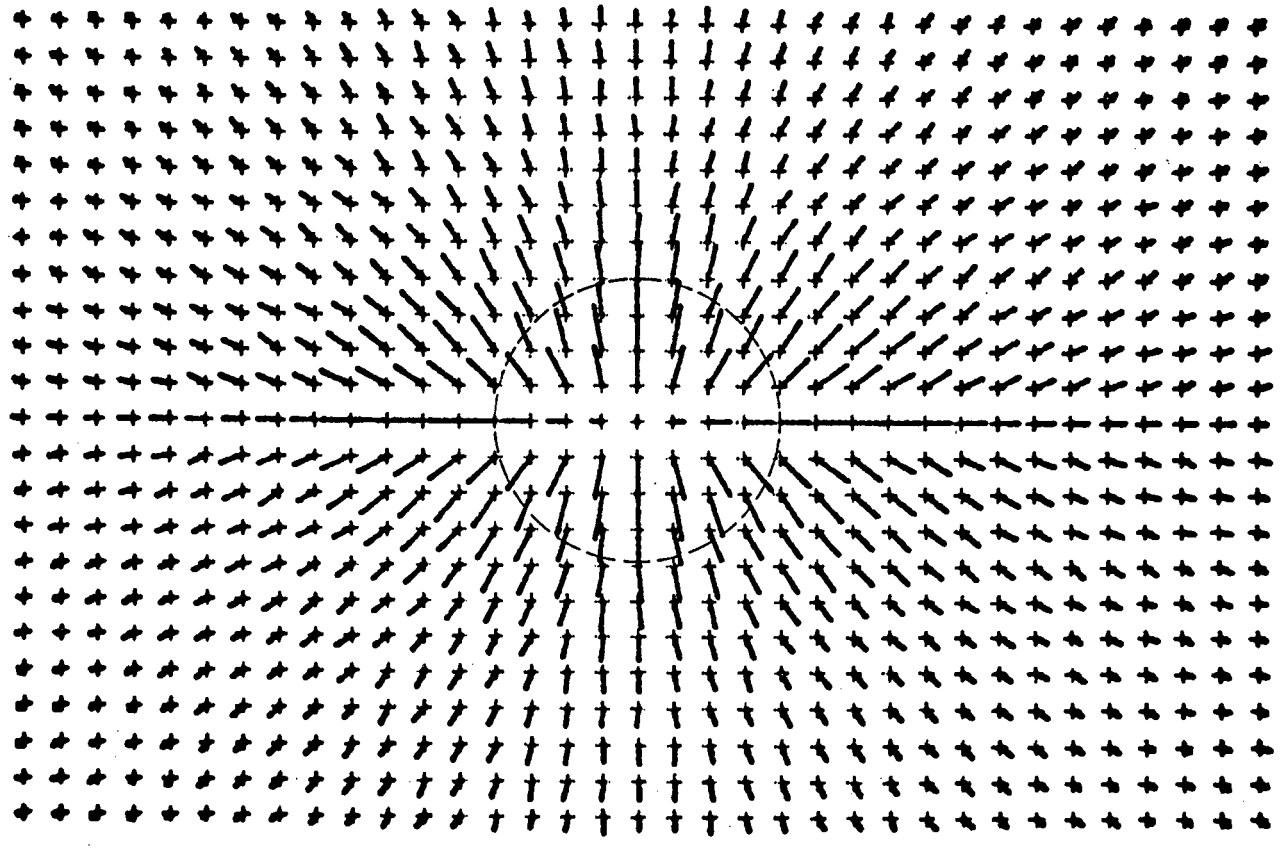

(b) Y=2cms

FIGURE 6.4 CURRENT DISTRIBUTION IN X-Z PLANE FOR SINGLE ELECTRODE

1mm. accuracy. The distribution is, as should be expected radially symmetric. Surprisingly, current flows in areas quite far removed from the electrode, but the main flow reaches the bottom of the tank within a circle of 20cm. diameter. Figure 6.5 is an indication of the lines along which the current flows. The flow lines have been drawn through points at which the current magnitude has dropped to a certain fraction of the maximum value in that plane. The dotted line shows the boundary where the field drops to one third of its maximum value in the tank. This is a similar shape to that proposed by Kjolseth and confirms Andreae's reasoning that the power from an electrode is dissipated within a sphere with a radius equal to one electrode diameter (assuming power dissipation is due to resistance heating). A contour plot of the power distribution in the XY plane is shown in Figure 6.6. The dimensional plots in Figure 6.7 show the power distribution in the XY plane at different levels below the electrode. The magnitude of E^2 has been plotted vertically over the whole plane. From these it is quite clear that most of the power dissipation is within two centimetres of the electrode surface. The value of E can be evaluated at any point in the power cycle and squared to give a figure related to power because, it was observed, that at any time the field pattern remained the same - it only varied in magnitude and sign, the actual current flow-lines remain the same. Hence the timing was set to give maximum E and greatest accuracy. This cannot be done in the polyphase case.

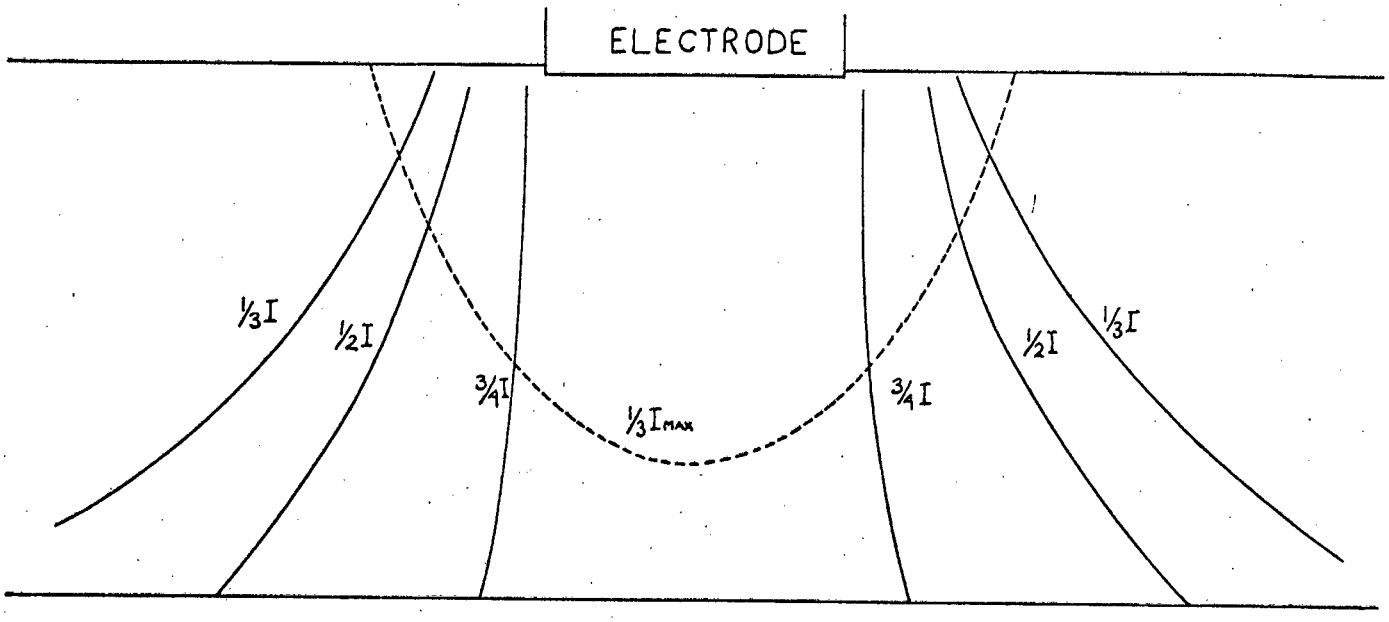

FIGURE 6.5 CURRENT FLOW-LINES IN ELECTROLYTE (X-Y PLANE)

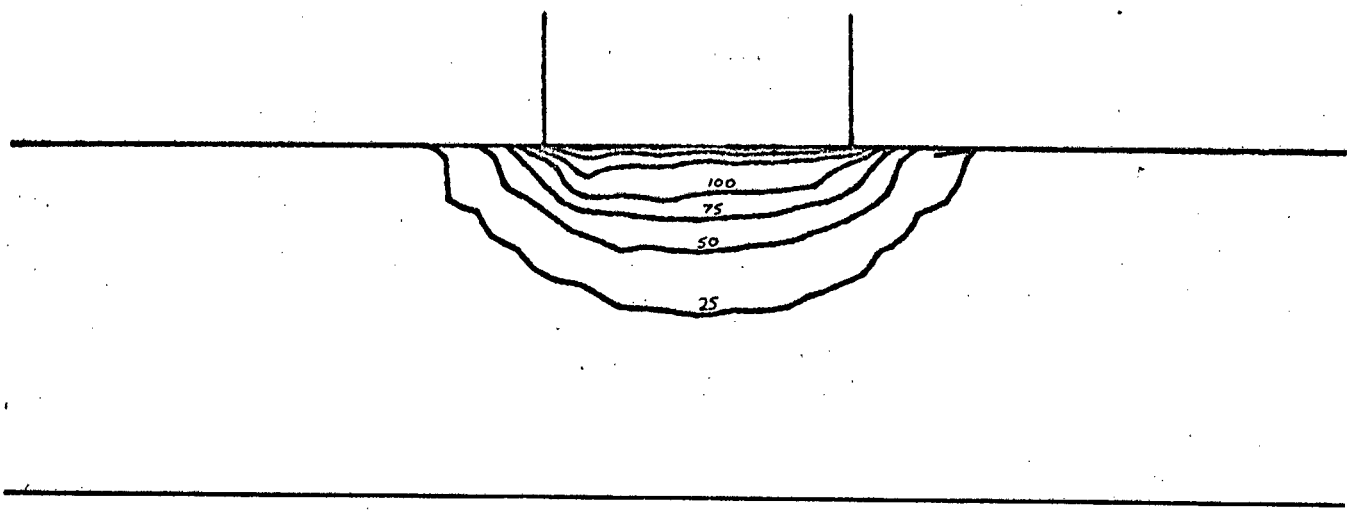

FIGURE 6.6 POWER DISTRIBUTION IN X-Y PLANE (Z=0cms)

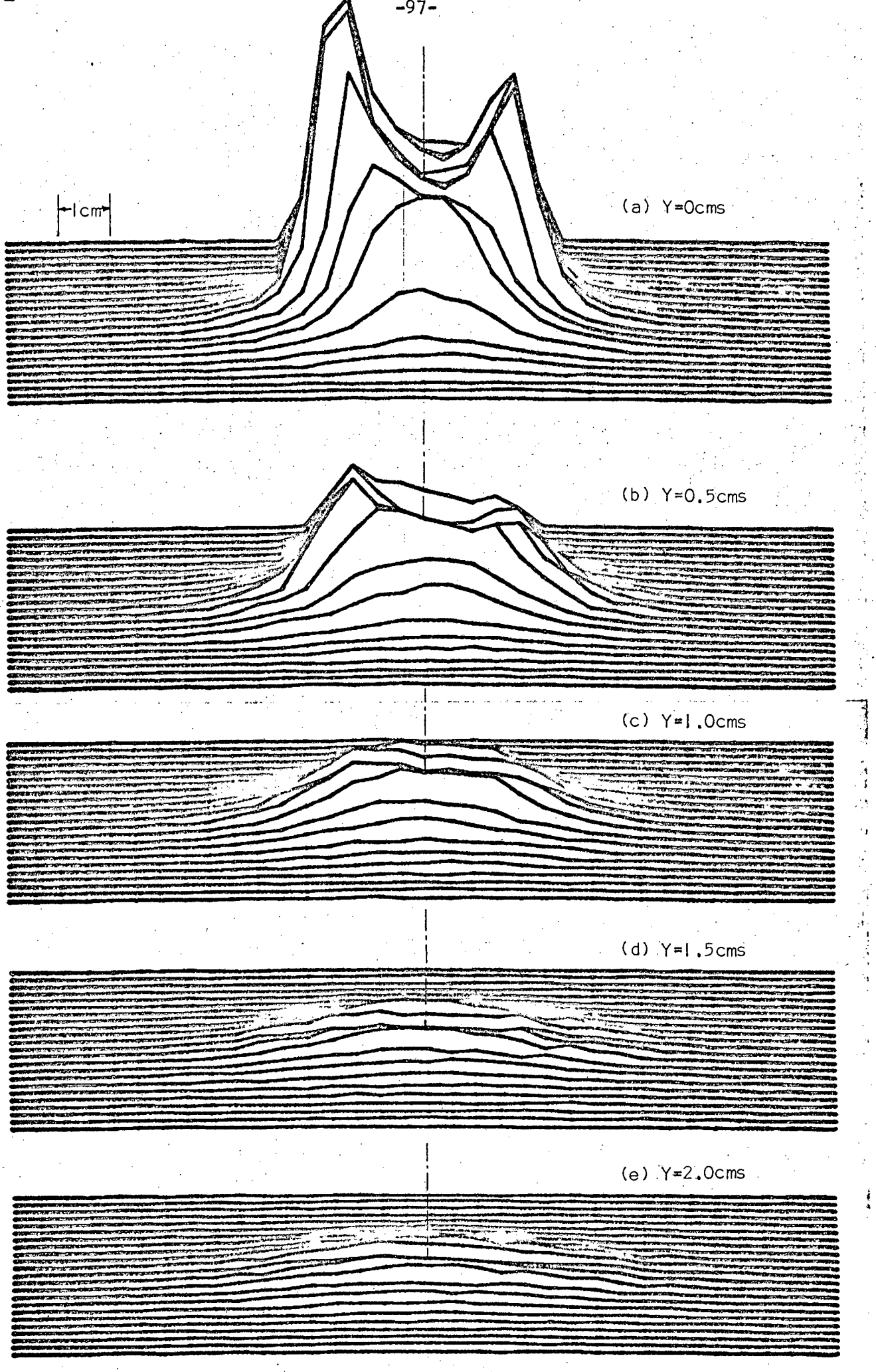

FIGURE 6.7 POWER DISTRIBUTION OVER HORIZONTAL(X-Z) PLANES FOR SINGLE ELECTRODE

The shape of the power field can be explained if one considers how it is derived. The $\underline{E}$ field is taken as the gradient of the V field. Hence the peaks of power at the electrode circumference - the voltage gradient has to start decreasing at some stage as a peak is reached, and this (as shown in Figure 6.1) is approximately at the position of the electrode boundaries, because these conductors are at a constant potential. It is the familiar result from electrostatics that the largest fields occur at the sharpest boundaries. The power on the axis of the electrode will not be zero because the E_y component here is non zero. The peak of power around the circumference explains why the base of a real electrode has rounded edges - obviously this will be the hottest place, so the carbon will burn away fastest here.

Turning to a more practical case, the two electrode single phase furnace can be shown to be made up of two single electrode systems (see Figure 6.8). 6.8(a) shows the field when two electrodes are connected and the bottom is left floating. (b) and (c) show the fields when the power is connected between one electrode and the earth plate, and (d) shows the result when these two fields are summed. Power distributions of the individual systems cannot be simply added as they involve the square of the current. First the resultant current distribution must be found and then this can be squared.

The single phase two electrode furnace was studied further. The current distribution in various planes has

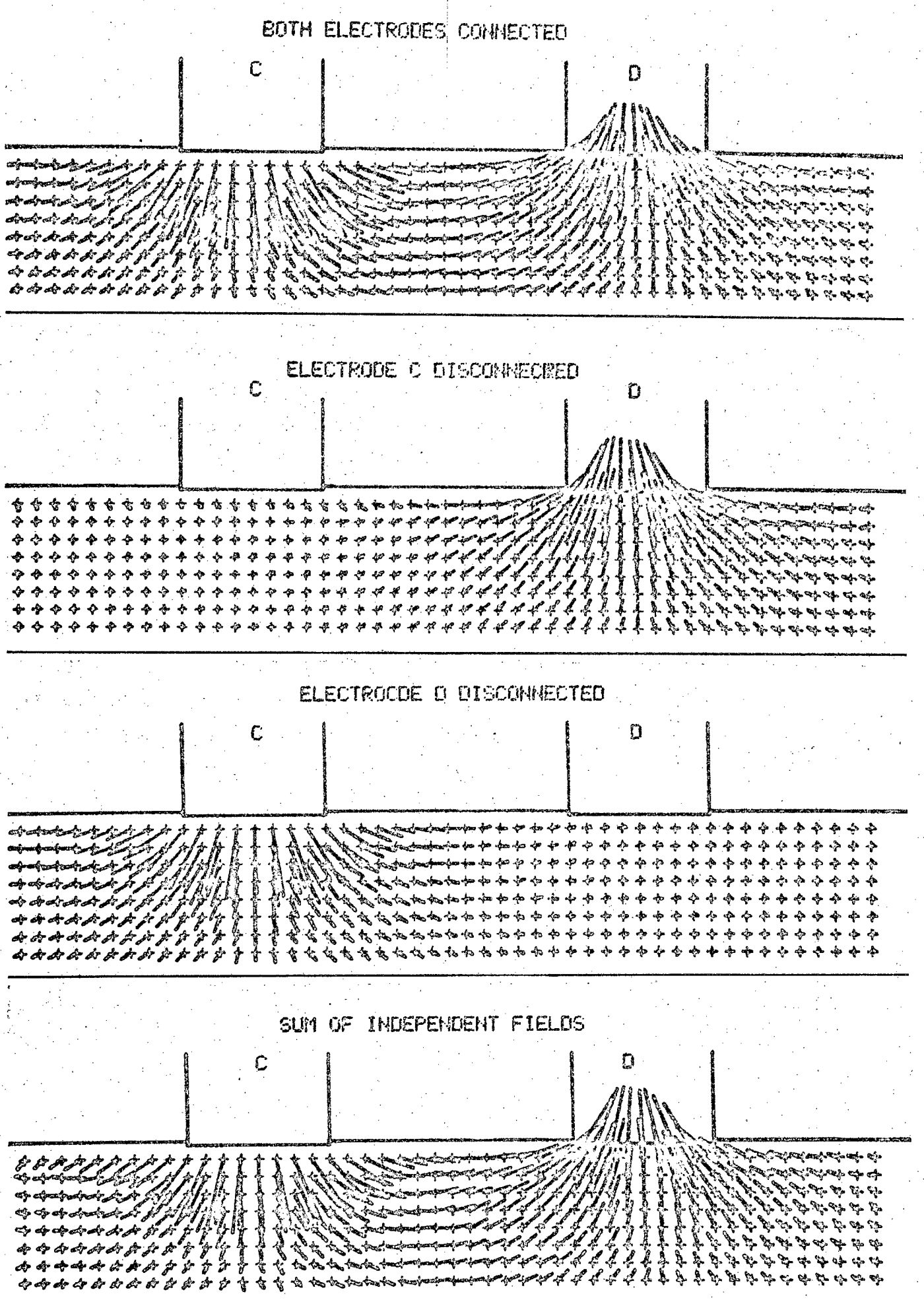

FIGURE 6.8 DIAGRAM TO SHOW SUPERIMPOSITION PROPERTY OF FIELDS

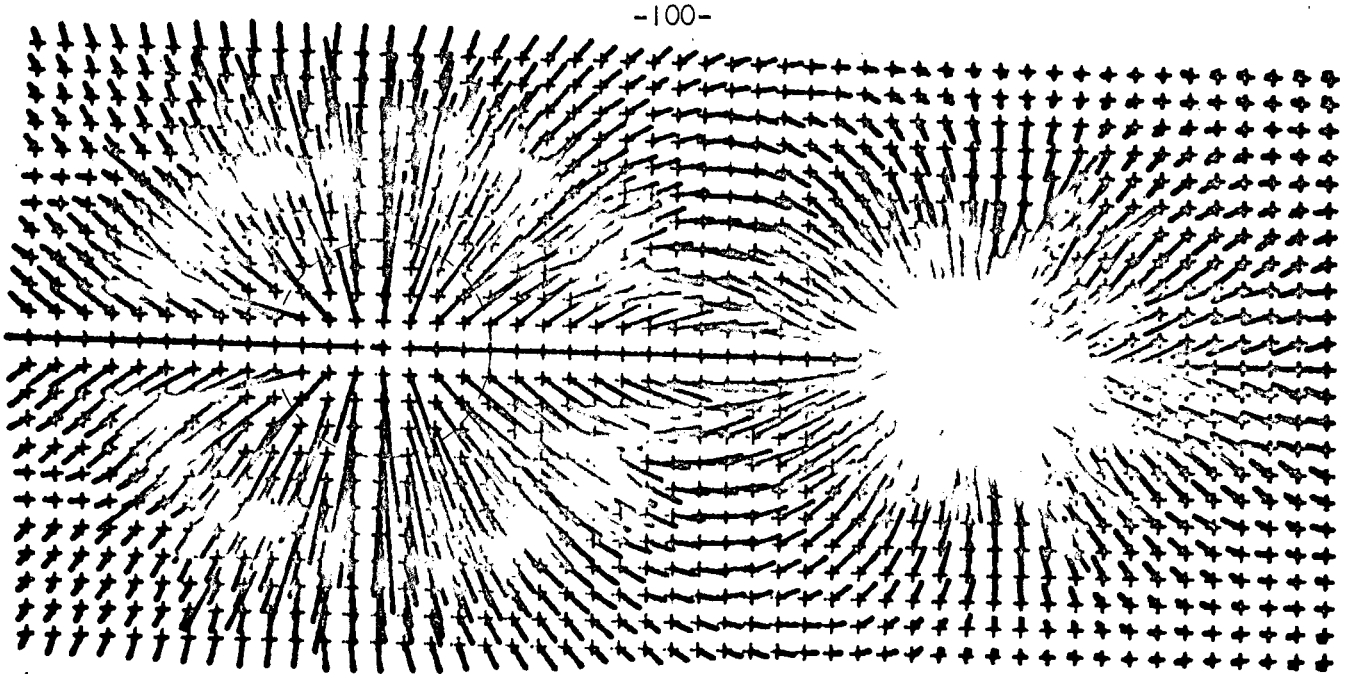

(a) X-Z PLANE Y=0.5cms

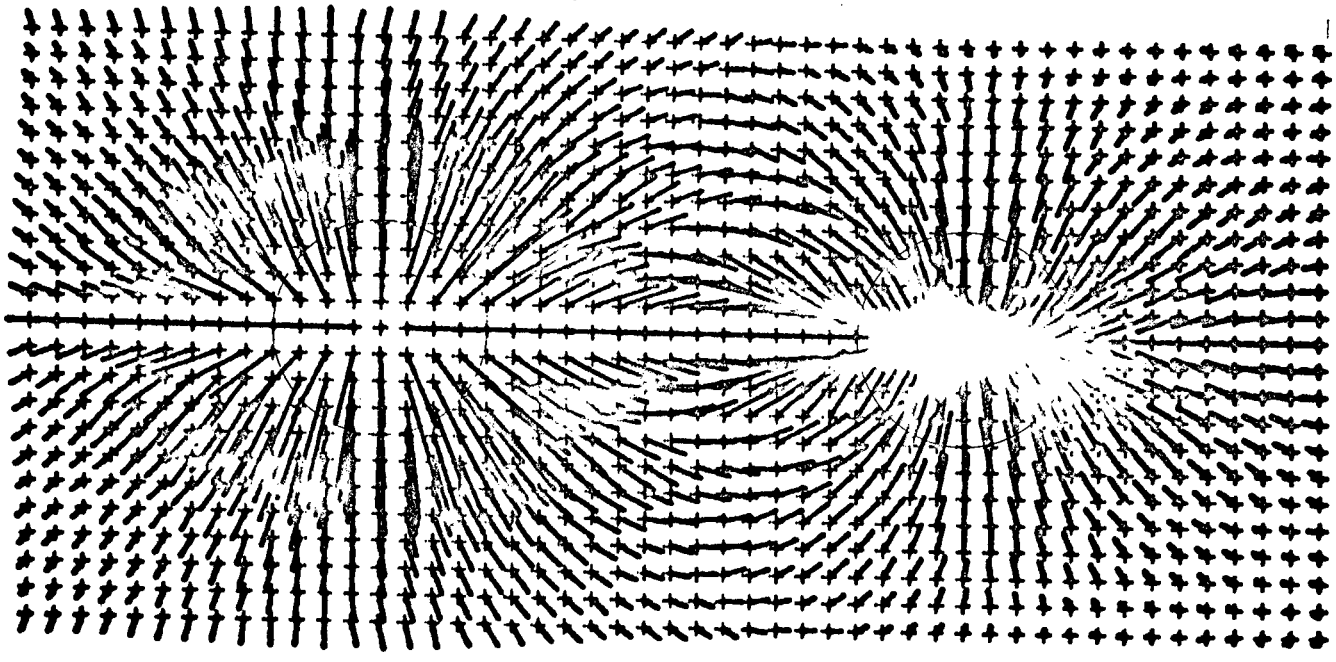

(b) X-Z PLANE Y=1.5cms

(c) X-Y PLANE Z=0.0cms

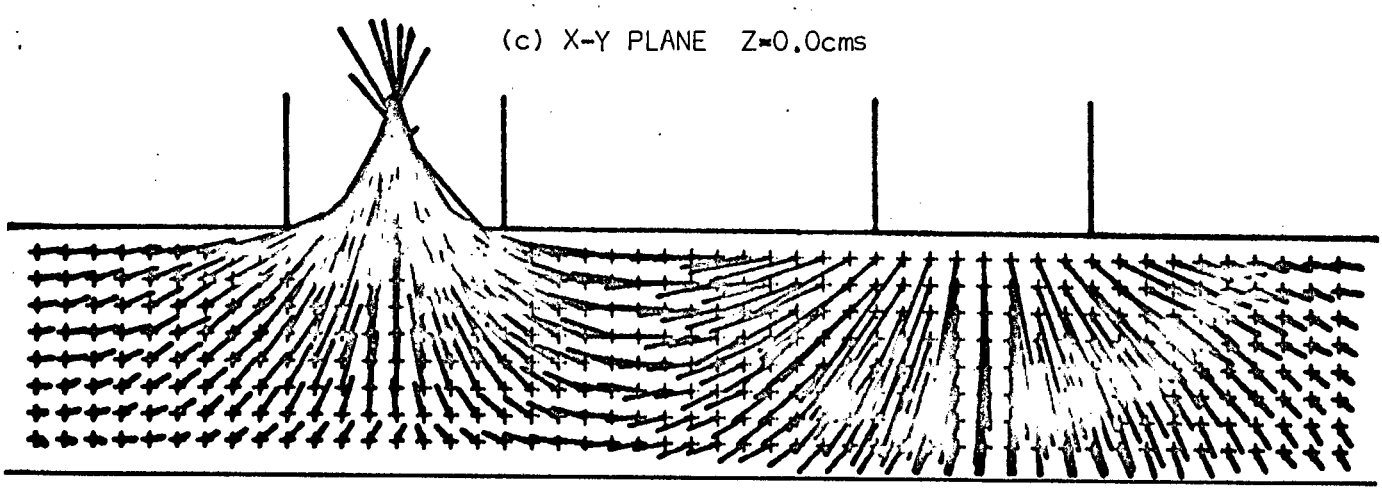

FIGURE 6.9 CURRENT DISTRIBUTION FOR TWO ELECTRODE CASE

been shown in Figure 6.9. From these it was calculated that about seventy per cent of the current flow is via the hearth - this agrees with NIM's findings (Reference 9). The voltage plot in a plane through the electrodes is shown in Figure 6.10. In this case the presence of the second electrode tends to increase the voltage gradient on the inside of the electrodes which should give a larger $\underline{E}$ and hence greater power density in this region. This can be seen in Figure 6.12. The lower planes have been enlarged by a factor of 5 in Figure 6.13 to show that the two power peaks merge into one at a level about 3cm. below the electrode. Again the power dissipation can be seen to be concentrated in a very small area around the electrode tips. This is further illustrated by means of contour maps (Figures 6.14 and 6.15). Although there is no area in which the power is actually zero, very little extends beyond a radius of 4cm.

Theoretically the power dissipation should approximate to the temperature distribution, but the curves obtained here bear no relation to the temperature measurements made on the real furnace. This is because no account for heat conduction has been made. If the power dissipation can be equated to heat production and the medium assumed homogeneous, the gradient of this field should indicate the heat flow pattern (Figure 6.16). Note that the heat flows both ways from the perimeter of the electrode, hence the spot in the middle will become one of the hottest points.

So far only a symmetric furnace has been investi-

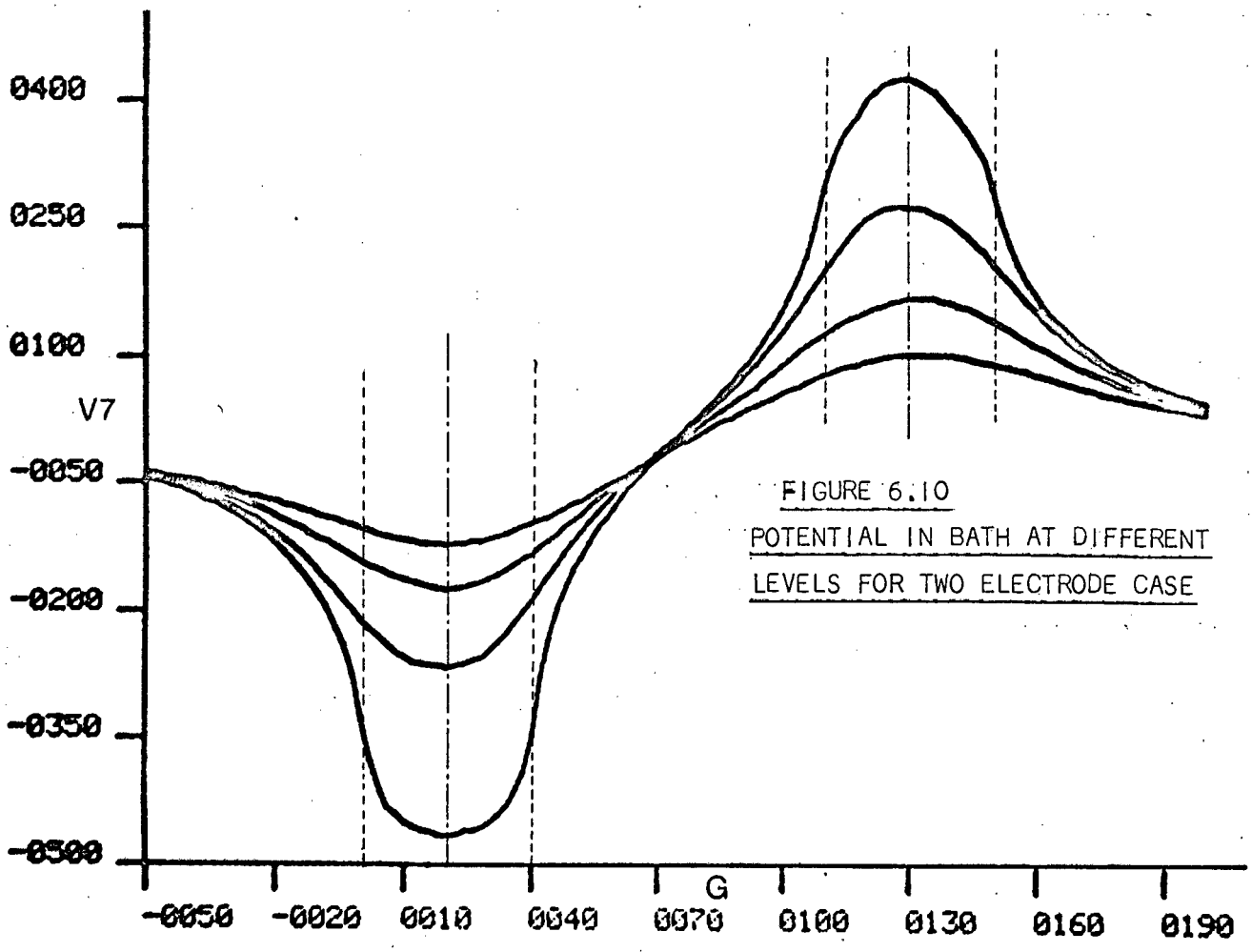

FIGURE 6.10
POTENTIAL IN BATH AT DIFFERENT LEVELS FOR TWO ELECTRODE CASE

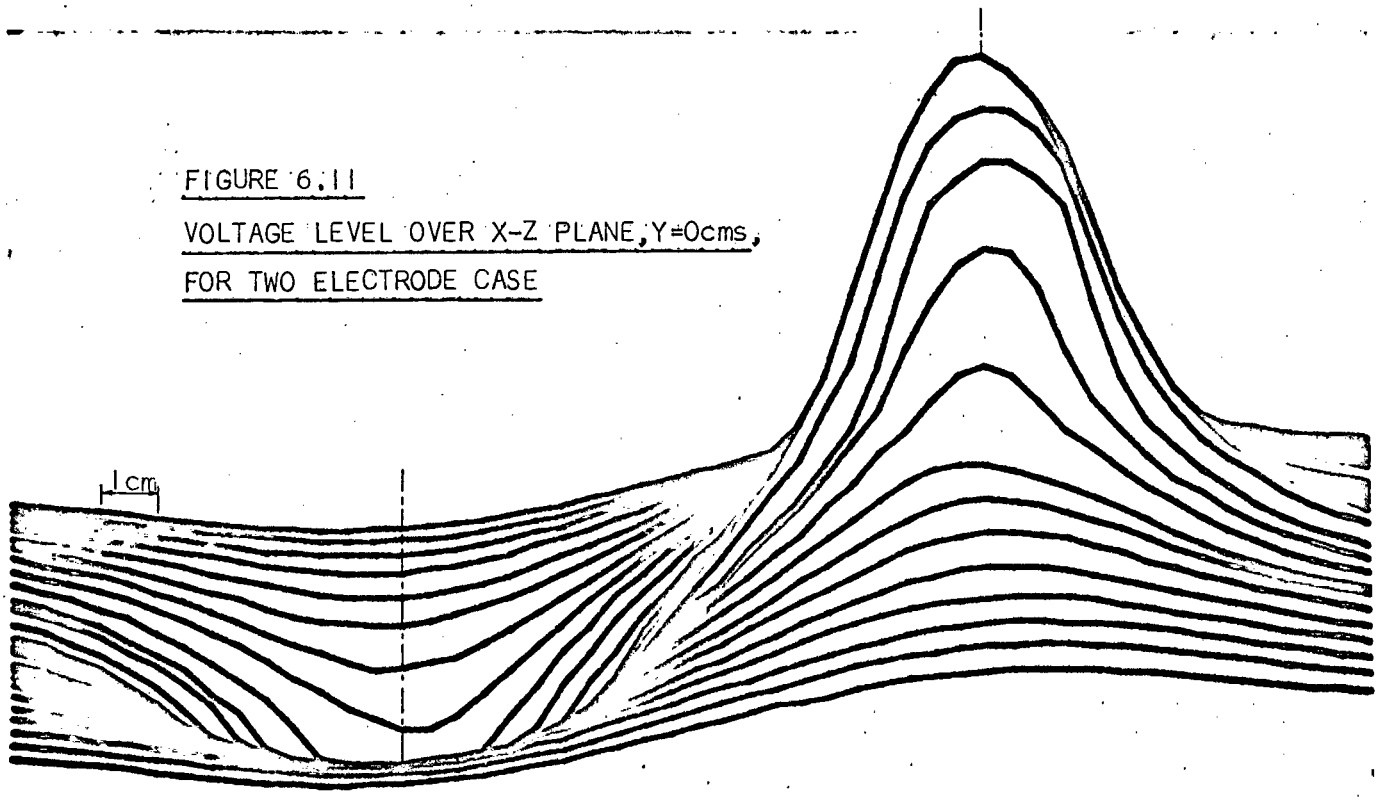

FIGURE 6.11
VOLTAGE LEVEL OVER X-Z PLANE, Y=0cms, FOR TWO ELECTRODE CASE

FIGURE 6.12 POWER DISTRIBUTION OVER X-Z PLANE FOR TWO ELECTRODE CASE

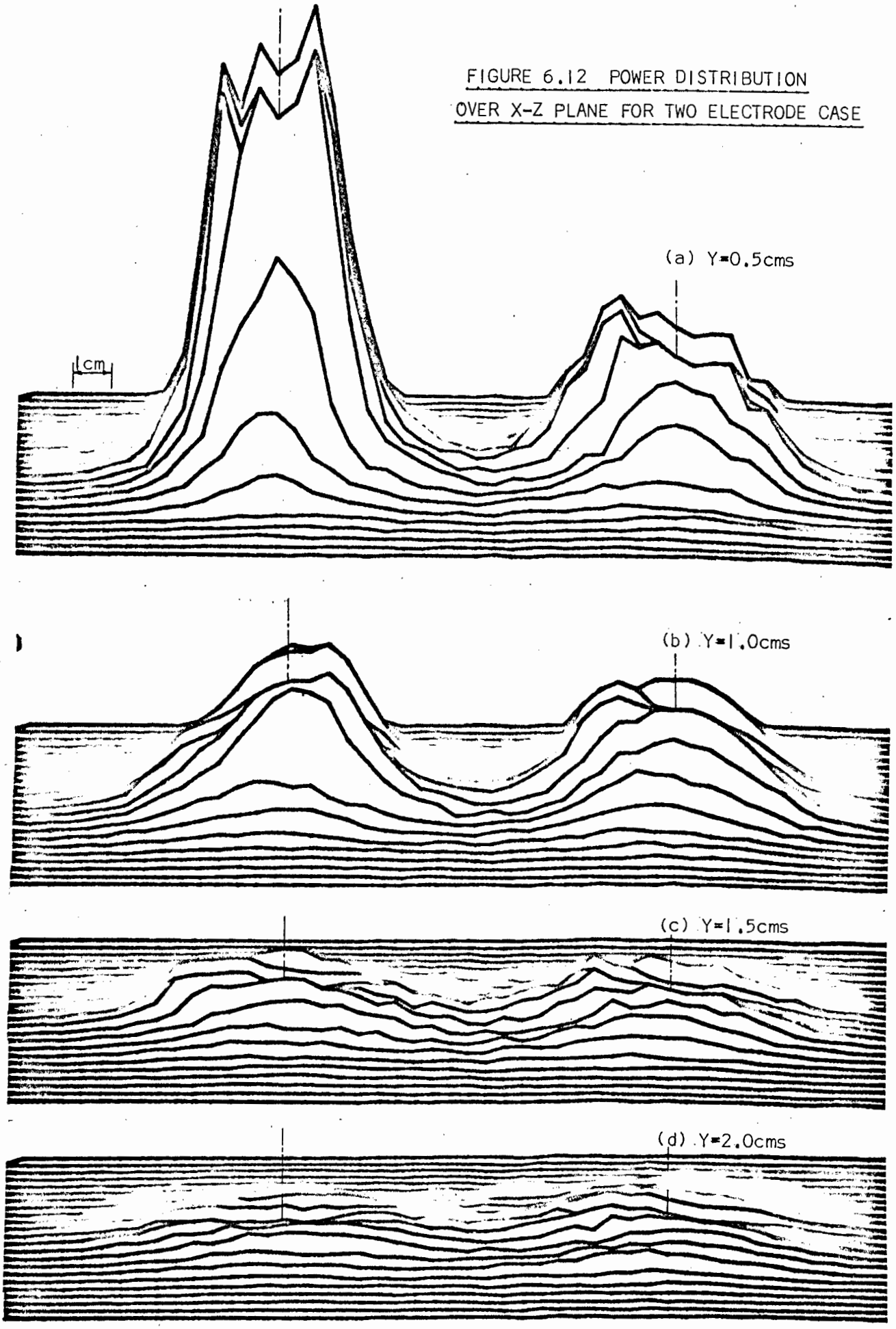

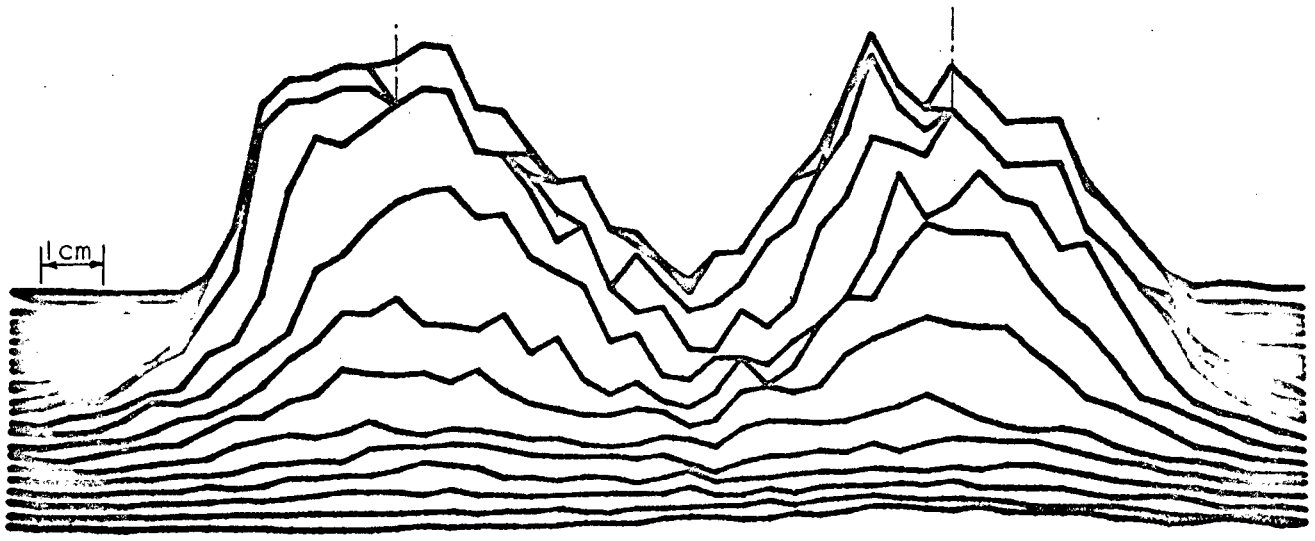

(a) Y=2.0cms

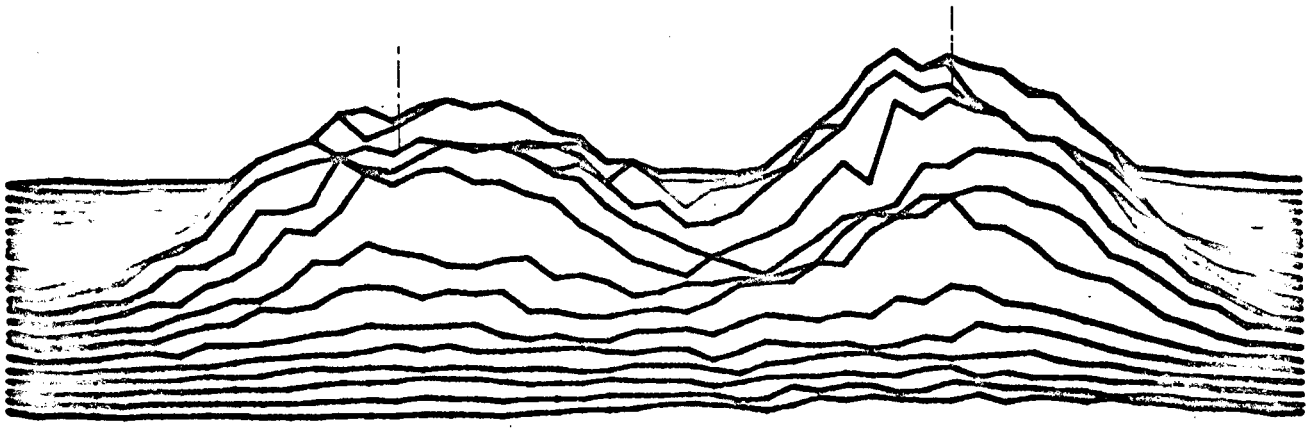

(b) Y=2.5cms

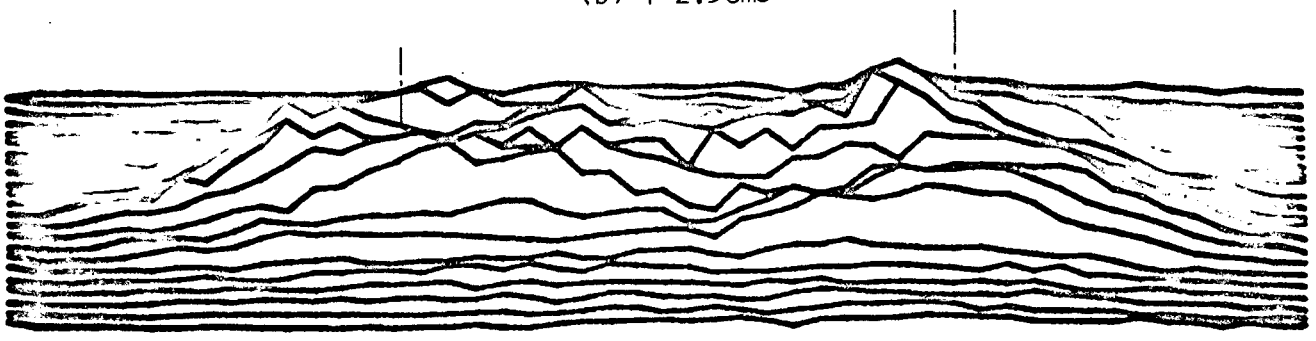

(c) Y=3.0cms

FIGURE 6.13 POWER DISTRIBUTION (ENLARGED) IN LOWER LAYERS OF BATH

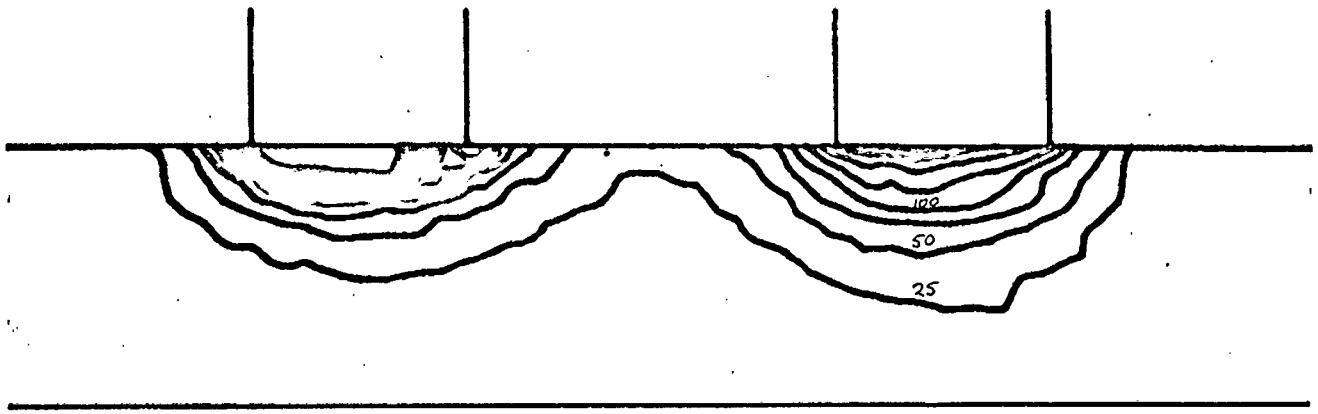

FIGURE 6.14 POWER CONTOURS IN X-Y PLANE (Z=0cms)

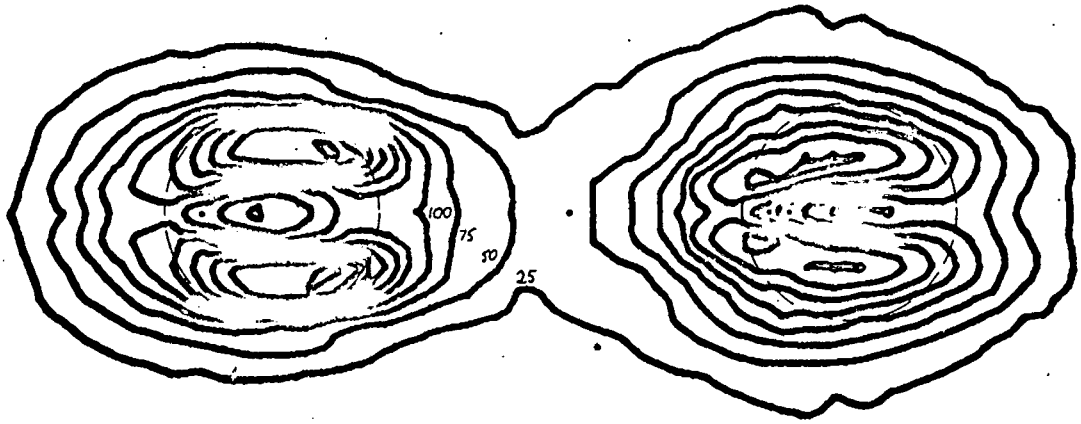

FIGURE 6.15 POWER CONTORS IN X-Z PLANE (Y=0cms)

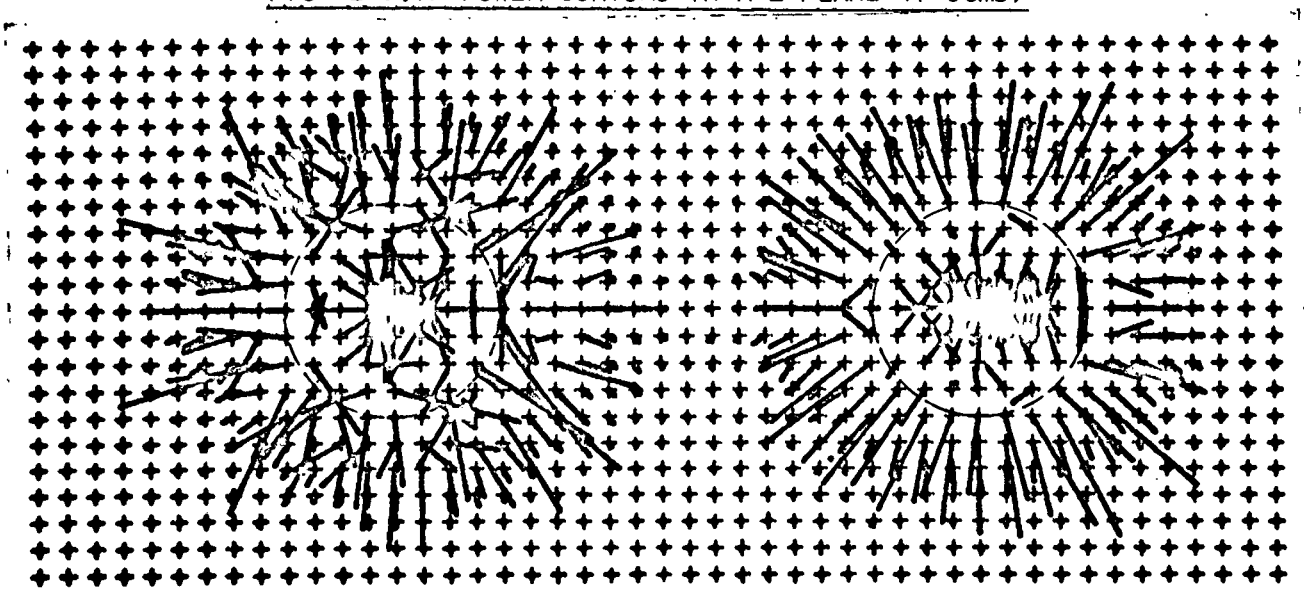

FIGURE 6.16 HEAT FLOW IN THE X-Z PLANE (Y=0cms)

gated where both electrodes lie on the surface. Figure 6.17 shows the effect of lowering one electrode. The inter-electrode current does increase slightly and the flow-lines change direction to enter the electrode at right angles (characteristic of an electric field at the surface of a perfect conductor). The power distribution for an asymmetric system shows one or two interesting features. The voltage distribution in the XZ plane is shown in Figure 6.18. Electrode 3 was submerged to a depth of 2cms. The plateau-like projection indicates its position. This plateau seems to point to the carbon having some finite resistance and hence is not at an equipotential. At the surface plane along the centre-line the voltage curve is continuous to the electrode surface, but elsewhere on the perimeter there is a sudden step which is the cause of the massive power peaks in Figure 6.19(a) and (b). This error is very difficult to eliminate since one cannot measure the potential inside the electrode. If one disregards this false internal power it can be seen that very little energy escapes through the side walls of the submerged electrode. The interesting point is that the shape and size of the power curve beneath electrode 3(6.19(c)) is the same as that at an equivalent level below electrode 4 (6.19(a)). This indicates that the same amount of power is dissipated around each electrode, no matter what its submersion (within reasonable limits i.e. not too close to the matte).

The three phase furnace can be considered to be

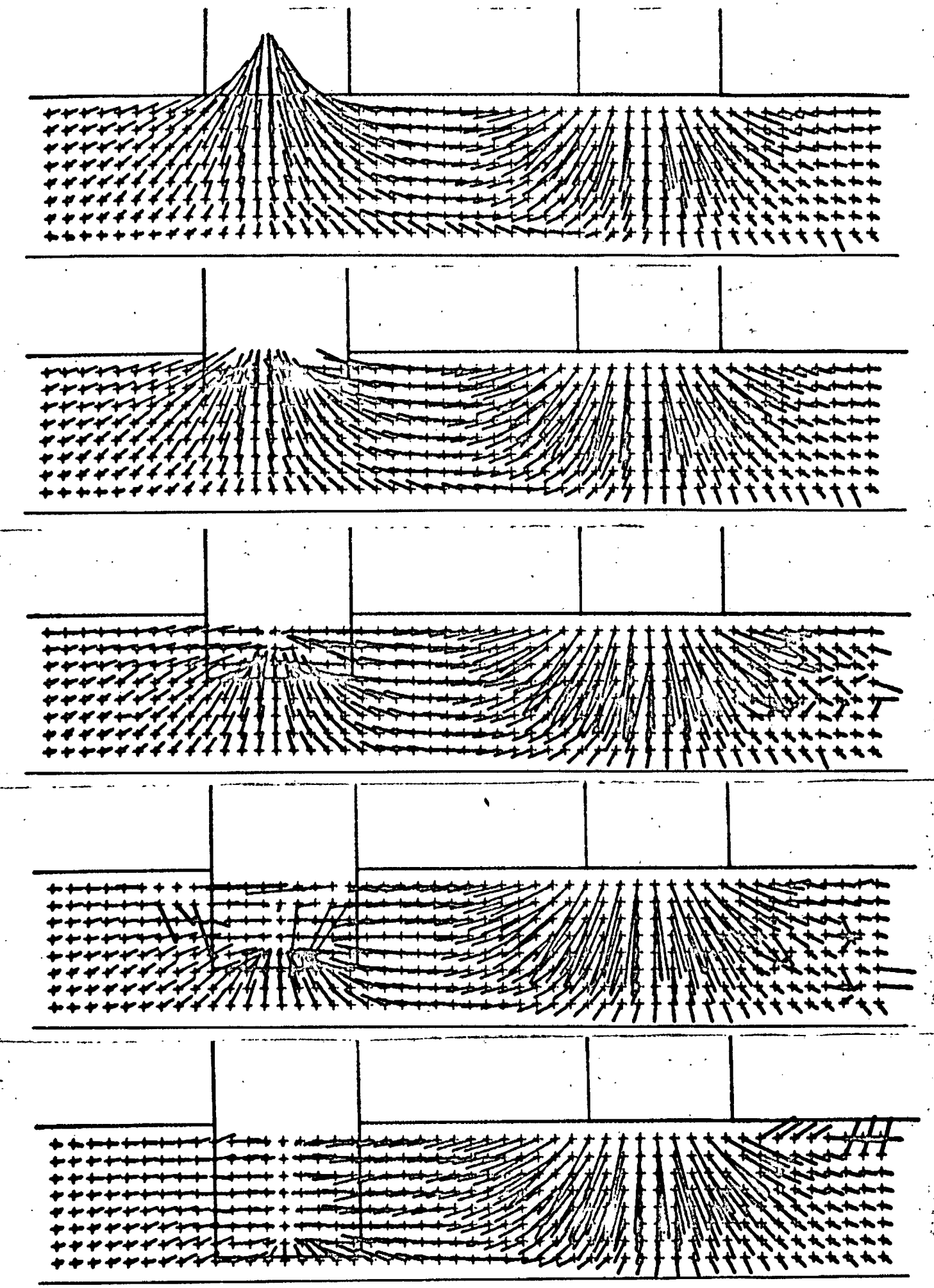

FIGURE 6.17 EFFECT ON CURRENT WHEN ELECTRODE IS IMMERSED

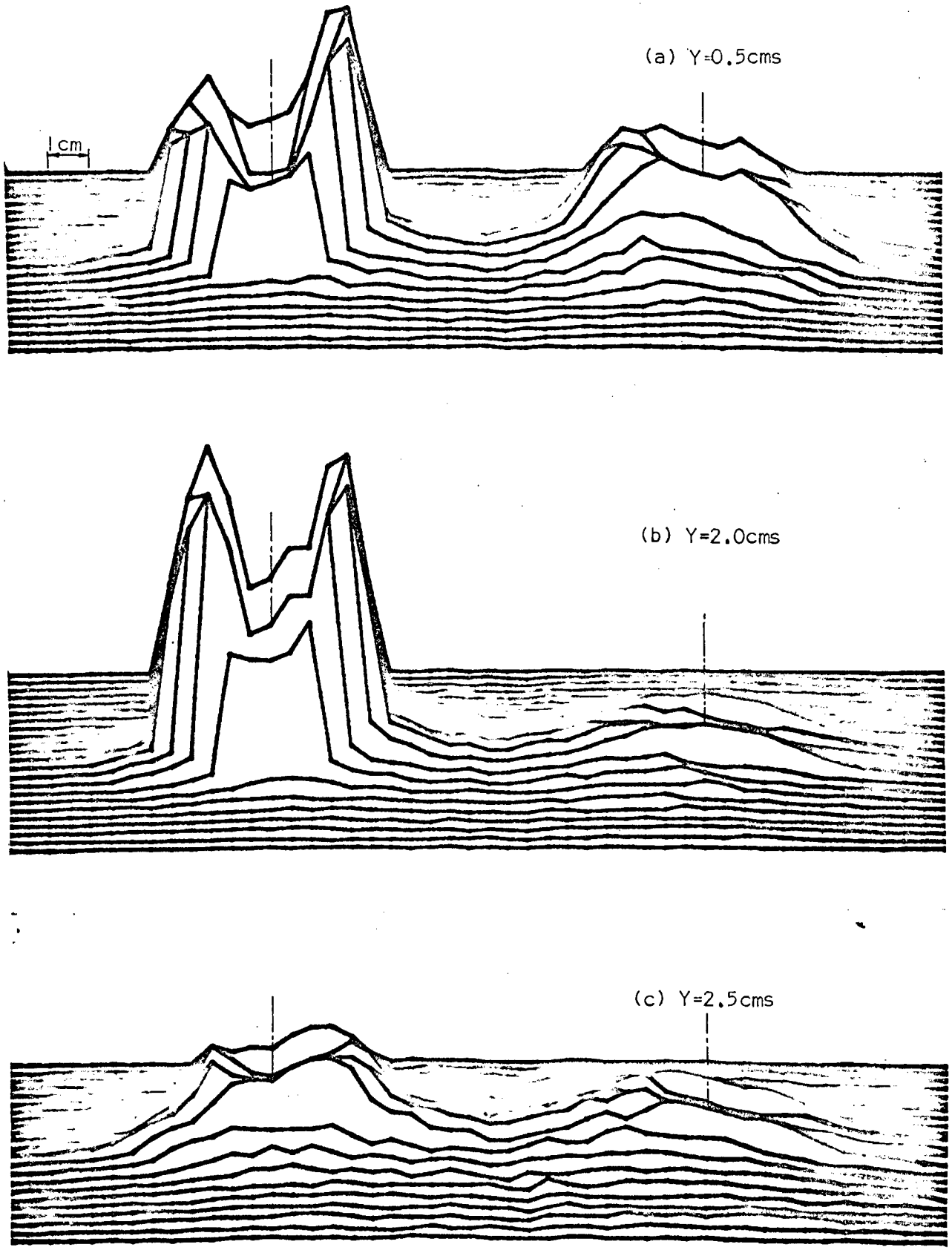

FIGURE 6.19 POWER DISTRIBUTION OVER X-Z PLANE FOR ASSYMETRIC ELECTRODE SUBMERSIONS

made up of three single phase furnaces. Figure 6.20 shows that the instantaneous field can be made up of the sum of the two individual fields. This result is not representative of the current distribution over the whole cycle because phase differences have been introduced. The field between two electrodes of different phases is no longer merely a sinusoidal varying quantity, but now is a rotating vector with a sinusoidally changing magnitude. The field in the full furnace at different points in the cycle is shown in Figure 6.21. The timing is relative to the zero-crossing of the red phase (electrodes 5 and 6). Also the power distribution cannot be ascertained with one set of readings. A number of sets of readings must be taken at different time instants, the instantaneous power distribution calculated for each and the whole lot added and averaged out to get the mean pattern. This was attempted but the accuracy of the result obtained was dubious. To collect such a set of readings at sufficiently small time steps to justify an integration by a summation takes nearly four hours, and in this time the experimental conditions must vary. Figure 6.22 shows the power distribution between electrodes 4 and 5 at different points in the cycle. The average power distribution will be something akin to the two electrode case since the peaks are very localised around the electrode tips.

Finally, an attempt to correlate the experiment with the theory. Figures 6.23 to 6.26 show curves of horizontal and vertical components of current for different levels, in

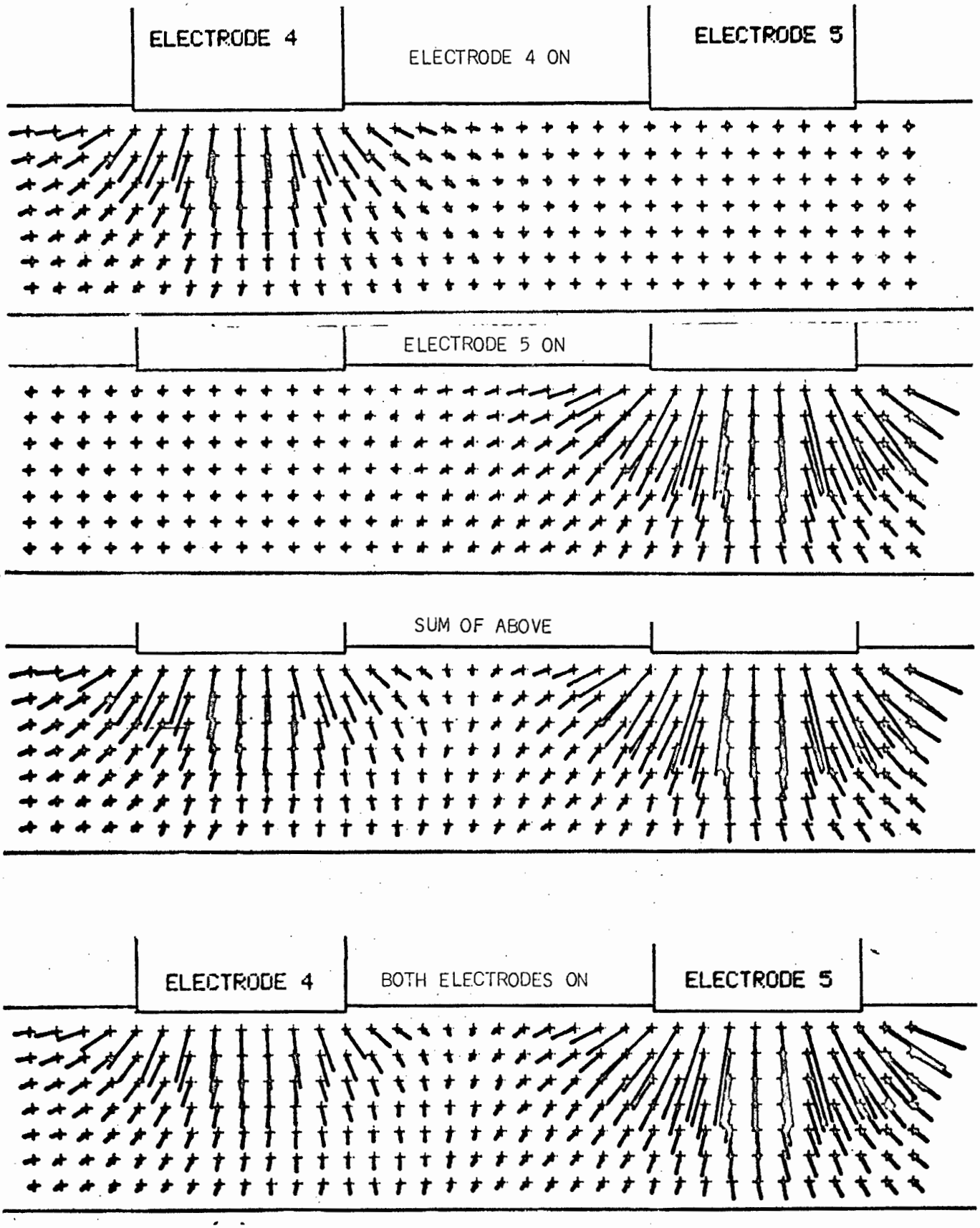

FIGURE 6.20 SUMMATION OF INDEPENDENT FIELDS FOR POLYPHASE EFFECT

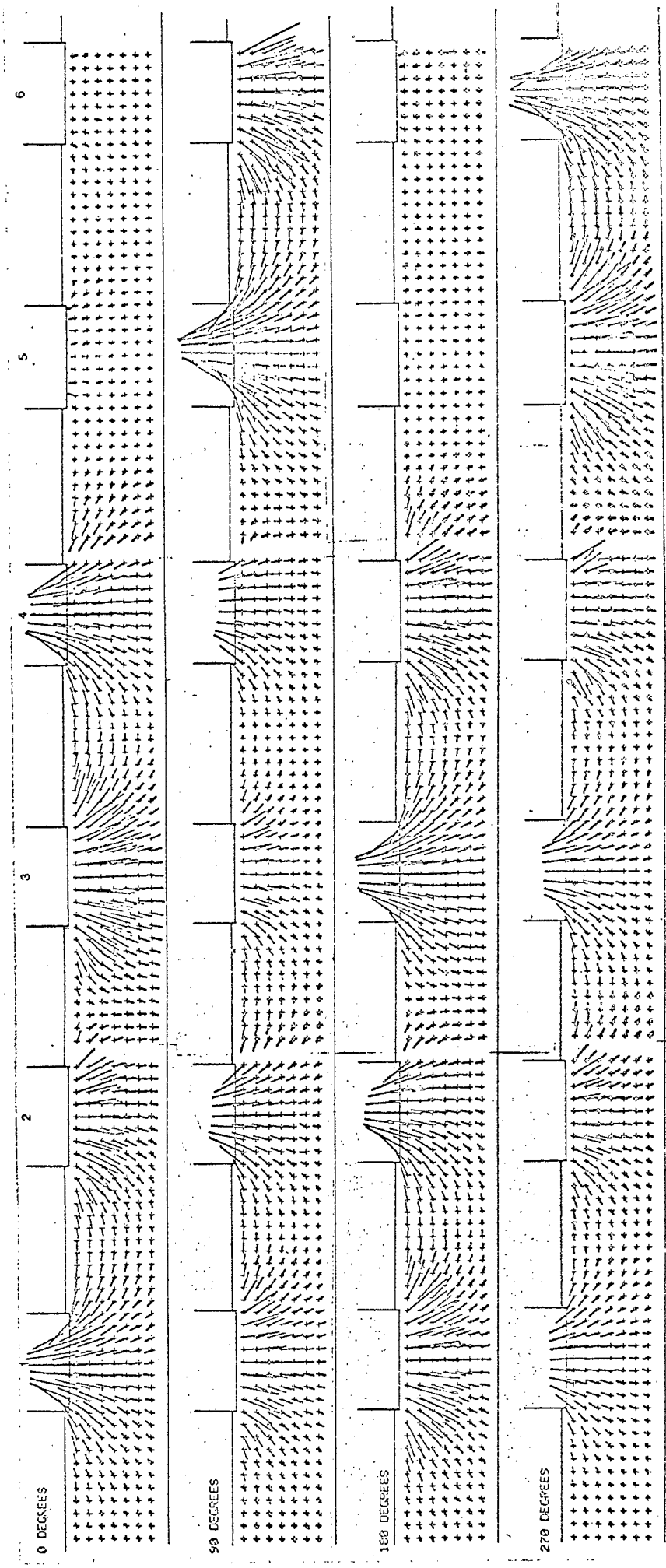

FIGURE 6.21 FIELDS IN A THREE PHASE FURNACE AT DIFFERENT INSTANTS IN THE CYCLE

FIGURE 6.22 POWER IN A POLYPHASE SYSTEM AT DIFFERENT INSTANTS IN THE CYCLE

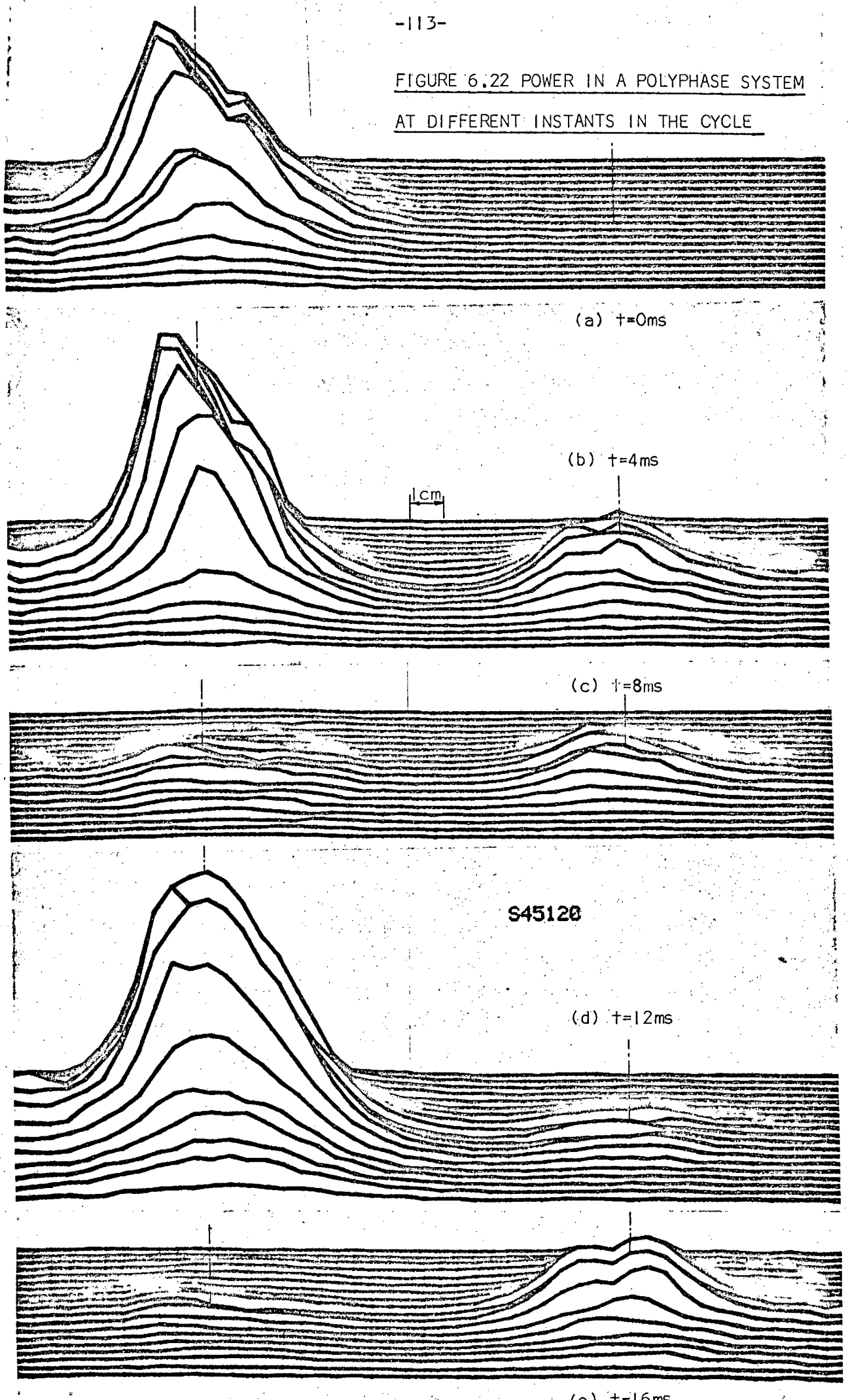

a plane through the electrodes, using experimental results, the static model and the field model (2cm electrode and 60cm electrode). For the static case (6.24) the horizontal component is much larger (in relation to the vertical component) than in the other models. This is because no account for the magnetic fields has been made. These will tend to force the current flow to the lower layers of the slag and hence reduce the interelectrode component. The field model gives a better approximation to the pattern obtained in the physical model (cf. Figures 6.23 and 6.25) which justifies using this to scale-up the dimensions of the furnace (Figure 6.26). For this large model the electrical constants of the system viz. electrode conductivity, must be altered to suit the new operating temperatures. Note that there is very little change in the field distribution except for a small area around the electrode tip where the non-uniform current input has an effect. There is no concentration of current at the sides or surface of the slag. This is because the skin depth for this material is about 4m and the depth of the slag is only 2m. The strange inflexion in the Ex component near the surface indicates that just below the electrode current will flow in from the circumference to the axis to set up a steady field. Increasing the current input to the theoretical model had no effect on the shape of the field pattern - only on magnitude. This was rather puzzling at first, but is obvious if one recalls the assumptions made in the model - the medium is linear and isotropic i.e. no saturation will occur.

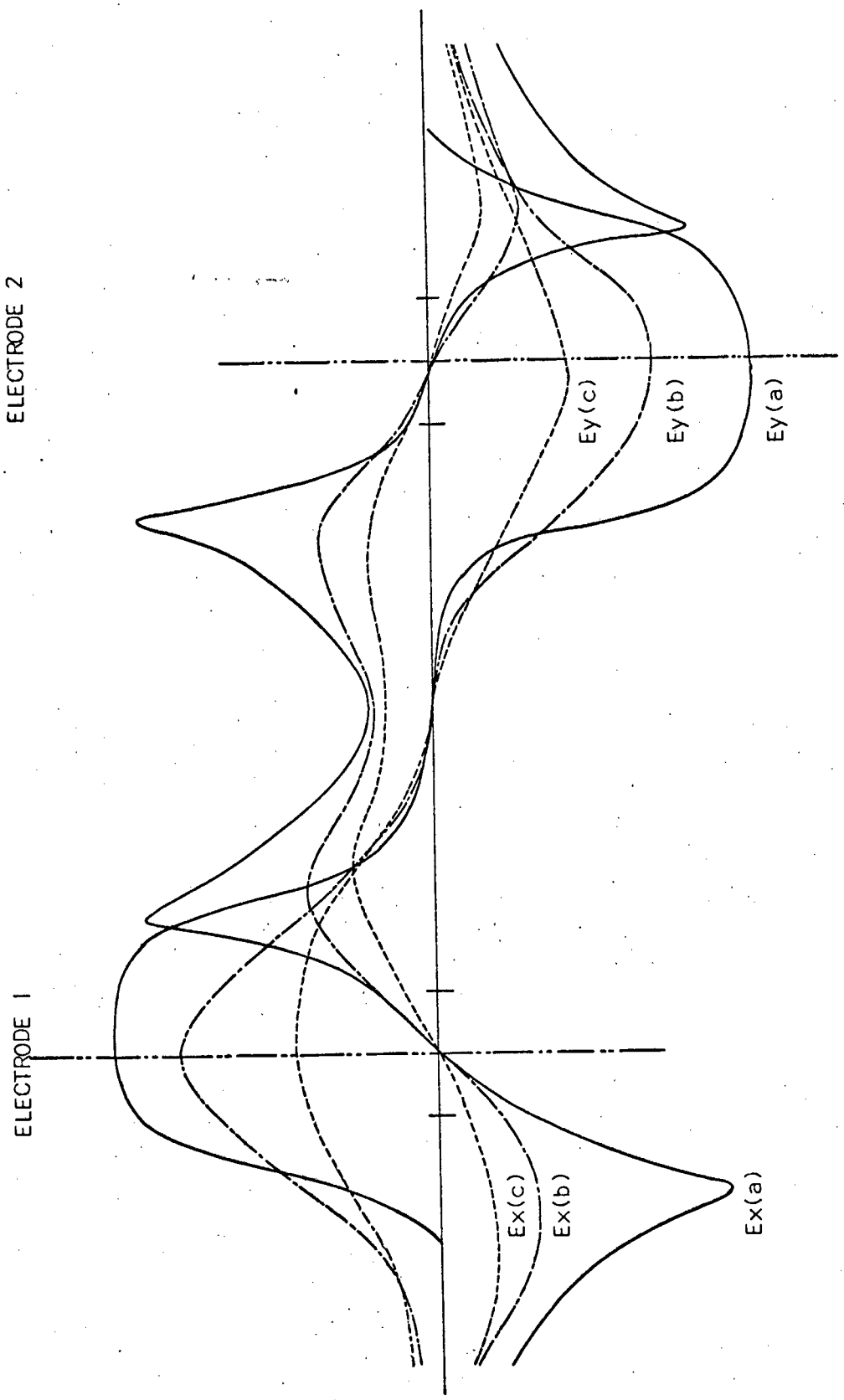

FIGURE 6.23 COMPONENTS OF CURRENT IN PHYSICAL MODEL IN PLANE Z=0

(a) Y=0.5cms
(b) Y=1.5cms
(c) Y=2.5cms

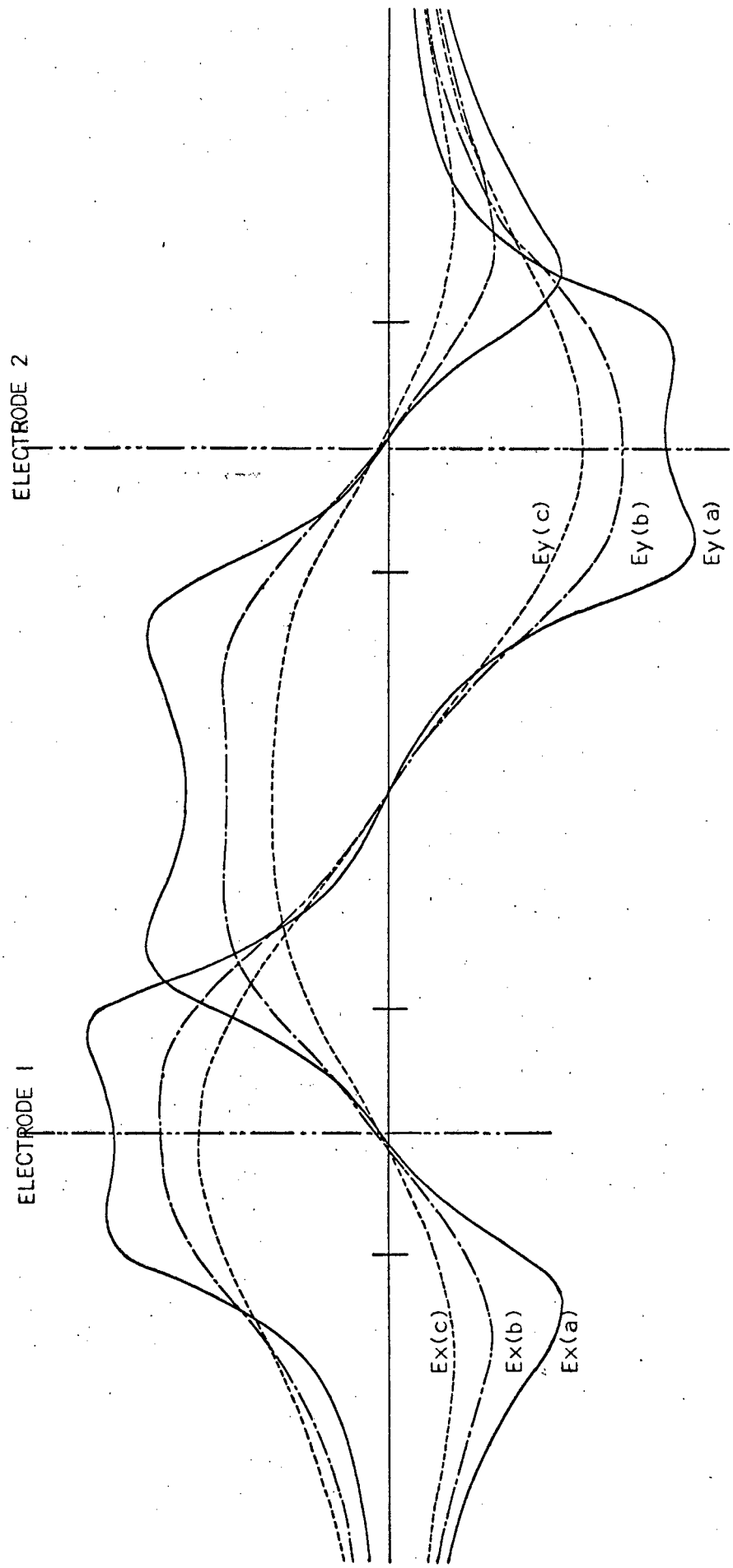

FIGURE 6.24 COMPONENTS OF CURRENT FROM STATIC MODEL

(a) Y=0.5cms
(b) Y=1.5cms
(c) Y=2.5cms

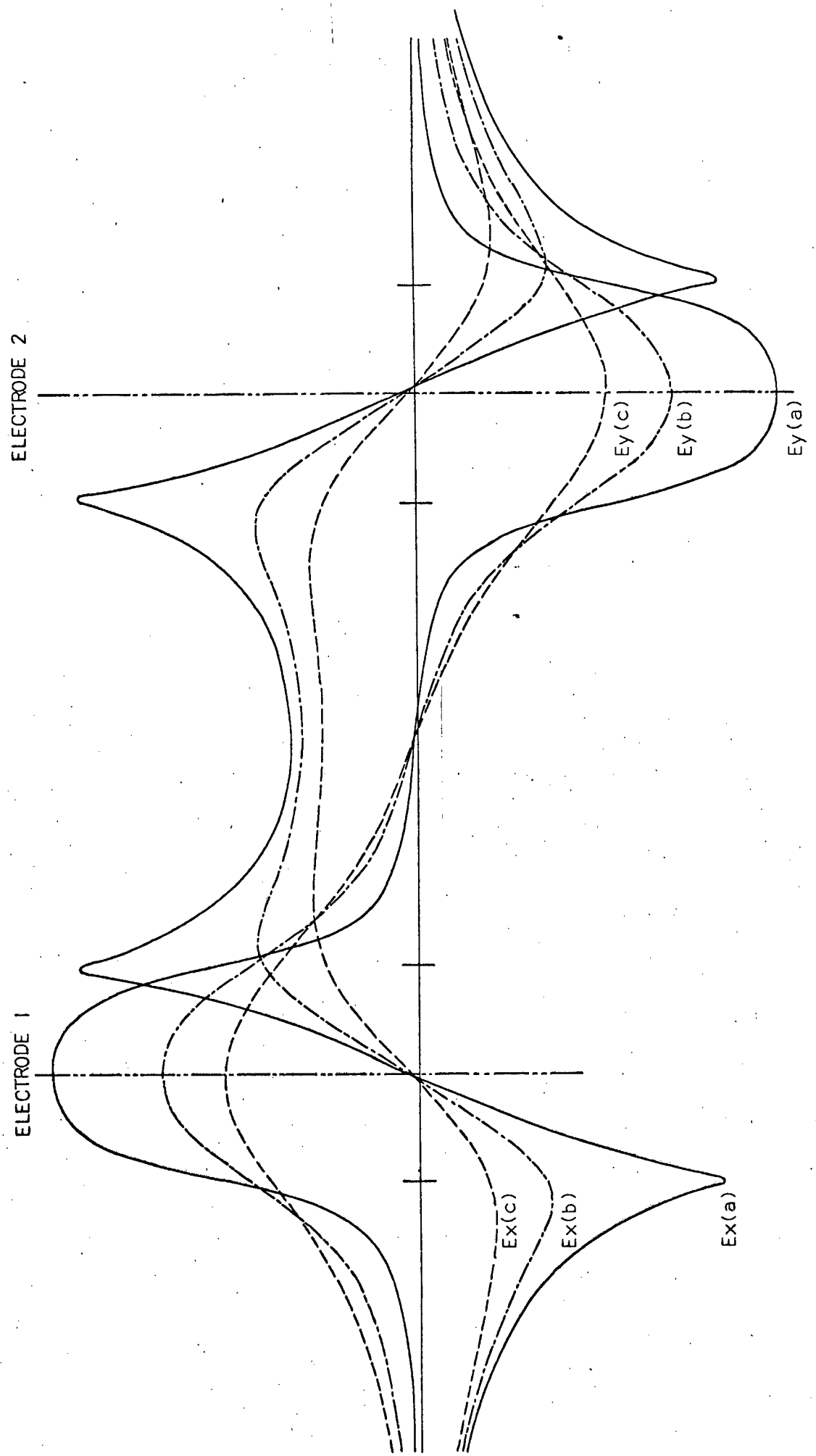

FIGURE 6.25 COMPONENTS OF CURRENT FROM FIELD MODEL - RADIUS OF ELECTRODE = 2.0cms

(a) Y=0.5cms
(b) Y=1.5cms
(c) Y=2.5cms

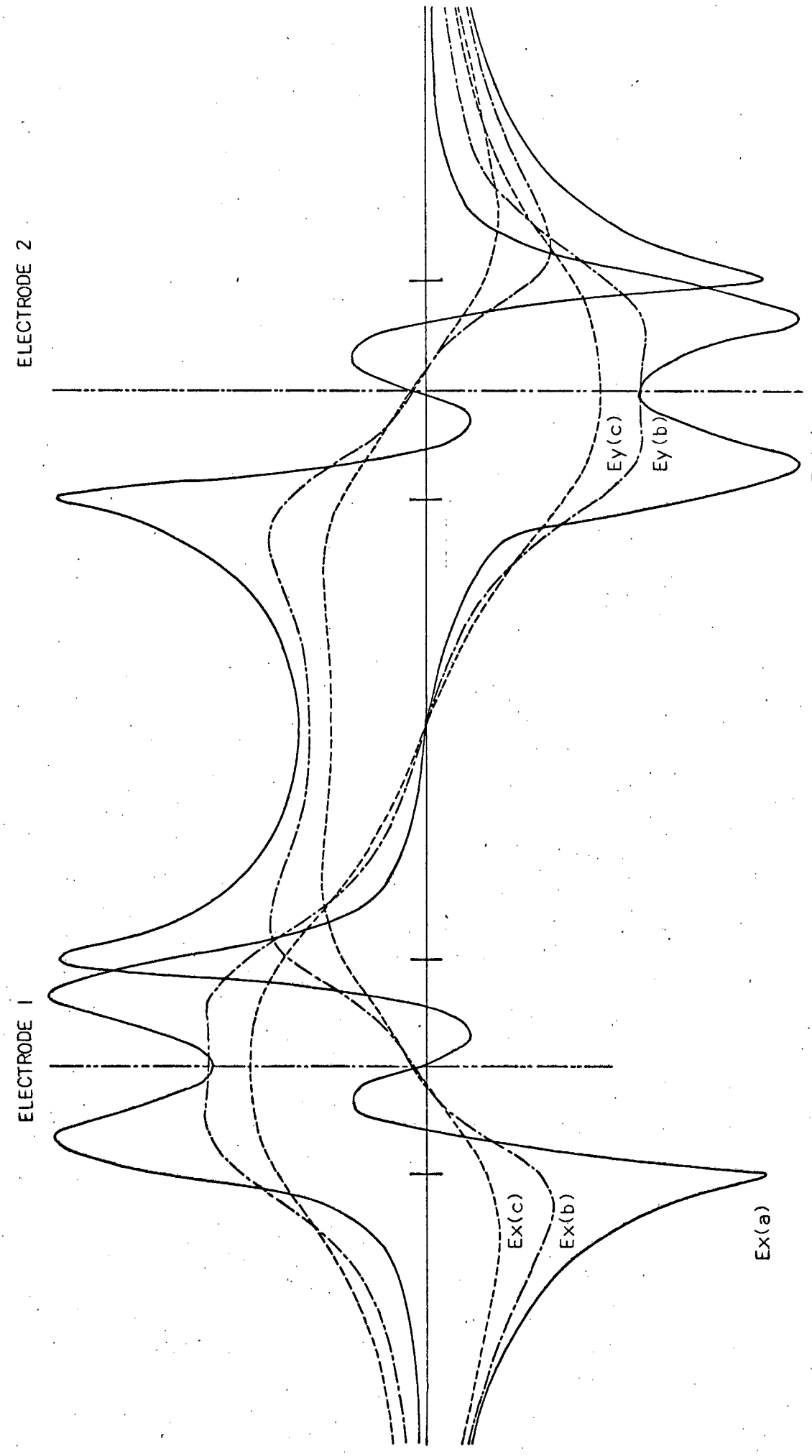

FIGURE 6.26 COMPONENTS OF CURRENT FROM FIELD MODEL - RADIUS OF ELECTRODE = 60cms

(a) Y=0.5cms
(b) Y=1.5cms
(c) Y=2.5cms

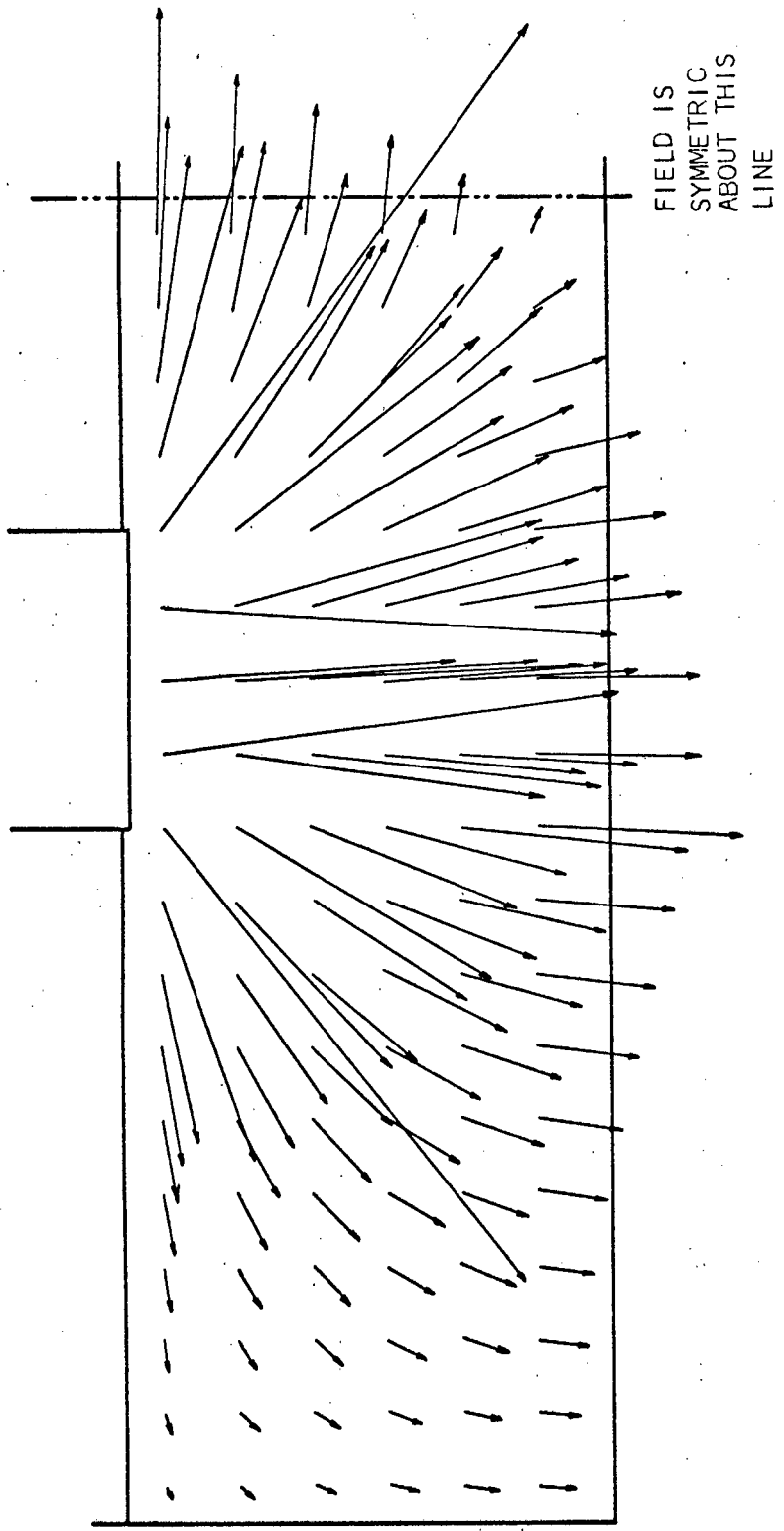

FIGURE 6.27 PROPOSED CURRENT DISTRIBUTION IN FURNACE (FROM FIELD MODEL)

It would appear that the power distribution plots obtained from the physical model are not as inaccurate as at first thought. The only change on scale-up will be that the peaks at the perimeter of the electrode will be more prominent - the rest of the field remains fairly constant. The model developed by no means gives a completely accurate description of the furnace at Rustenburg, but it will show the basic trend of change when one scales up a laboratory model. How accurate the assumption that the current distribution in the electrode is the same as that in an infinite length rod is difficult to say. The truncation of the line as it enters the electrolyte will definitely have some effect but the current will, in the very large conductors, still tend to congregate in the outer regions, though maybe not as much as proposed here. In a real furnace the arcing may tend to draw the current towards the electrode axis. Further work in this field will probably result in a more accurate model taking into account saturation effects, heat conduction and changes in conductivity due to temperature. This will no doubt give a better picture of the interior of a furnace, but the basic change will be the same as indicated here. Hence, although the model does have its limitations and would appear to be a poor representation of a real furnace, the field patterns set up in it are closely related to those in the operational plant so the results as regards power distribution can be applied to the large system.

REFERENCES

1. ANDREAE, F.V. Design and control of ferro-alloy furnaces. Trans. A.I.E.E. vol. 69. 1950 pp. 557-562.

2. KELLY, W.M. Design and construction of the submerged-arc furnace. Carbon and Graphite News, vol. 5, No. 1 April - May, 1958.

3. LOE, L.T. Aspects of Smelting Pig Iron in Electric Reduction Furnaces. The Canadian Mining and Metallurgical Bulletin, August 1970.

4. OTANI, SAITO, USUI, CHINO. The Inner Structure of the Submerged Arc Furnace. 6th International Congress on Electroheat, Brighton, 1968.

5. MOSTERT, J.C. and ROBERTS, P.N. Electric Smelting at Rustenburg Platinum Mines Ltd. of copper-nickel concentrates containing platinum-group metals. J.S.A.I.M.M. vol. 73, No. 9, 1973, pp. 290-299.

6. KJOLSETH, O. Electrochemical conditions of the Tysland-Hole furnace. Tids. Kemji. Bergv. Metall., vol. 21, 1961, pp. 27-33

7. HALLVARD NILSEN, P. Determination of the electrical resistance in idealised-resistance furnaces from model experiments. Tids. Kemji. Bergv. Metall., vol. 24, No. 11, 1964, pp. 203-208

8. DOWNING, J.H. and URBAN, L. Electrical conduction in submerged-arc furnaces. J. Metals, N.Y., March 1966, pp. 337-344

9. NIM TECHNICAL REPORT. The smelting of copper-nickel concentrates in an electric furnace. 1974.

10. SELMER-OLSEN, S. Lectures in Electro-smelting given at the University of Witwatersrand, September, 1968.

11. PERSSON, J.A. The significance of electrode-to-hearth voltage in electric smelting furnaces. Electric Furnace Proceedings, 1970, vol. 28, pp. 168-169

12. MORKRAMER, M. Design principles for arc reduction furnaces. Proc. 4th Int. Cong. on Electro-heat, 1959.

13. BRETTHAUER, K. and TIMM, K. The Measurement of electrical variables on the secondary side of three phase furnaces. Electro warme International 29, 1971.

14. URQUART, R. The production of high-carbon ferrochromium in a submerged-arc furnace. Minerals Science and Engineering vol. 4, No. 4, 1972, pp. 48-65

15. SCHWABE, W.E. The mechanics of consumption of graphite electrodes in electric steel furnaces. Journal of Metals, November 1972, pp. 65-71

16. JOHNSTONE, R.E. and THRING, M.W. Pilot Plants, Models and Scale Up Methods in Chemical Engineering, New York, McGraw-Hill, 1957

17. CADZOW, J.A. Discrete Time and Computer Control Systems, Prentice-Hall, 1970

18. THORNING, G. A High Speed Data Link. M.Sc. (Eng.) Thesis, U.C.T., 1974

19. BRADLOW, H. A digital investigation into arc furnace fields. B.Sc. (Eng.) Thesis, U.C.T., 1973

20. PANOFSKY, W.K.H. and PHILLIPS, M. Classical Electricity and Magnetism. Addison-Wesley, 1962

21. SILVESTER, P. Modern Electro-magnetic Fields. Prentice-Hall, Inc.

22. VITKOVITCH, O. Field Analysis, Van Nostrand, 1966

23. ARTLEY, J. Fields and Configurations. Holt, Rinehart and Winston, Inc., 1965

24. SOUTHWELL, R.V. Relaxation Methods in Theoretical Physics. Oxford, Clarendon Press, 1946

25. SMITH, G.D. Numerical Solution of Partial Differential Equations. Oxford University Press, 1965

26. VAN BLADEL, J. Electro magnetic Fields. McGraw-Hill, Inc. 1964

APPENDIX A : STEPPER MOTORS

With so much of the world turning to digital systems for control purposes inevitably some positioning device had to be developed which could be controlled digitally. This was the stepping motor, so called because instead of rotating smoothly like any conventional motor it jerks around in discrete steps of a fixed angle. Essentially there are two types of stepper motor - the permanent magnet type and the reluctance type. In each the stator consists of several windings which can be energised sequentially to produce a rotating magnetic field. The rotor is made up of either a permanent magnet or a toothed iron core which follows this wave to maintain a position of minimum potential energy. The motors used in this project are the permanent magnet type and have two multipole, centre-tap stator coils. A simplified sketch of the motor is given in Figure A.1. With the switches (1 and 2) as shown, the rotor will line up as in the diagram. If switch 1 is thrown to position A' the direction of the field in coil 1 will be reversed, hence the polarity of the pole pair will be changed and the rotor will swing ninety degrees in a clockwise direction to maintain the potential energy. By switching in the sequence given, one can get the rotor to turn through one complete revolution. To go round in the opposite direction the switching sequence must be reversed. The more pole pairs/coil, the smaller the step angle. The motors used have two hundred

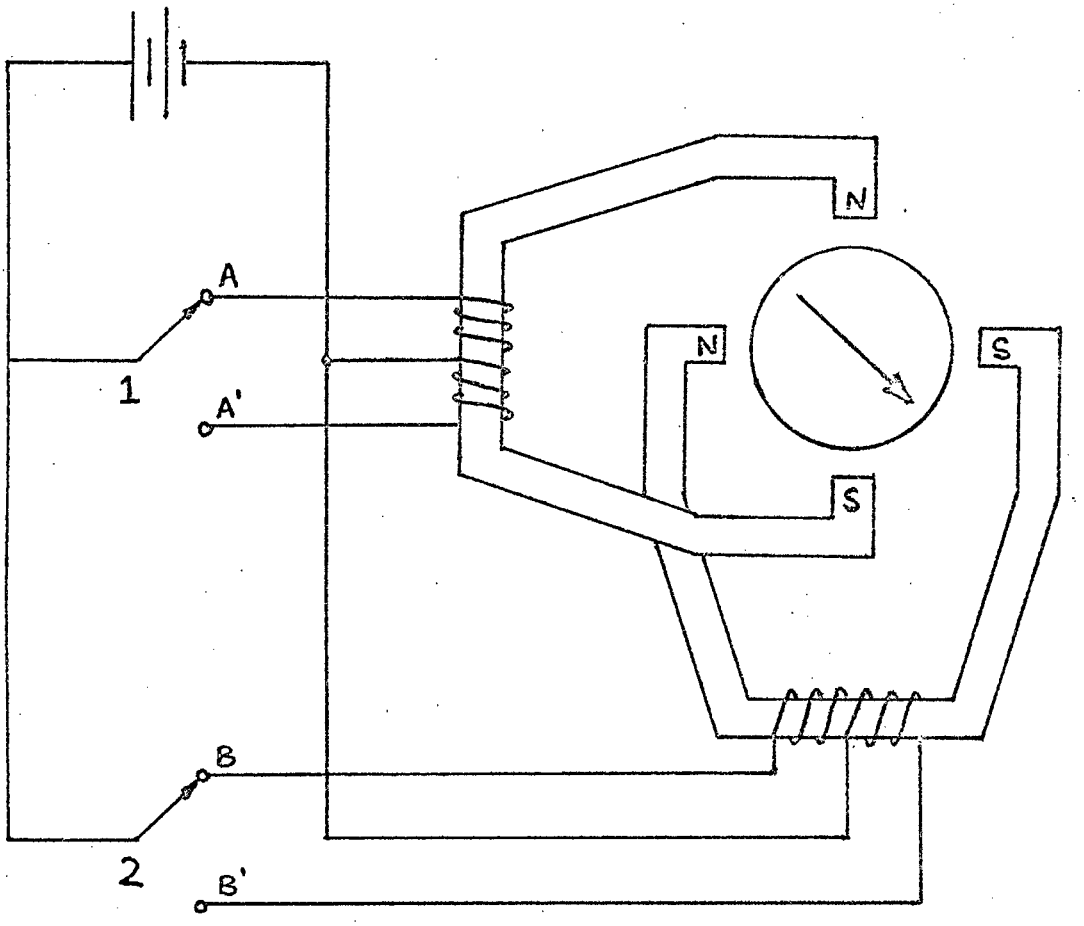

SWITCHING SEQUENCE FOR ROTATION OF MOTOR

CLOCKWISE		ANTICLOCKWISE	
A	B	A	B
A'	B	A	B'
A'	B'	A'	B'
A	B'	A'	B
A	B	A	B

FIGURE A.1 DIAGRAMMATIC CIRCUIT OF A STEPPER MOTOR

steps/revolution and this is attained by using fifty pole pairs per coil. In general, the stepping angle, D, is

$$D = \frac{360}{2n}$$ where n = total no. of pole pairs

To drive the motors from the computer some sort of interface had to be built up. The computer outputs the information i.e. how many steps to move, as a series of pulses and the direction of rotation by a line which is set either high or low. The interface (Figure A.2.) has to take these pulses and convert them into four signals which control the switching of the coils. Each pulse from the computer represents one step of rotation. The speed of stepping is limited if one is to maintain a reasonable torque. This timing is done by the computer's real-time clock which limits the pulse rate to 100Hz.

The advantage of using stepper motors with a digital control system is quite clear - no feedback is necessary. If two pulses are fed to the motor it will turn by two steps - no more and no less. The disadvantages are that the motors are slow (half a revolution per second in this case) and large for the amount of torque they give. This is due to the fact that only half of the stator coils are used at any one time, so for any large system, they would be prohibitively expensive.

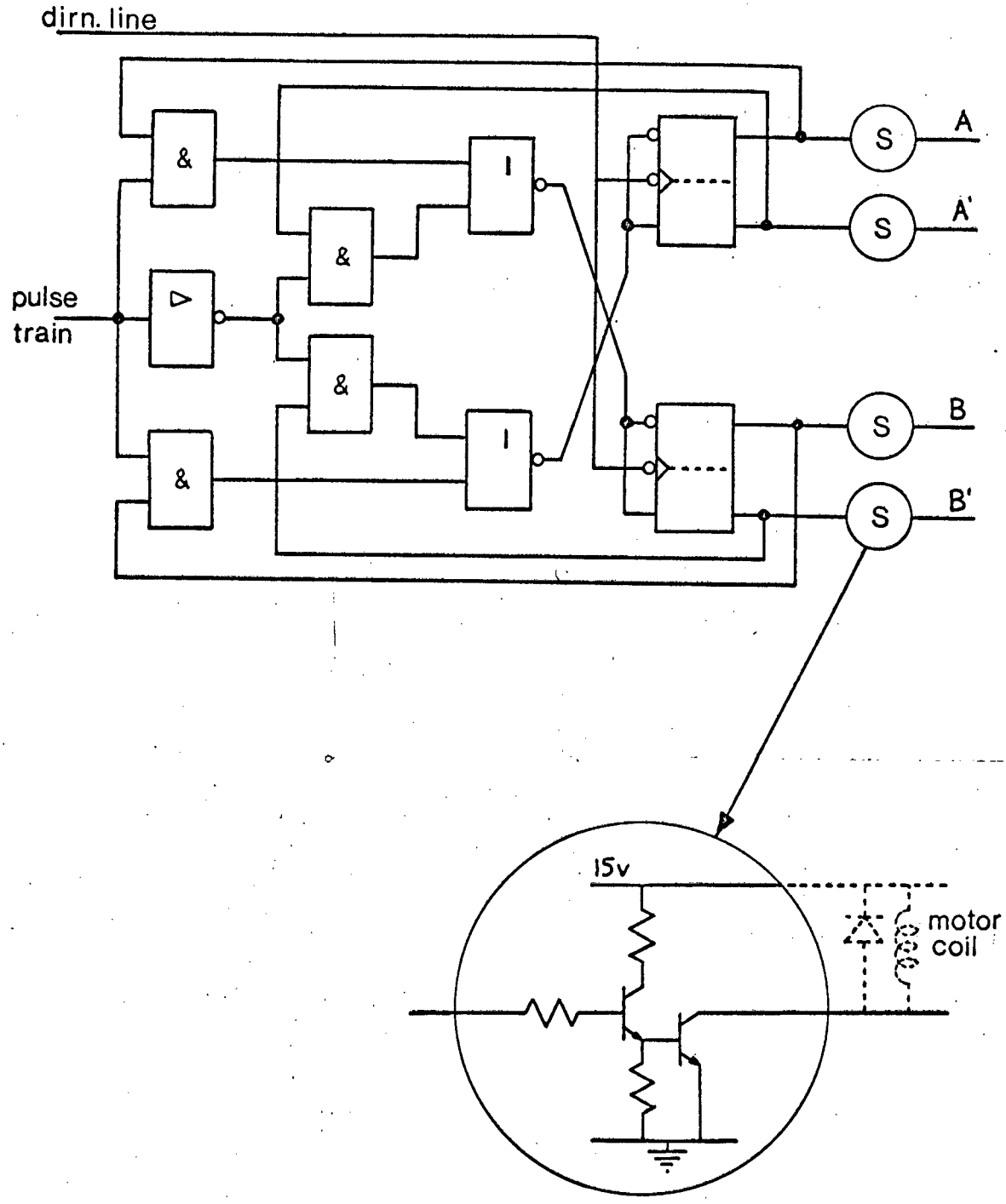

FIGURE A.2 INTERFACE TO STEPPER MOTORS

APPENDIX B : COMPUTER PERIPHERALS

In the discussion on the means of data acquisition reference has been made to several facilities which were conveniently called and used. A more detailed description of their purpose and operation follows.

B.1. ANALOGUE-TO-DIGITAL CONVERTER

The analogue signals being measured are converted to digital values which can be used by the processor via the analogue input module. This is under direct control of the computer. The block diagram of the system is shown in Figure B.1.1

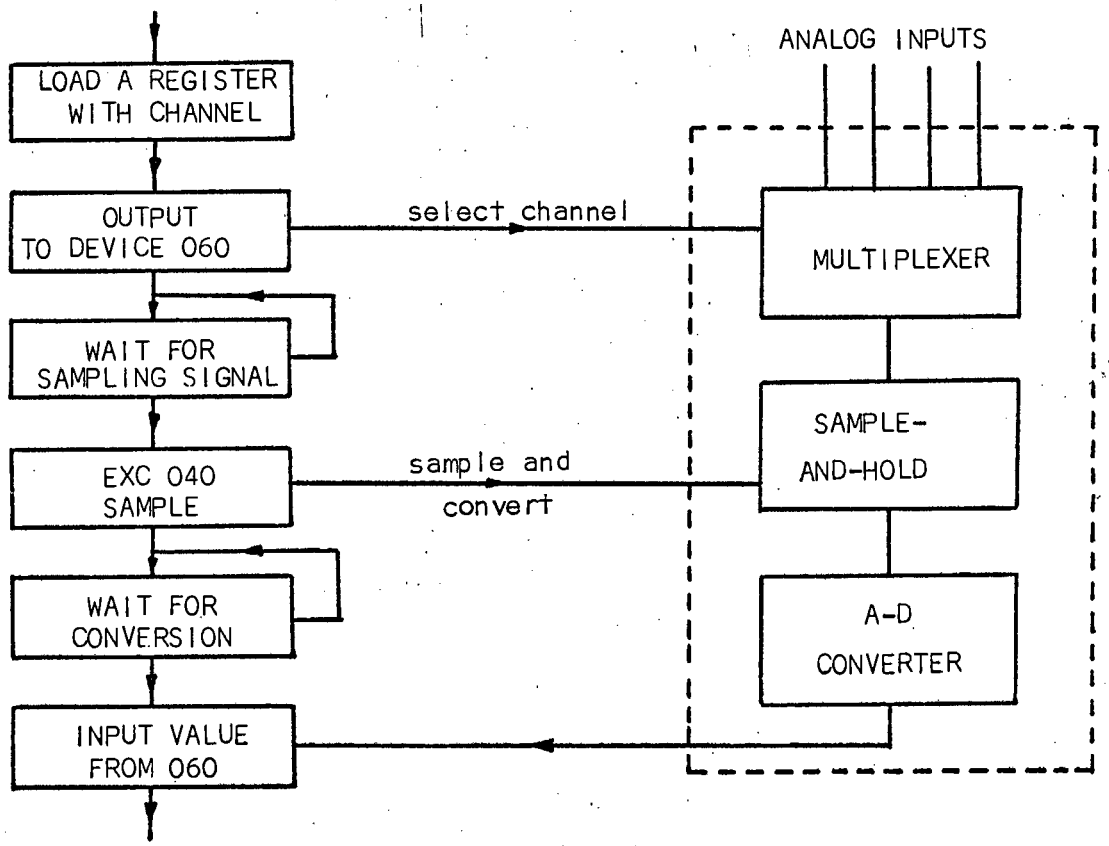

FIGURE B1.1 A-D CONVERTER

The module consists of a 16 channel multiplexer, a sample-and-hold circuit and an A-D converter. The peripheral device number is 060. First the channel number is selected by outputting the desired number to the multiplexer. When the computer receives the signal to sample it sends a pulse to the module and the analogue input is sampled and digitised. The conversion takes some time (about thirty-five microseconds) so the computer must wait in a loop before inputting the digital value. The resolution of the converter is ten bits, and the signal can vary from -10 volts to +10 volts. The maximum sampling rate is about 30kHz.

B.2. THE PRIORITY INTERRUPT MODULE

When dealing with alternating signals there must be some sort of synchronising signal between the computer and the system i.e. there must be some means of informing the processor of the time in the real world. This is achieved by the Priority Interrupt Module (P.I.M.) which performs the following functions :

(i) Establishes eight levels of interrupt priority for selected peripheral device controllers.

(ii) Stores interrupt requests originated by connected peripheral controllers placing them on the I/O bus in order of their established priorities.

The priority levels of the various peripherals are established by their connection to the interrupt cable.

The P.I.M. also provides entry to a memory location predetermined for each of the controllers connected. Interrupts from selected lines can be inhibited by a mask if so programmed so that these lines do not monopolise computer time.

The eight interrupt lines are scanned every nine hundred nano-seconds (except during double word or I/O instructions) and if an interrupt pulse is detected (the lines are normally high) the P.I.M. stores the line number in the interrupt register. If more than one line is low, the one with highest priority is administered first. The remaining interrupts are stored and dealt with later. When the computer acknowledges the interrupt the P.I.M. specifies a memory address which must hold the next instruction to be executed. This can be any instruction except an I/O command (normally it is a jump instruction to some specific routine). The P.I.M. is disabled either by a jump-and-mark instruction or a special programmed execution. In the VARIAN 620I, the interrupt locations are from 0100 - 0120 (number one line jumps to 0100, number two to 0102 etc.)

A sample program for using the interrupt facility is given in Figure B.2.1. Interrupt line 1 is used to initiate a routine, TEST, at a given signal. When TEST has been run, the processor returns to the main program, continuing from the location at which it was interrupted.

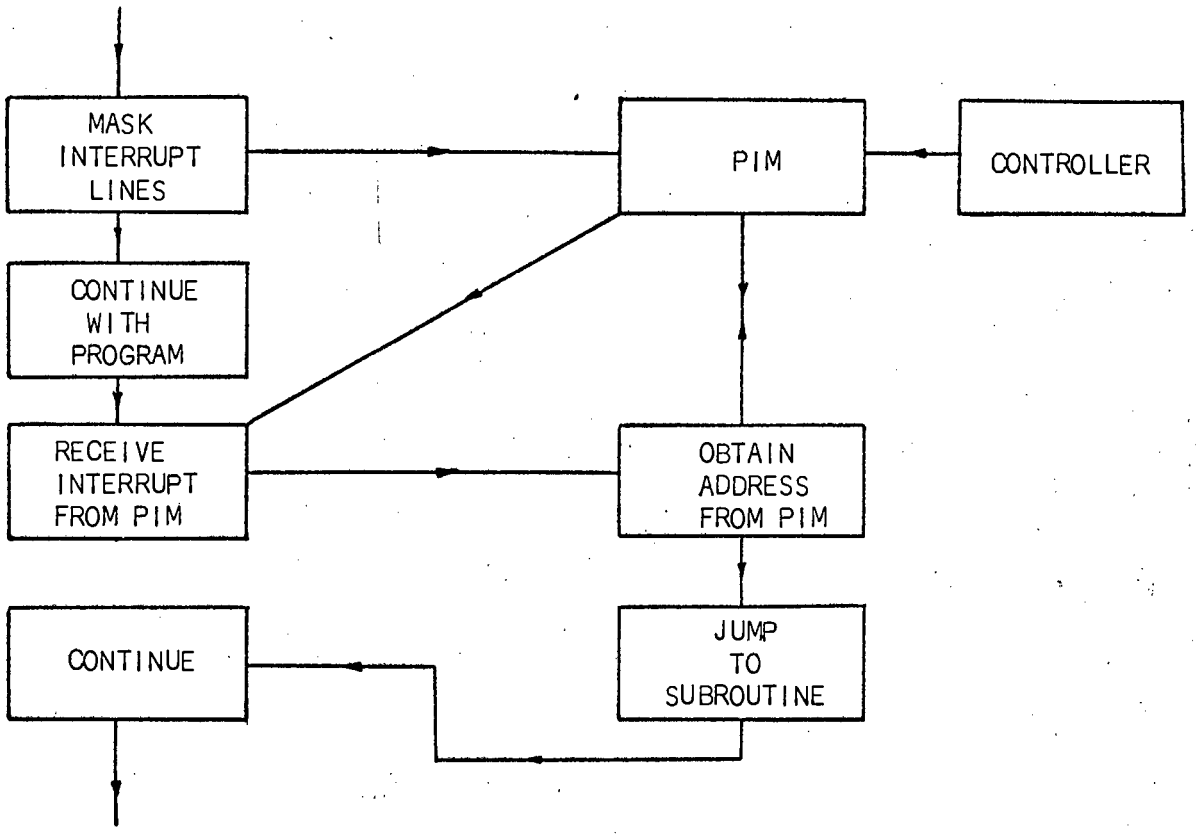


```
        ORG     0100            SPECIFY LOCATION TO JUMP TO
        JMPM    TEST            AT INTERRUPT SIGNAL
          .
          .
        LDAI    0376            SELECT INTERRUPT LINE WITH MASK
        OAR     047
        EXC     047             ENABLE PIM
          .
          .
          .
TEST    ENTR                    ROUTINE CALLED BY INTERRUPT
          .
          .
        JMP*    TEST            JUMP BACK TO SECTION OF PROGRAM
                                THAT WAS INTERRUPTED
```

FIGURE B.2.1 OPERATION OF INTERRUPT MODULE

B.3. REAL TIME CLOCK

Often one requires some sort of time delay in a program e.g. the pulses to drive the motors must be at least ten milliseconds apart. One could use the P.I.M. facility but this would require an external timing circuit and generally add complexity to the system. A much simpler and more convenient method is to use the computer's real-time clock. This is a unit contained on one of the control cards which can be programmed to give an interrupt after a predetermined time interval. In the system used this delay could be any multiple of one millisecond up to a maximum of sixteen seconds. The mode of operation and a sample program is shown in Figure B.3.1.

The real time clock actually uses two interrupts for its operation. When the unit has been enabled an interrupt causing the computer to execute the instruction at location 044 is generated every millisecond. The second interrupt is generated when the fifteenth bit of the word in location 045 changes from zero to one i.e. when the value reaches 040000. The execution address specified for this interrupt is 046.

The means of using the clock should now become apparent. Location 044 is set to instruct the computer to increment the value held in 045 by one. Assume a time delay of T milliseconds is required. The value 040000-T is loaded into 045 and the clock is enabled. Every milli-

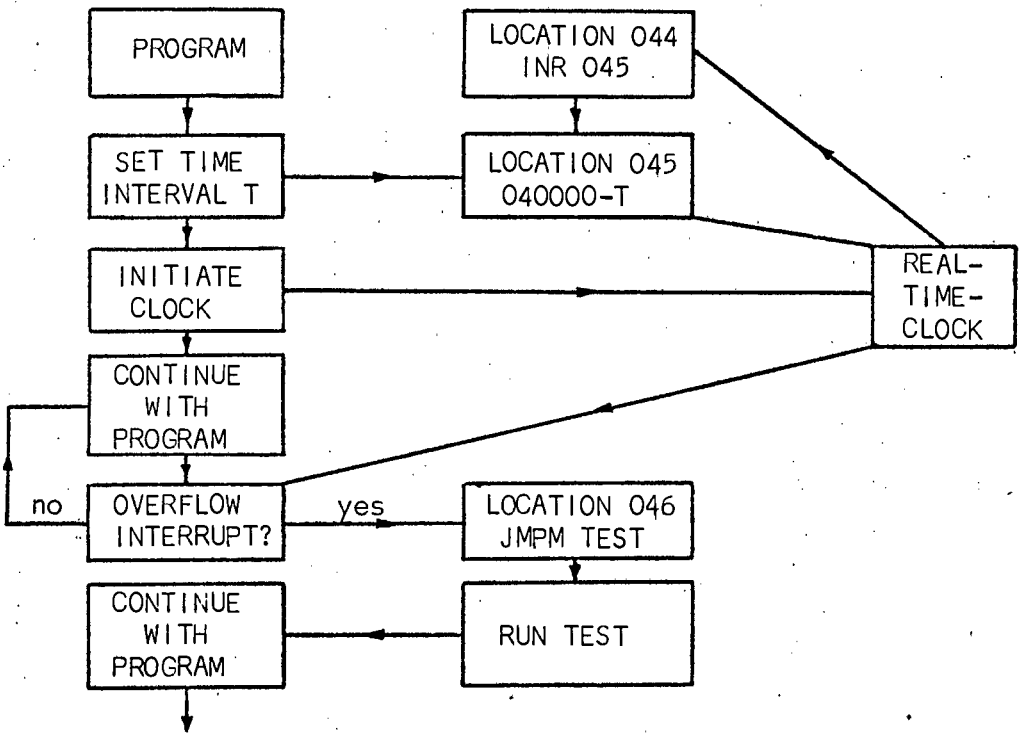


```
044     INR     045.        SET TO INCREMENT 045
045     DATA    DELAY       INITIALLT SET TO VALUE TO GIVE Tms DELAY
046     JMPM    TEST        JUMP AND MARK TO TEST ROUTINE
          .
          .
   MAIN PROGRAM
          .
          .
        LDA     DELAY
        STA     045         SET TIME  LAPSE
        EXC     0147        ENABLE REAL-TIME-CLOCK
          .
TEST    ENTR                SUBROUTINE TEST(CALLED BY RTC)
          .
        JMP*    TEST        RETURN TO MAIN PROGRAM
```

FIGURE B.3.1 OPERATION OF REAL-TIME-CLOCK

second 045 will be incremented until, after T interrupts, it will reach 040000 and the computer will execute the instruction at 046 - this will normally be an instruction to jump to some specific routine in the program.

The accuracy of the clock is only about five per cent, so it cannot be used for applications requiring perfect timing as for example the sampling of an alternating signal. Here the P.I.M. must be used. However for approximate delays such as a second wait while the storage screen of a cathode-ray tube is cleared it is ideal.

B.4. EXTERNAL CONTROL LINES

Direct digital data flow to and from the computer is achieved with a set of thirty six external control lines. The EXC card, from which these lines originate, is an interface built by the Electrical Engineering Department, U.C.T., for digital control of various systems using a VARIAN minicomputer. This card is plugged directly into the E-bus - the main input/output set of busbars in the computer.

The state of the output lines can be programmed to be either logical one or logical zero. Control is effected using the two external commands

(0100XXX)	EXC	XXX	-	line XXX low
(0104XXX)	EXC2	XXX	-	line XXX high

where XXX specifies the line number. The number in the

bracket is the machine code instruction (in octal). When such an instruction is executed the last nine bits of the word (i.e. XXX) are placed on the E-bus. During an EXC instruction the tenth line of the E-bus is high and for an EXC2 instruction the eleventh is high. The interface card accepts this information, decodes it and accordingly changes the relevant output line. Hence, to obtain a pulse from the computer to, say, line 054 the program would be

```
EXC2      .      054
          .
          .
        DELAY
          .
          .
EXC       .      054
```

The DELAY will give the pulse width. This can be done using the real time clock, the P.I.M. (if accurate timing is required) or with a series of NOP commands (an instruction during which the computer does nothing for one cycle).

The digital input is achieved by sensing the state of the various input lines using the SEN instruction viz :

(101XXX) SEN XXX, HIGH - sense the state of line XXX.

If the state of XXX is true (logical one) the next instruction executed will be at location HIGH. If false, the next instruction in sequence is executed.

APPENDIX C : INTERRUPT GENERATOR

As mentioned in the text the timing for the data sampling is controlled by an interrupt pulse to the P.I.M. This ensures that each sample is taken at the same instant of the model's power cycle. For different experiments different sampling instants will be required so the phase difference between the pulse train and the supply voltage must be variable. The circuit diagram of the system used is shown in Figure C.1. It merely consists of a simple voltage zero detector and two monostables. The zero detector is connected across the transformer to one phase of the model and triggers the first monostable at the beginning of each power cycle. This monostable has a variable pulse width (0-20msecs i.e. one period at 50Hz). The second one-shot is triggered on the trailing edge of this pulse and sends a short interrupt signal to the P.I.M.

A system using the computer to generate the delay was tried but found unsuitable due to the inaccuracy of the real-time clock.

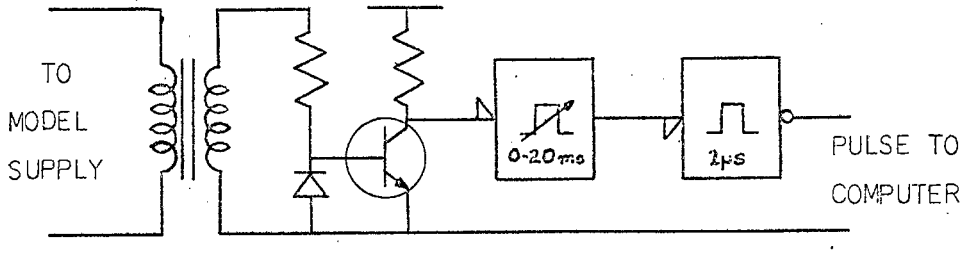

FIGURE C.1 INTERRUPT PULSE GENERATOR

APPENDIX D : DAS

The Varian 620/I assembler language (DAS) specifies instructions, addresses, address modifications and constants in a straightforward manner. Instruction mnemonics replace the usual numerical codes. Memory addresses can be referenced symbolically, and comments can be added to the statements to facilitate check-out. Each statement comprises a label, operation, variable and comment field, and on compilation it generally generates one computer word. A full listing of the instructions available, together with its meaning and binary equivalent is given in the table below.

Mnemonic	Octal	Definition
ADD	120000	Add to A Register
ADDE	006120	Add to A Register Extended
ADDI	006120	Add to A Register Immediate
ANA	150000	AND to A Register
ANAE	006150	AND to A Register Extended
ANAI	006150	AND to A Register Immediate
AOFA	005511	Add OF to A Register
AOFB	005522	Add OF to B Register
AOFX	005544	Add OF to X Register
ASLA	004200+n	Arithmetic Shift Left A n Places
ASLB	004000+n	Arithmetic Shift Left B n Places
ASRA	004300+n	Arithmetic Shift Right A n Places
ASRB	004100+n	Arithmetic Shift Right B n Places
CIA	102500	Clear and Input to A Register
CIAB	102700	Clear and Input to A and B
CIB	102600	Clear and Input to B Register
COMPL	005000	Complement Source to Destination
CPA	005211	Complement A Register
CPB	005222	Complement B Register

TABLE D 1 of 5

Mnemonic	Octal	Definition
CPX	005244	Complement X Register
DAR	005311	Decrement A Register
DBR	005322	Decrement B Register
DECR	005000	Decrement Source to Destination
DIV	170000	Divide AB Register
DIVE	006170	Divide AB Register Extended
DIVI	006170	Divide AB Register Immediate
DXR	005344	Decrement X Register
ERA	130000	Exclusive OR to A Register
ERAE	006130	Exclusive OR to A Register Extended
ERAI	006130	Exclusive OR to A Register Immediate
EXC	100000	External Control Function
HLT	000000	Halt
IAR	005111	Increment A Register
IBR	005122	Increment B Register
IME	102000	Input to Memory
INA	102100	Input to A Register
INAB	102300	Input to A and B Registers
INB	102200	Input to B Register
INCR	005000	Increment Source to Destination
INR	040000	Increment and Replace
INRE	006040	Increment and Replace Extended
INRI	006040	Increment and Replace Immediate
IXR	005144	Increment X Register
JAN	001004	Jump if A Register Negative
JANM	002004	Jump and Mark if A Register Negative
JAP	001002	Jump if A Register Positive
JAPM	002002	Jump and Mark if A Register Positive
JAZ	001010	Jump if A Register Zero
JAZM	002010	Jump and Mark if A Register Zero

TABLE D 2 of 5

Mnemonic	Octal	Definition
JBZ	001020	Jump if B Register Zero
JBZM	002020	Jump and Mark if B Register Zero
JIF	001000	Jump if Combined Conditions
JIFM	002000	Jump and Mark if Combined Conditions
JMP	001000	Jump Unconditionally
JMPM	002000	Jump and Mark Unconditionally
JOF	001001	Jump if Overflow On
JOFM	002001	Jump and Mark if Overflow On
JS1M	002100	Jump and Mark if Sense Switch 1 On
JS2M	002200	Jump and Mark if Sense Switch 2 On
JS3M	002400	Jump and Mark if Sense Switch 3 On
JSS1	001100	Jump if Sense Switch 1 On
JSS2	001200	Jump if Sense Switch 2 On
JSS3	001400	Jump if Sense Switch 3 On
JXZ	001040	Jump X Register Zero
JXZM	002040	Jump and Mark X Zero
LASL	004400+n	Long Arithmetic Shift Left n Places
LASR	004500+n	Long Arithmetic Shift Right n Places
LDA	010000	Load A Register
LDAE	006010	Load A Register Extended
LDAI	006010	Load A Register Immediate
LDB	020000	Load B Register
LDBE	006020	Load B Register Extended
LDBI	006020	Load B Register Immediate
LDX	030000	Load X Register
LDXE	006030	Load X Register Extended
LDXI	006030	Load X Register Immediate
LLRL	004440+n	Long Logical Rotate Left n Places
LLSR	004540+n	Long Logical Shift Right n Places

TABLE D 3 of 5

Mnemonic	Octal	Definition
LRLA	004240+n	Logical Rotate Left A n Places
LRLB	004040+n	Logical Rotate Left B n Places
LSRA	004340+n	Logical Shift Right A n Places
LSRB	004140+n	Logical Shift Right B n Places
MERGE	005000	Merge Source to Destination
MUL	160000	Multiply B Register
MULE	006160	Multiply B Register Extended
MULI	006160	Multiply B Register Immediate
NOP	005000	No Operation
OAB	103300	Output OR of A and B Registers
OAR	103100	Output from A Register
OBR	103200	Output from B Register
OME	103000	Output from Memory
ORA	110000	Inclusive OR to A Register
ORAE	006110	Inclusive OR to A Register Extended
ORAI	006110	Inclusive OR to A Register Immediate
ROF	007400	Reset Overflow
SEN	101000	Sense Input/Output Lines
SOF	007401	Set Overflow
SOFA	005711	Subtract OFLO from A Register
SOFB	005722	Subtract OFLO from B Register
SOFX	005744	Subtract OFLO from X Register
STA	050000	Store A Register
STAE	006050	Store A Register Extended
STAI	006050	Store A Register Immediate
STB	060000	Store B Register
STBE	006060	Store B Register Extended
STBI	006060	Store B Register Immediate

TABLE D 4 of 5

Mnemonic	Octal	Definition
STX	070000	Store X Register
STXE	006070	Store X Register Extended
STXI	006070	Store X Register Immediate
SUB	140000	Subtract from A Register
SUBE	006140	Subtract from A Register Extended
SUBI	006140	Subtract from A Register Immediate
TAB	005012	Transfer A to B Register
TAX	005014	Transfer A to X Register
TBA	005021	Transfer B to A Register
TBX	005024	Transfer B to X Register
TXA	005041	Transfer X to A Register
TXB	005042	Transfer X to B Register
TZA	005001	Transfer Zero to A Register
TZB	005002	Transfer Zero to B Register
TZX	005004	Transfer Zero to X Register
XAN	003004	Execute A Register Negative
XAP	003002	Execute A Register Positive
XAZ	003010	Execute A Register Zero
XBZ	003020	Execute B Register Zero
XEC	003000	Execute Unconditionally
XIF	003000	Execute if Combined Conditions
XOF	003001	Execute Overflow Set
XS1	003100	Execute SENSE Switch 1 Set
XS2	003200	Execute SENSE Switch 2 Set
XS3	003400	Execute SENSE Switch 3 Set
XXZ	003040	Execute X Register Zero
ZERC	005000	Zero Register

TABLE D 5 of 5